

 $K_L - K_S$ Mass Difference and Rare K-Decays

In a Phenomenological Gauge Model

SATISH D. JOGLEKAR

Fermi National Accelerator Laboratory, Batavia, Illinois 60510

and

Institute for Theoretical Physics, SUNY at Stony Brook, LI, NY 11790

ABSTRACT

We discuss the $K_L - K_S$ mass difference and many rare decay modes of K mesons in a phenomenological unified gauge model of strong, electromagnetic and weak interactions. The strong interactions of the system of pseudoscalar mesons which belong to a 15-dimensional representation of SU(4) are described by a phenomenological Lagrangian which possesses approximate chiral SU(4) \times SU(4) symmetry. The additional quantum number is charm. The weak and electromagnetic interactions are described by the Weinberg-Salam model. In general, the results are in qualitative agreement with those of the free quark model calculations. Results on the $K_L - K_S$ mass difference indicate that charmed hadrons must not be very heavy. As in the quark model calculation, we also find a surprising cancellation of the leading terms in $K^0 \rightarrow \mu\mu^-$ amplitude. The result for the $K^+ \rightarrow \pi^+ e\bar{e}$ branching ratio is in reasonably good agreement with the recent experimental result. Calculations of the branching ratios for the decays $K^+ \rightarrow \pi^+ \nu\bar{\nu}$, $K_{L,S} \rightarrow \pi^0 \nu\bar{\nu}$ and $K_{L,S} \rightarrow \pi^0 e\bar{e}$ are also performed.



I. INTRODUCTION

Recently, several models^{1, 2} which unify weak and electromagnetic interactions through spontaneously broken gauge theories have been proposed. Such models are renormalizable and as such they have finite predictions for higher order weak processes. Mostly, the weak interactions of the hadrons are incorporated² in such models by postulating that hadrons are constituted of quarks and by assigning the quarks to representations of the weak gauge group. In terms of quarks, p, n and λ , the hadronic weak (charged) current is expressed as

$$(J_{\mu}^{-}(c))^{+} = (J_{\mu}^{+}(c)) = \bar{p} \gamma_{\mu} (1 - \gamma_5) (n \cos \theta + \lambda \sin \theta) = \bar{p} \gamma_{\mu} (1 - \gamma_5) n_c \quad (1.1)$$

where θ is the Cabbibo angle. In these gauge invariant theories the neutral current J_{μ}^3 defined by,

$$J_{\mu}^3(x) = \frac{1}{2} \left[J_{\mu}^{+(c)}(x), \int d^3y J_0^{-}(c)(y) \right] \quad (1.2)$$

together with $J_{\mu}^{\pm}(c)$ satisfy the algebra of SU(2), and $J_{\mu}^3(x)$ couples to the neutral weak gauge bosons with the same strength as the charged weak current. With the charged weak current $J_{\mu}^{+(c)}(x)$ of Eq. (1.1), it is well known that $J_{\mu}^3(x)$ contains pieces which can change strangeness. Thus the strangeness changing ($\Delta S = 1, \Delta Q = 0$) hadronic weak processes will proceed with rates of the same order of magnitude as the $\Delta S = \Delta Q = \pm 1$ processes; in contradiction to the observed suppression of the $|\Delta S| = 1,$

$\Delta Q = 0$ processes. In quark models, this situation is remedied by the addition of one or more new quarks. In the case of the Weinberg-Salam model, which we shall be using this, this situation is remedied by the introduction of a new quark p' [the Glashow-Iliopoulos-Maiani mechanism]³ which has the charge, the strangeness and the hypercharge of p quark and is distinguished from p by the introduction of an additional quantum number, the charm. Charm is assumed to be conserved by strong interactions.

Since the charm is introduced⁴ to suppress the $\Delta S = 1$ neutral currents, the calculation of $|\Delta S| = 1$, $\Delta Q = 0$ processes can provide us with information about (the mass of) the charmed quark Lee and Gaillard⁵ have recently performed these calculations in connection with the rare decay modes of K-mesons in the Weinberg-Salam model.⁶ These calculations yield bounds on the quark masses and predictions for several of the suppressed decays. However, one does not know as to how these quark masses will be related⁷ to the masses of hadrons containing the charmed quark p' . Further, one does not know to what extent the strong interactions will modify the free quark model results and therefore one does not know how reliable these estimates are.

With this motivation, we have performed similar calculations in a phenomenological unified gauge model of the strong, electromagnetic and weak interactions. It is assumed that Chiral $SU(4) \times SU(4)$ is an approximate symmetry of the strong interaction dynamics, and it is

broken only by the "mass terms" [which can give a higher mass to the charmed particles as compared to the uncharmed ones]. It is assumed that the pseudoscalar mesons belong to the 15 dimensional representation of the SU(4) and that this 15 dimensional representation contains the octet of the uncharmed pseudoscalar mesons. A phenomenological model⁸ of the strong interactions of the pseudoscalar mesons, which will incorporate the results of current algebra of the chiral SU(4) \times SU(4) group and PCAC in the tree approximation, is constructed by an analog to the σ -model⁹ and the SU(3) version¹⁰ of the σ -model. Such a model consists of a set of 16 pseudoscalar (\equiv II) and 16 pseudoscalar (\equiv Σ) mesons which are assigned to $(4, \bar{4}) + (\bar{4}, 4)$ representations of the chiral SU(4) \times SU(4) group, and with an appropriate choice of the potential term, the masses of the scalar mesons are made arbitrarily large via spontaneous breakdown of symmetry (analogous to the σ -model). In order to incorporate the weak and the electromagnetic interactions in a renormalizable way, we have coupled this model to the Weinberg-Salam model⁶ of the weak and the electromagnetic interactions by assigning transformation properties to Σ and II under the weak gauge group. We have chosen the Weinberg-Salam model as this is the simplest model which is reasonably consistent with the present data on neutral currents.¹¹

In Sec. II, we have described the model in detail. We have explained how the SU(4) symmetry breaking is produced and how the weak and electromagnetic interactions are incorporated. In Sec. III, we have

explained the phenomenological point of view taken while performing the calculations [i. e., while drawing the Feynman diagrams for a relevant process] to lowest order in the weak and electromagnetic interactions and to all orders in the strong interactions. In subsequent sections, we have performed the calculations of the amplitudes for (i) $K_L \rightarrow \mu \bar{\mu}$ (ii) $K^+ \rightarrow \pi^+ \nu \bar{\nu}$ (iii) $K_{L,S}^0 \rightarrow \pi^0 \nu \bar{\nu}$ (iv) $K^+ \rightarrow \pi^+ e \bar{e}$ (v) $K_{S,L}^0 \rightarrow \pi^0 e \bar{e}$ and the calculation of the $K_L - K_S$ mass difference. These calculations are done in the approximate $\mu^2 \gg M^2 \gg m_c^2 \gg m_K^2 \gg m_\pi^2$, where μ , M and m_c are respectively, the masses of the scalar mesons, the W^\pm and the charmed pseudoscalar meson. It is interesting to note that even though individual diagrams may not have a finite limit¹² as $\mu^2 \rightarrow \infty$ [through terms like μ^2 , $\ln \mu^2$, etc.] the total amplitude in all cases have a finite limit as $\mu^2 \rightarrow \infty$. Furthermore, all the results are found to be independent of the parameters $\mu_0^2, \alpha, \beta, \gamma$ which enter the phenomenological Lagrangian of the strong interactions [see Eq. (2.3)]. This is very important for otherwise the results will be useless. The results depend only on the observable parameters like m_c, f_K, M_W etc. It is important to note that the only unknown parameter the results may sensitively depend on is m_c . [The dependence on M_W in the final form, is at most logarithmic.]

In several cases, it is obvious that the corrections to the amplitude due to the SU(3) symmetry breaking ($m_K \neq m_\pi \neq 0$) are small as compared to the leading order contribution. In such cases, we shall perform the

calculation in the exact $SU(3) \times SU(3)$ limit and set $m_K = m_\pi = 0$, wherever possible.¹³

In Appendix A, we have summarized many of the Feynman rules, used in the calculations. Since the use of the Ward-Takahashi (WT) identities simplifies the calculations considerably, in Appendix B, we have derived the WT identities relevant to the calculations. The Appendices C and D are added to make it more transparent the facts that the results are finite and independent of the parameters α, β, γ as $\mu_0^2 \rightarrow \infty$. The Appendices E, F, G, H and I deal with some specific calculations which are rather lengthy or less important, but essential.

In Sec. X, we have made the numerical estimates of the decay rates and branching ratios.

We find that the results are in qualitative agreement with those of the free quark model of Ref. [5] [i. e., with respect to the order of magnitude.] Thus, it was found in the free quark model calculation of Ref. (5) that there is an unexpected cancellation of the terms of the leading order in the amplitude for $K_{L,S} \rightarrow \mu\bar{\mu}$. We also find a similar cancellation of terms of $O(G_F \alpha \frac{m_c^2}{M^2} \ln \frac{M^2}{m_c^2})$ in the amplitude for $K_0 \rightarrow \mu\bar{\mu}$. Thus our result indicates that the cancellation found in the free quark model holds even in presence of the strong interactions.¹⁴ The amplitude we have computed is found to be of two orders of magnitude lower than the amplitude for $K_L \rightarrow \gamma\gamma \rightarrow \mu\bar{\mu}$ as a result of this cancellation. The result for $K^+ \rightarrow \pi^+ e\bar{e}$ is found to be in good agreement with the recent

experimental result.¹⁵ The calculation of the $K_L - K_S$ mass difference in this model puts stringent upper bound on the masses of the charmed mesons. The amplitude for the process $K^+ \rightarrow \pi^+ \nu \bar{\nu}$ is found to be sensitive to the charmed meson mass (m_c); however, present experimental bound is not sufficiently strong to use this result to put a meaningful bound on m_c . Calculations of the branching ratios for the decay processes $K_{S,L}^0 \rightarrow \pi^0 e \bar{e}$ and $K_{S,L}^0 \rightarrow \pi^0 \nu \bar{\nu}$ are also performed. The results can obviously be extended to $K^\pm \rightarrow \pi^\pm \mu \bar{\mu}$ and $K^0 \rightarrow \pi^0 \mu \bar{\mu}$.

II. THE MODEL

(II. 1) The Model for Strong Interactions

The model for strong interactions is a natural extension of the σ -model⁹ and the SU(3) version of the σ -model¹⁰ to incorporate the chiral SU(4) \times SU(4) symmetry. It consists of a set of 16 pseudoscalar fields and 16 scalar fields which are assigned to $(4, \bar{4}) + (\bar{4}, 4)$ representation of the chiral SU(4) \times SU(4). The scalar and the pseudoscalar fields may be written as 4×4 hermitian matrices Σ and Π respectively. These are given below:

$$\Pi = \begin{bmatrix} \eta_c & X_c^0 & \pi_c^+ & K_c^+ \\ \bar{X}_c^0 & \frac{\pi_0}{\sqrt{2}} + \frac{\eta_8}{\sqrt{6}} + \frac{\eta_0}{\sqrt{3}} & \pi^+ & K^+ \\ \pi_0^- & \pi^- & -\frac{\pi_0}{\sqrt{2}} + \frac{\eta_8}{\sqrt{6}} + \frac{\eta_0}{\sqrt{3}} & K_0 \\ K_c^- & K^- & \bar{K}_0 & -\frac{2\eta_8}{\sqrt{6}} + \frac{\eta_0}{\sqrt{3}} \end{bmatrix}$$

and,

$$\Sigma = \begin{bmatrix} \xi_c & Y_c^0 & \phi_c^+ & \kappa_c^+ \\ \bar{Y}_c^0 & \frac{\phi_0}{\sqrt{2}} + \frac{\xi_8}{\sqrt{6}} + \frac{\eta_0}{\sqrt{3}} & \phi^+ & \kappa^+ \\ \phi_c^- & \phi^- & -\frac{\phi_0}{\sqrt{2}} + \frac{\xi_8}{\sqrt{6}} + \frac{\xi_0}{\sqrt{3}} & \kappa_0 \\ \bar{\kappa}_c^- & \kappa^- & \bar{\kappa}_0^- & -\frac{2\xi_8}{\sqrt{6}} + \frac{\xi_0}{\sqrt{3}} \end{bmatrix} \quad . (2.1)$$

In terms of the quark language, the basis chosen for the four dimensional representation is (p', p, n, λ) . In addition to the SU(3) nonet, there are 7 scalar and pseudoscalar particles whose quark contents are:

$$\begin{aligned} \xi_c, \eta_c &\sim \bar{p}' p' & X_c^0, Y_c^0 &\sim \bar{p} p' \\ \pi_c^+, \phi_c^+ &\sim \bar{n} p' & K_c^+, \kappa_c^+ &\sim \bar{\lambda} p' \text{ etc.} \end{aligned}$$

We assign $M = \Sigma + i\Pi$ and $M^\dagger = \Sigma - i\Pi$ to $(4, \bar{4})$ and $(\bar{4}, 4)$ representation of the chiral $SU(4) \times SU(4)$ group; i.e., the fields M and M^\dagger transform under the chiral $SU(4) \times SU(4)$ transformation as

$$\begin{aligned} [Q_i^+, M_{\alpha\beta}] &= -\frac{1}{2} (\lambda_i)_{\alpha\gamma} M_{\gamma\beta} \\ [Q_i^+, M_{\alpha\beta}^\dagger] &= \frac{1}{2} M_{\alpha\gamma}^\dagger (\lambda_i)_{\gamma\beta} \\ [Q_i^-, M_{\alpha\beta}] &= \frac{1}{2} M_{\alpha\gamma} (\lambda_i)_{\gamma\beta} \\ [Q_i^-, M_{\alpha\beta}^\dagger] &= -\frac{1}{2} (\lambda_i)_{\alpha\gamma} M_{\gamma\beta}^\dagger \end{aligned} \quad (2.2)$$

where, $(\frac{1}{2} \lambda_i)$ are 4×4 matrix representation of SU(4) and Q_i^\pm are the

generators of the chiral $SU(4) \times SU(4)$.

We write down the most general Lagrangian which is invariant under the chiral $SU(4) \times SU(4)$ transformations and has dimensions four or less [to ensure renormalizability after it is coupled to the Weinberg-Salam model of the weak and electromagnetic interactions.]

$$\begin{aligned} \mathcal{L}_0 &= \frac{1}{2} \text{tr} (\partial_\mu M^\dagger \partial^\mu M) - V(M, M^\dagger) \\ V(M, M^\dagger) &\equiv \mu_0^2 \text{tr} (M^\dagger M) \\ &+ \mu_0^2 \{ \alpha \text{tr} (M^\dagger M)^2 + \beta [\text{tr}(M^\dagger M)]^2 + \gamma [\det M + \det M^\dagger] \}. \end{aligned} \quad (2.3)$$

The coefficients α, β, γ are arbitrary to the extent that they produce the potential $V(M, M^\dagger)$ such that $V \rightarrow \infty$ as any linear combination of fields $\rightarrow \infty$.

We shall not discuss this model in detail. We shall only note that like the σ -model and its $SU(3)$ version,^{8,9} if we let μ_0^2 be negative, spontaneous symmetry breakdown will occur, M will develop a vacuum expectation value (which may be chosen to be real). Then \mathcal{L}_0 will describe a theory¹⁶ containing 15 massless pseudoscalar fields and 16 scalar and one pseudoscalar ($\frac{1}{2} \text{tr} \Pi$) massive fields. Furthermore, the tree diagrams with external pseudoscalar lines will, in the limit⁸ $-\mu_0^2 \rightarrow \infty$ reproduce the results of the current algebra (extended to the $SU(4) \times SU(4)$ group) with PCAC, and thus will contain the low energy phenomenology. [As far as the model of the strong interactions is

concerned, we may add to \mathcal{L}_0 a term of the form $\text{tr } A(M + M^\dagger)$ so as to break the SU(4) symmetry and make the charmed particles massive. However, as we shall see, to maintain the gauge invariance with respect to the weak gauge group such a term cannot be added arbitrarily, but must be produced through the Higgs' scalar couplings.] Further, in the spirit of a phenomenological model of strong interactions, such tree diagrams will be assumed to represent the effect of strong interactions to all orders.

(II. 2) Extention of the Model to Incorporate Weak and Electromagnetic Interactions

In order to incorporate the weak and the electromagnetic interactions into the Lagrangian \mathcal{L}_0 of Eq. (2.3), in a renormalizable way, we assign to M and M, transformation properties under the weak gauge group SU(2) \times U(1) of the Weinberg-Salam model.⁶ This model is so well known that we shall not describe it in detail, except to introduce our notations. The basic Lagrangian^{1,2} consists of gauge fields B_μ^α ($\alpha = 0, 1, 2, 3$) and a complex doublet of Higgs' scalars $\Phi = \begin{pmatrix} s^+ \\ s_0 \end{pmatrix}$ which belong to the representation of the local SU(2) \times U(1) gauge group. This Lagrangian is described by

$$\begin{aligned} \mathcal{L}_1 = & -\frac{1}{4} F_{\mu\nu}^\alpha F^{\mu\nu}_\alpha \\ & + \frac{1}{2} D_\mu \Phi^\dagger D^\mu \Phi - m_0^2 \Phi^\dagger \Phi + \lambda (\Phi^\dagger \Phi)^2 \end{aligned} \quad (2.4)$$

where

$$F_{\mu\nu}^{\alpha} = \partial_{\mu} B_{\nu}^{\alpha} - \partial_{\nu} B_{\mu}^{\alpha} + \epsilon^{\alpha\beta\gamma} B_{\mu}^{\beta} B_{\nu}^{\gamma}$$

$$(\alpha, \beta, \gamma \neq 0)$$

$$F_{\mu\nu}^0 = \partial_{\mu} B_{\nu}^0 - \partial_{\nu} B_{\mu}^0$$

$$D_{\mu} \Phi = \partial_{\mu} \Phi - \frac{i}{2} g \tau^{\alpha} B_{\mu}^{\alpha} \Phi - \frac{i}{2} g' B_{\mu}^0 \Phi$$

$$\lambda > 0.$$

When m_0^2 is negative, spontaneous symmetry breaking occurs and Φ develops a vacuum expectation value which may be chosen to be

$$\langle \Phi \rangle_0 = \begin{pmatrix} 0 \\ v/\sqrt{2} \end{pmatrix}$$

where v is real. Then \mathcal{L}_1 describes a theory of a charged doublet of massive vector bosons (W^{\pm}) a massive neutral vector boson (Z) and a massless vector boson (A) which is identified with the photon. The masses of W^{\pm} and Z are given by,^{6, 17}

$$M_W = \frac{1}{2} g v$$

$$M_Z = \frac{1}{2} \sqrt{g^2 + g'^2} v \equiv \frac{1}{2} G v .$$

We define the fields,

$$W_{\mu}^{\pm} \equiv \frac{B_{1\mu} \mp i B_{2\mu}}{\sqrt{2}}$$

$$\begin{aligned}
Z_{\mu} &\equiv \frac{g B_{3\mu} - g' B_{0\mu}}{\sqrt{g^2 + g'^2}} \\
A_{\mu} &\equiv \frac{g' B_{3\mu} + g B_{0\mu}}{\sqrt{g^2 + g'^2}} .
\end{aligned} \tag{2.6}$$

We shall work in some special case of the R_{ξ} gauges¹⁸ for which the gauge term is given by

$$\begin{aligned}
\mathcal{L}_{\text{gauge}} &\equiv \frac{1}{2} \sum_{\alpha} F_{\alpha}^2(B, \Phi) \\
&= \xi \left| \partial^{\mu} W_{\mu}^{+} + \frac{i g v}{2 \xi} s^{+} \right|^2 + \frac{1}{2} \eta \left| \partial_{\mu} Z^{\mu} - \frac{1}{2} \frac{G v}{\eta} \chi \right|^2 \\
&\quad + \frac{1}{2\alpha} (\partial^{\mu} A_{\mu})^2
\end{aligned} \tag{2.7}$$

where we define the fields s^{\pm} and χ by:

$$\Phi = \begin{pmatrix} s^{+} \\ v + \psi_0 + i\chi \\ \sqrt{2} \end{pmatrix}; \quad s^{-} = (s^{+})^{\dagger} . \tag{2.8}$$

In these gauges the unphysical scalars s^{\pm} and χ are decoupled from W^{\pm} and Z .

To assign the transformation properties to M and M^{\dagger} under the weak gauge group, we refer to the quark version of the Weinberg-Salam model for hadrons.^{2,6} There the quark quartets $(p', p, n, \lambda)_L$ and $(p', p, n, \lambda)_R$ form reducible representations of the gauge group $SU(2) \times U(1)$. They transform under a local $SU(2) \times U(1)$ gauge

transformation described by parameters $\theta_\alpha(x)$ as

$$\begin{bmatrix} p'(x) \\ p(x) \\ n(x) \\ \lambda(x) \end{bmatrix}_{L,R} \xrightarrow{e^{-i T_{L,R}^\alpha \theta_\alpha(x)}} \begin{bmatrix} p'(x) \\ p(x) \\ n(x) \\ \lambda(x) \end{bmatrix}_{L,R} \quad (2.9)$$

where T_L^α and T_R^α form reducible representations of $SU(2) \times U(1)$ and are given by

$$\begin{aligned} T_L^\alpha &= T^\alpha \quad (\alpha = 1, 2, 3), \quad T_L^0 \equiv Y_L \\ T_R^\alpha &= 0 \quad (\alpha = 1, 2, 3), \quad T_R^0 \equiv Y_R \\ T_+ &\equiv \frac{T_1 + iT_2}{\sqrt{2}} = (T_-)^\dagger \\ &= \frac{1}{\sqrt{2}} \begin{bmatrix} 0 & 0 & -\sin \theta & \cos \theta \\ 0 & 0 & \cos \theta & \sin \theta \\ 0 & 0 & 0 & 0 \\ 0 & 0 & 0 & 0 \end{bmatrix} \\ T_3 &= \text{Diag} \left(\frac{1}{2}, \frac{1}{2}, -\frac{1}{2}, -\frac{1}{2} \right) \\ Y_L &= \frac{1}{3} \mathbb{1} \\ Y_R &= \text{Diag} \left(\frac{4}{3}, \frac{4}{3}, -\frac{2}{3}, -\frac{2}{3} \right). \end{aligned} \quad (2.10)$$

The generator of the electromagnetic gauge transformation, Q , is given by

$$Q = T_3 + \frac{1}{2}(Y_L + Y_R) \quad (2.11)$$

We define the transformation properties of M and M^\dagger under an $SU(2) \times U(1)$ local gauge transformation as:

$$\begin{aligned} M(x) &\rightarrow e^{-iT_L^\alpha \theta_\alpha(x)} M(x) e^{iT_R^\alpha \theta_\alpha(x)} \\ M^\dagger(x) &\rightarrow e^{-iT_R^\alpha \theta_\alpha(x)} M^\dagger(x) e^{iT_L^\alpha \theta_\alpha(x)} \end{aligned} \quad (2.12)$$

so that, denoting quarks by q_α ($\alpha = 1, 2, 3, 4$); $M_{\alpha\beta}$ transforms as $q_{\alpha L} \bar{q}_{\beta R}$ and $M_{\alpha\beta}^\dagger$ as $q_{\alpha R} \bar{q}_{\beta L}$.

The gauge-covariant derivative $D_\mu M$ is given by,

$$D_\mu M \equiv (\partial_\mu M - ig T^\alpha B_\mu^\alpha M - \frac{i}{2} g' Y_L B_\mu^0 M + \frac{i}{2} g' M Y_R B_\mu^0). \quad (2.13)$$

Then the Lagrangian which incorporates \mathcal{L}_0 of Eq. (2.3) and is gauge invariant under the gauge transformations of the weak gauge group is:¹⁷

$$\begin{aligned} \mathcal{L} = & \frac{1}{2} \text{tr} (D_\mu M^\dagger D^\mu M) - \mu_0^2 M^\dagger M \\ & - \mu_0^2 \left[\alpha \text{tr} (M^\dagger M)^2 + \beta (\text{tr} M^\dagger M)^2 + \gamma (\det M + \det M^\dagger) \right] \\ & + \mathcal{L}_1 + \mathcal{L}_{M\Phi} \end{aligned} \quad (2.14)$$

where $\mathcal{L}_{M\Phi}$ is a gauge-invariant interaction (up to quartic terms) of M and Φ fields.

$\mathcal{L}_{M\Phi}$ can be chosen such that it can produce the $SU(4)$ and $SU(3)$ symmetry breaking. For simplicity, we shall first consider the $SU(4)$ symmetry breaking. To construct gauge invariant couplings, it is

convenient to write M with the basis (p', λ_c, p, n_c) ; [where

$$\lambda_c \equiv \lambda \cos \theta - n \sin \theta$$

$$n_c \equiv n \cos \theta + \lambda \sin \theta \quad (\theta \equiv \text{the Cabbibo angle}).]$$

Let us call it M' . Then the coupling

$$\mathcal{L}_{M\Phi} = \sqrt{2} \zeta \eta^\dagger (M')^\dagger \tilde{\Phi} + \text{h. c.}$$

where,

$$\eta = \begin{bmatrix} 1 \\ 0 \\ 0 \\ 0 \end{bmatrix} \quad \tilde{\Phi} \equiv \begin{bmatrix} s^+ \\ 0 \\ -s^- \\ 0 \\ 0 \end{bmatrix} \quad (2.15)$$

is gauge invariant. Explicitly,¹⁹

$$\begin{aligned} \mathcal{L}_{M\Phi} = & 2 \zeta \left[\xi_c (v + \psi_0) - \eta_c \chi \right] \\ & + \left\{ \sqrt{2} \zeta s^- \left[(\kappa_c^+ \cos \theta - \phi_c^- \sin \theta) - i (K_c^- \cos \theta - \pi_c^- \sin \theta) \right] + \text{h. c.} \right\}. \end{aligned} \quad (2.16)$$

If we let μ_0^2 be negative, M will develop vacuum expectation value which may be chosen to be real and diagonal. In this case, with the SU(4) symmetry breaking,¹⁶

$$\langle M \rangle = \begin{bmatrix} f' & & & \\ & f & & \\ & & f & \\ & & & f \end{bmatrix} . \quad (2.17)$$

The vacuum expectation values f' and f satisfy the constraints which follow from the requirement that there should not be terms linear in fields (here ξ_c and ξ_0). These can be obtained from Eqs. (2.14), (2.16) and (2.17). They are:

$$-\mu_0^2 f' - \mu_0^2 \{4\alpha f'^3 + 4\beta(f'^2 + 3f^2)f' + 2\gamma f^3\} + 2v\xi = 0,$$

i. e. ,

$$4\alpha f'^2 + 4\beta(f'^2 + 3f^2) + 2\gamma \frac{f^3}{f'} + 1 = \frac{2v\xi}{f' \mu_0^2} \quad (2.18)$$

and

$$4\alpha f'^2 + 4\beta(f'^2 + 3f^2) + 2\gamma f f' + 1 = 0 . \quad (2.19)$$

From Eqs. (2.18) and (2.19), it is clear that as $\mu_0^2 \rightarrow -\infty$, $f' \rightarrow f$.

Let us define

$$f' \equiv f(1 + \epsilon) .$$

Then, to the first order in ϵ , Eqs. (2.18) and (2.19) yield:

$$\epsilon = \frac{v\xi}{2\mu_0^2 f^3 (2\alpha - \gamma)} . \quad (2.20)$$

The mass terms in the Lagrangian of Eq. (2.14) can be computed and simplified using Eqs. (2.18), (2.19) and (2.20). We shall only quote the results. We obtain, to the first order in ϵ :

$$\begin{aligned} \text{(i)} \quad m_{X_0}^2 &= m_{K_c}^2 = m_{\pi_c}^2 \equiv m_c^2 \\ &= 2\mu_0^2 f^2 \epsilon (2\alpha - \gamma) \end{aligned}$$

$$= \frac{v\zeta}{f} \quad \text{using Eq. (2.20)} \quad (2.21)$$

Thus,

$$\zeta = \frac{m_c^2 f}{v} = \frac{g f m_c^2}{2M} \quad (2.22)$$

$$(ii) \quad m_K^2 = m_\pi^2 = m_{\eta_8}^2 = 0 \quad (2.23)$$

$$(iii) \quad m_{\xi_8}^2 = m_\kappa^2 = m_\phi^2 \equiv \mu^2 \\ = 4\mu_0^2 f^2 (2\alpha - \gamma) - 4\mu_0^2 \gamma f^2 \epsilon \quad (2.24)$$

$$(iv) \quad m_{Y_0}^2 = m_{\kappa_c}^2 = m_{\phi_c}^2 \equiv \mu_c^2 \\ = \mu^2 + 3m_c^2 \quad (2.25)$$

(v) The mass terms containing the diagonal pseudoscalar fields

are:

$$- \frac{1}{2} \left\{ -8\mu_0^2 \gamma f^2 \left(\frac{\eta_c + \sqrt{3}\eta_0}{2} \right)^2 - 6\mu_0^2 \gamma f \epsilon \eta_0^2 \right. \\ \left. + 2(m_c^2 + \mu_0^2 \gamma f \epsilon) \eta_c^2 \right\} . \quad (2.26)$$

Thus there is mixing between η_c and η_0 . The SU(4) singlet $\frac{1}{2} \text{tr} \Pi \equiv \eta'_0 = \frac{1}{2}(\eta_c + \sqrt{3}\eta_0)$ and $\eta'_c \equiv \frac{1}{2}(\sqrt{3}\eta_c - \eta_0)$ are approximate eigenstates of the (mass)² operator [to zeroth order in ϵ] with eigenvalues

$$m_0'^2 \sim 0 \quad (-\mu_0^2) \quad \text{and} \quad m_c'^2 = \frac{3}{2} m_c^2 \quad (2.26a)$$

respectively.

(vi) There will be similar mixing between ξ_c and ξ_0 . To the zeroth order in ϵ ,

$$\xi_1 \equiv \frac{1}{2} \text{tr } \tilde{\Sigma} = \frac{1}{2} (\xi_c + \sqrt{3} \xi_0)$$

and,

$$\xi_2 = \frac{1}{2} (\sqrt{3} \xi_c - \xi_0)$$

are the eigenstates of the (mass)² operator with the eigenvalues:

$$\mu_1^2 = -2\mu_0^2; \quad \mu_2^2 = \mu^2 \quad (2.26b)$$

respectively.

Next consider the SU(3) mass splitting. We can introduce an SU(3) splitting by the addition of terms to $\mathcal{L}_{M\Phi}$ which are similar to that of Eq. (2.15) with suitable choices of η 's and Φ 's so that the isospin and hypercharge are still exactly conserved by strong interactions. For convenience let us consider such an SU(3) symmetry breaking that will still keep pions massless. This can be achieved by the addition of the following type to $\mathcal{L}_{M\Phi}$:

$$(a_1 \eta_1^\dagger + a_2 \eta_2^\dagger) (M')^\dagger \Phi_1 + (b_1 \eta_1^\dagger + b_2 \eta_2^\dagger) (M')^\dagger \Phi_2 + \text{h. c.} \quad (2.27)$$

where

$$\eta_1 = \begin{pmatrix} 0 \\ 1 \\ 0 \\ 0 \end{pmatrix} \quad \eta_2 = \begin{pmatrix} 0 \\ 0 \\ 0 \\ 1 \end{pmatrix}$$

$$\Phi_1 = \begin{pmatrix} s^\dagger \\ 0 \\ s \\ 0 \\ 0 \\ 0 \end{pmatrix} \quad \Phi_2 = \begin{pmatrix} 0 \\ 0 \\ s^\dagger \\ s \\ 0 \\ s \end{pmatrix} .$$

Given the Cabbibo angle, the constants a_1, a_2, b_1, b_2 must be so constrained that they produce:

(i) no $K_0 \chi$ and $\bar{K}_0 \chi$ couplings, since there are no $K_0 Z, \bar{K}_0 Z$ couplings.

(ii) no $\pi^+ s^-$ and $\pi^- s^+$ couplings since we want π^\pm to be massless.

[These requirements follow from the gauge invariance of the tree diagrams containing Z and W^\pm internal lines. These conditions may be rephrased as there are to be no linear terms in $\kappa_0, \bar{\kappa}_0$ and $(-\frac{\phi_0}{\sqrt{2}} + \frac{\xi_8}{\sqrt{6}} + \frac{\xi_0}{\sqrt{3}})$. This is all very similar to the Higgs couplings in the corresponding quark model.]

These conditions leave only one free parameter which may be chosen to be m_K^2 .

The details of these constraints are unimportant to us. We shall only need the mass splitting. For this purpose we note that now $\langle M_0 \rangle$ takes the form:

$$\langle M \rangle_0 = \begin{bmatrix} f(1 + \epsilon) & & & \\ & f & & \\ & & f & \\ & & & f(1 + \delta) \end{bmatrix} . \quad (2.28)$$

With this $\langle M \rangle_0$ we may carry out the steps outlined in Eqs. (2.17) - (2.26). The relevant results are:

$$(i) \quad m_\pi^2 = 0, \quad m_K^2 = 2 \mu_0^2 f^2 (2\alpha - \gamma) \delta. \quad (2.29)$$

(ii) The mass terms containing the diagonal pseudoscalar fields to the first order in δ and ϵ now, are:

$$\begin{aligned} & -\frac{1}{2} \left\{ -8 \mu_0^2 \gamma f^2 \left(\frac{\eta_c + \sqrt{3} \eta_0}{2} \right)^2 - 6 \mu_0^2 \gamma f^2 \epsilon \eta_0^2 + 2(m_c^2 + \mu_0^2 \gamma f^2 \epsilon) \eta_c \right. \\ & \left. - 2 \mu_0^2 \gamma f^2 \delta \left(\eta_c + \frac{2\eta_0}{\sqrt{3}} + \frac{2\eta_8}{\sqrt{6}} \right)^2 + 2(m_K^2 + \mu_0^2 \gamma f^2 \delta) \left(-\frac{2\eta_8}{\sqrt{6}} + \frac{\eta_0}{\sqrt{3}} \right)^2 \right\}. \end{aligned} \quad (2.30)$$

Since at $\delta = 0$, η_8 was an exact eigenstate of $(\text{mass})^2$; in the approximation $\delta/\epsilon \ll 1$, the corresponding eigenstate of $(\text{mass})^2$ in Eq. (2.30) will be of the form $\eta' = \eta_8 + 0(\delta)(x\eta_c + y\eta_0)$. Therefore, the $(\text{mass})^2$ of η'_8 to the first order in δ can be read from Eq. (2.30) as the coefficient of $-\frac{1}{2} \eta_8^2$. Hence

$$m_8^2 = \frac{4}{3} m_K^2 \quad (2.31)$$

which, incidently, is the GMO mass formula with $m_\pi^2 = 0$.

(iii) The $(\text{mass})^2$ of some of the charmed pseudoscalars and of scalars may also be changed by an amount of $0(m_K^2)$.

In some calculations, [the calculations of the amplitudes for $K^+ \rightarrow \pi^+ e \bar{e}$ and $K^0 \rightarrow \pi^0 e \bar{e}$] it is not possible to let $m_\pi^2 = 0$ because of a $(\log m_\pi^2)$ dependence of the amplitude. There we shall need to keep pions massive. The pion mass can be generated similar to the generation of kaon mass. The terms that one needs to add to $\mathcal{L}_{M\Phi}$ for this purpose

are similar to those that generate the (nonzero) mass for the p quark, $m_p (= m_n)$.

Finally we note that the leptons are coupled to the gauge fields and the Higgs fields in the usual way.⁶

The Feynman rules for the leptonic and the mesonic weak and electromagnetic couplings are given in the Appendix A. We shall note some of relevant characteristics which will be useful later.

(i) Couplings of the Z with the mesons are always $\Delta S = \Delta Q = 0$.

(ii) The only couplings which have $\Delta S = \Delta Q = \pm 1$ involve a singlet W^\pm or a single s^\pm . Couplings with two W^\pm are necessarily $\Delta S = \Delta Q = 0$.

(iii) There is no scalar meson - Z nor a scalar meson - χ two point vertex. Only the diagonal pseudoscalar mesons couple to Z in a two-point vertex

III. PHENOMENOLOGICAL APPROXIMATION

We shall, briefly, explain the point of view taken while performing the calculations to the leading order in the weak and the electromagnetic interactions and to all orders in the strong interactions.

It is well known that the tree graphs containing only the external pseudoscalar lines (and no weak vertices) in such models with the chiral symmetry of strong interactions will reproduce the results of the corresponding current algebra with PCAC. Thus the strong interaction Lagrangian in Eq. (2.3) is phenomenological in that the tree approximation

of this Lagrangian produces the results to all orders in strong interactions (of some underlying field theory of strong interactions).

It is essential to make a similar assumption regarding the vertices involving the gauge bosons. Here, we take the point of view similar to the one used in calculating electromagnetic corrections (like $\pi^+ \rightarrow \pi^0$ mass difference) using a phenomenological Lagrangian.²⁰ For example, we may consider the $\pi_c^+ \pi^0 W_\mu^-$ vertex. See Fig. 1. It is assumed that the $\pi_c^+ \pi^0 W_\mu^-$ vertex is described by the sum of the diagrams 1(a) and 1(b). [In a renormalizable gauge, there will be a $\pi_c^+ \pi^0 s^-$ vertex as in 1(c)] to all orders in strong interactions and to the lowest order [here to $O(g)$] in weak interactions. Thus such couplings of vector bosons to mesons (pseudoscalar and scalar) are assumed to arise only via :
 (i) possible direct coupling and (ii) their mixing with the mesons. And even though one can draw Feynman diagrams for this vertex with higher loops and of $O(g)$, e. g., like the one shown in Fig. 2, they are to be discarded.

For the sake of clarity, let us discuss some examples which will, later, be useful. There are two kinds of diagrams. These are shown in Fig. 3(a) and 3(b).

The $K_0 Z$ coupling [which is zero to $O(g)$] arises in several possible ways. Among them are (i) $K_0 \rightarrow W^+ W^- \rightarrow Z$ diagram and (ii) through the mixing of Z with the pseudoscalar mesons. These are shown in Figs. 3(c) and 3(d).

Then with the above rules, we may draw the shaded $K_0 \rightarrow W^+ W^-$ vertex which is of $O(g^2)$. There is no direct $K_0 \rightarrow W^+ W^-$ vertex. The diagrams that will contribute to this vertex to $O(g^2)$ are shown in Fig. 4.

The $K_0 \pi_0$ self-energy diagrams in Fig. 3(d) [which are of $O(g^2)$ in the leading order] are to be constructed by drawing all possible tree diagrams for the process $K_0 \rightarrow \pi_0 W^+ W^-$ and then closing the W-loop. Thus to $O(g^2)$ in the weak interactions and to all orders in the strong interactions, the $K_0 \pi_0$ self-energy is described by the diagrams in Fig. 5 [and the diagrams with the unphysical scalars in a renormalizable gauge.]

We shall use the same criteria while drawing the diagrams for the other decay processes and the $K_0 \rightarrow \bar{K}_0$ transition amplitude. We shall not discuss this in detail in these cases.

In the subsequent sections, we shall discuss in detail the calculation of the $K_L - K_S$ mass difference and several decay amplitudes of the K mesons. These are (i) $K_{L,S} \rightarrow \mu \bar{\mu}$; (ii) $K^+ \rightarrow \pi^+ \nu \bar{\nu}$; (iii) $K^0 \rightarrow \pi^0 \nu \bar{\nu}$; (iv) $K^+ \rightarrow \pi^+ e \bar{e}$; (v) $K_{L,S} \rightarrow \pi^0 e \bar{e}$.

We shall always use the Landau gauge for the W-propagator. As a result, any diagram containing a meson-W vertex (2-point vertex) vanishes identically in this gauge. Therefore, we shall not draw those diagrams in the following discussion.

IV. $\underline{K_{L,S} \rightarrow \mu \bar{\mu}}$

The diagrams that contribute to this process are of two kinds:

(i) The one particle reducible diagrams; (ii) The one particle irreducible diagrams. We shall first consider the one particle reducible diagrams. These consist of (i) $K_0 \rightarrow Z, \chi \rightarrow \mu\bar{\mu}$; (ii) $K_0 \rightarrow \gamma \rightarrow \mu\bar{\mu}$; (iii) $K_0 \rightarrow \psi_0 \rightarrow \mu\bar{\mu}$, (ψ_0 is the Higgs scalar). The $K_0 \rightarrow \gamma \rightarrow \mu\bar{\mu}$ diagram is zero because the $K_0\gamma$ vertex is proportional to p_μ , the momentum of the photon and when it is contracted with the electromagnetic muon current (on mass shell) the result is zero.

(IV-A) Z-Reducible Diagrams

Let us first consider the $K_0 \rightarrow Z, \chi \rightarrow \mu\bar{\mu}$ diagrams. If we denote the truncated $K_0 Z$ Green's function by $E_\mu(p) \equiv p_\mu E(p)$ and the truncated K, χ Green's function by $F(p)$ then the Ward-Takahashi identity, in the one loop approximation [see Appendix B] states that

$$p_\mu E^\mu(p) = -i M_Z F(p) . \quad (\text{B. 28})$$

Putting in the Z and the χ propagators, the above statement can be easily shown to imply that the sum of the diagrams $K_0 \rightarrow Z \rightarrow \mu\bar{\mu}$ and $K_0 \rightarrow \chi \rightarrow \mu\bar{\mu}$ is independent of the gauge parameter η [see Eq. (2.7)] in the one-loop approximation. [This is not surprising since these are the only diagrams that depend on η in the one-loop approximation.] We shall use this fact conveniently.

Let us choose the Landau gauge for the Z -propagator ($\eta \rightarrow \infty$). Then $K_0 \rightarrow Z \rightarrow \mu\bar{\mu}$ diagrams vanish since the $K_0 Z_\mu$ vertex is proportional to p_μ , the Z -momentum. Hence, we need to compute only the $K_0 \chi$ vertex. The diagrams that contribute to the $K_0 \chi$ vertex are shown in

Fig 6. We shall put $m_\pi^2 = 0$.

The diagram in Fig. 6(a) is finite for each of the intermediate states. When the intermediate states are scalars ($\kappa_c^+, \phi_c^-, \kappa_c^+$), the amplitudes are proportional to $\frac{1}{\mu^2}$ and therefore may be neglected as $\mu^2 \rightarrow \infty$. We shall compute the results to the leading order. The diagrams in Fig. 6(a) with the intermediate states K_c^+, π_c^- are proportional to m_c^2 , while with the intermediate state K^+ , it is proportional to m_K^2 and therefore we shall neglect the diagram with the intermediate state K^+ .

The contributions of the diagrams with the intermediate states K_c^+ and π_c^- are equal and their sum is given by

$$\mathcal{M}(6a.) = -(\sin \theta \cos \theta) \frac{p_\mu p_\nu g^3 f m_c^2}{M(2\pi)^4} \int \frac{d^4 k D^{\mu\nu}(k)}{(k^2 - M^2)(k+p)^2 [(k+p)^2 - m_c^2]} \quad (4.1)$$

where

$$D^{\mu\nu}(k) = g^{\mu\nu} - \frac{k^\mu k^\nu}{k^2} .$$

Next, we shall compute the one particle reducible diagram (the pole diagrams) contribution to the $K_0 \chi$ vertex. We note that the one particle irreducible vertex $m(6a)$ is directly proportional to p^2 ($= m_K^2$ on the mass shell). To the leading order, the contribution of the pole diagrams can have a term independent of p^2 as well as a term proportional to p^2 . Since the χ -propagator in the Landau gauge ($\eta \rightarrow \infty$) is $\frac{1}{p^2}$, the constant term in the $K_0 \chi$ vertex will give rise to a term in the amplitude which is proportional to $\frac{1}{m_K}$. We shall show that

(i) there are no terms in the $[K_0 \rightarrow Z \rightarrow \mu\bar{\mu} + K_0 \rightarrow \chi \rightarrow \mu\bar{\mu}]$

amplitude which are proportional to $\frac{1}{m_K^2}$, and

(ii) the contribution of the pole diagrams to the $K_0\chi$ vertex cancels the IPI contribution to it, in the limit of exact SU(3).

In computing the pole diagrams, we shall find it convenient to insert the eigenstates of the (mass)² matrix. Since we have let $m_\pi^2 = 0$, π^0 does not couple to χ . Let $\eta_8', \eta_c', \eta_0'$ be the eigenstates of the (mass)² matrix, which are "mostly" η_8, η_c and η_0 . Let m_8', m_c', m_0' be their masses. The couplings of $\eta_8', \eta_c', \eta_0'$ to χ are proportional to their (mass)² respectively. Let these Feynman rules be $i m_8'^2 a_8', i m_c'^2 a_c', i m_0'^2 a_0'$ respectively. Denote by Σ_8', Σ_c' and Σ_0' the self-energy diagrams for the $K_0 \rightarrow \eta_8', K_0 \rightarrow \eta_c'$ and $K_0 \rightarrow \eta_0'$ respectively. Then the pole diagram contribution to $K_0\chi$ vertex at $p^2 = m_K^2$ is

$$\begin{aligned} (K_0\chi)_{\text{pole}} = & \frac{i}{m_K^2 - m_8'^2} \cdot i m_8'^2 a_8' \cdot \Sigma_8' + \frac{i}{m_K^2 - m_c'^2} \cdot i m_c'^2 a_c' \cdot \Sigma_c' \\ & + \frac{i}{m_K^2 - m_0'^2} \cdot i m_0'^2 a_0' \cdot \Sigma_0'. \end{aligned} \quad (4.2)$$

From Eq. (2.31) we know that,

$$\frac{m_8'^2}{m_K^2 - m_8'^2} = -4 + O(\delta, \epsilon).$$

$$\text{Further, } m_c'^2 \approx \frac{3}{2} m_c^2 \gg m_K^2$$

$$m_0'^2 \sim 0 (-\mu_0^2) \gg m_K^2.$$

Hence,

$$\frac{m_c'^2}{m_K^2 - m_c'^2} = -1 + 0\left(\frac{m_K^2}{m_c^2}\right)$$

and,

$$\frac{m_0'^2}{m_K^2 - m_0'^2} = -1 + 0(\delta).$$

Using the above equations in Eq. (4.2), we obtain

$$(K_0\chi)_{\text{pole}} = 4\Sigma_8' a_8' + \Sigma_c' a_c' + \Sigma_0' a_0' + 0\left(\frac{m_K^2}{m_c^2}\right). \quad (4.3)$$

To compute $(K_0\chi)_{\text{pole}}$ in the exact SU(3) limit, we need to compute Σ_8' , Σ_c' and Σ_0' only to the zeroth order in the SU(3) symmetry breaking. In the zeroth order in the SU(3) symmetry breaking, $\eta_c' = \eta_8$. We shall not need to know the other two eigenstates η_c', η_0' exactly. We know that, at $\delta = 0$ (exact SU(3) symmetry)

$$\eta_c' = \frac{\sqrt{3}\eta_c - \eta_0}{2} + a\epsilon \left(\frac{\eta_c + \sqrt{3}\eta_0}{2} \right)$$

$$\eta_0' = \frac{\eta_c + \sqrt{3}\eta_0}{2} + b\epsilon \left(\frac{\sqrt{3}\eta_c - \eta_0}{2} \right)$$

where a and b are number we shall not need to know.

From the Appendix A, we note that the meson-Z two-point couplings are described by,

$$-\frac{Gf}{2} \partial_\mu \left[(1 + \epsilon)\eta_c - \frac{\eta_0}{\sqrt{3}} + \frac{2}{\sqrt{6}}\eta_8 + \sqrt{2}\pi_0 \right] Z^\mu$$

$$= - \frac{Gf}{\sqrt{3}} \partial_{\mu} \left[\eta'_c + c \epsilon \eta'_0 + \frac{1}{\sqrt{2}} \eta_8 + \frac{\sqrt{3}}{\sqrt{2}} \pi_0 \right] Z^{\mu} , \quad (4.4)$$

where c depends on a and b .

Gauge invariance requires that the meson- χ couplings are described by

$$- \frac{Gf}{\sqrt{3}M_Z} \left[m_c'^2 \eta'_c + c \epsilon m_0'^2 \eta'_0 + \frac{1}{\sqrt{2}} m_8^2 \eta_8 \right] \chi .$$

Therefore,

$$a_8 = - \frac{Gf}{\sqrt{6} M_Z} = - \frac{gf}{\sqrt{6} M} , \quad a_c' = \frac{gf}{\sqrt{3} M}$$

$$a_0' = c \epsilon \cdot \left(\frac{-gf}{\sqrt{3} M} \right) . \quad (4.5)$$

Since $a_0' = 0(\epsilon)$, only those terms in Σ_0' which are of $0(\mu^2)$ will survive in $\Sigma_0' a_0'$ as $\mu^2 \rightarrow \infty$. An inspection of the diagrams in Fig. 6 shows that there are no terms of $0(\mu^2)$ which are proportional to p^2 , while there are terms of $0(\mu^2)$ which are constant. However, as we shall see, we shall be able to avoid computing these.

Substituting the values of a_8' , a_0' and a_c' from Eq. (4.5) in Eq. (4.3) we obtain that in the exact SU(3) limit,

$$(K_0 \chi)_{\text{pole}} = \frac{-gf}{2M} \left[\frac{8}{\sqrt{6}} \Sigma_8 + \Sigma_c - \frac{1}{\sqrt{3}} \Sigma_0 + d \epsilon \Sigma_0' \right] \quad (4.6)$$

where d depends on a , b , and c ; and Σ_8 , Σ_c , Σ_0 have the obvious meaning.

First let us consider the terms proportional to p^2 in the right-hand side of the Eq. (4.6). The diagrams in Fig. 6(b) are proportional

to p^2 . The diagrams in Fig. 6(e) and 6(f) are independent of p^2 . The diagrams in Fig. 6(c) and 6(d) have terms proportional to p^2 which are of order $\left(p^2 \frac{m_c^2}{M^2}\right)$. However, these terms cancel in the linear combination of Σ 's appearing in Eq. (4.6). Thus the terms proportional to p^2 come entirely from the diagrams in Fig. 6(b). We quote the results:

$$\text{The contribution of 6(b) to } \Sigma_c = 2A(m_c) - 2A(\mu_c)$$

$$\text{The contribution of 6(b) to } -\frac{1}{\sqrt{3}}\Sigma_0 = \frac{2}{3}\left[A(m_c) + A(\mu_c) - 2A(\mu)\right]$$

$$\text{The contribution of 6(b) to } \frac{8}{\sqrt{6}}\Sigma_8 = \frac{4}{3}\left[-3A(0) + A(m_c) + A(\mu_c) + A(\mu)\right]$$

where,

$$A(\lambda) = -\frac{1}{2} \sin \theta \cos \theta \cdot \frac{g^2 p_\mu p_\nu}{(2\pi)^4} \int \frac{d^4 k D^{\mu\nu}(k)}{(k^2 - M^2) [(p+k)^2 - \lambda^2]} \quad (4.7)$$

Therefore, the total contribution of the diagrams in Fig. 6(b) to $(K_0 \chi)$ vertex is given by,

$$\begin{aligned} & -\frac{gf}{2M} \left\{ 4A(m_c) - 4A(0) \right\} \\ & = + (\sin \theta \cos \theta) \frac{p_\mu p_\nu g^3 f m_c^2}{(2\pi)^4 M} \int \frac{d^4 k D^{\mu\nu}(k)}{[k^2 - M^2] [(p+k)^2 - m_c^2] (p+k)^2} \end{aligned} \quad (4.8)$$

We note that for each of the intermediate states, the contribution to Σ is finite. However, each of these depends on the scalar mass through terms of the type $\ln\left(\frac{\mu^2}{M^2}\right)$, which would go to infinity if we let $\mu^2 \rightarrow \infty$. It is interesting to note that this μ -dependence cancels exactly in the

linear combination $\left(\frac{8}{\sqrt{6}} \Sigma_8 + \Sigma_c - \frac{1}{\sqrt{3}} \Sigma_0 \right)$.

We, further, note that the contribution to $(K_0 \chi)$ vertex in Eq. (4.8) cancels that of the IPI graphs in Eq. (4.1). Whatever its significance, we note that this cancellation is an exact one (i.e., to all orders in $\frac{m_c^2}{M^2}$) as $\mu^2 \rightarrow \infty$, $m_K^2 \rightarrow 0$.

Finally we shall show that there are no terms in the $K_0 \rightarrow \chi \rightarrow \mu\bar{\mu}$ amplitude which are proportional to $\frac{1}{m_K^2}$. As mentioned earlier, such terms arise out of the terms in the $(K_0 \chi)$ pole which are constant (i.e., independent of p^2) since the χ -propagator in the Landau gauge is $\frac{1}{p^2} = \frac{1}{m_K^2}$ on mass shell. However, it is much easier to verify this in the U-gauge ($\eta \rightarrow 0$). This is permissible since, as mentioned earlier, the sum of the amplitudes $(K_0 \rightarrow Z \rightarrow \mu\bar{\mu} + K_0 \rightarrow \chi \rightarrow \mu\bar{\mu})$ is independent of η . In the U-gauge, we need to consider the $K_0 Z$ vertex. In the $K_0 Z$ vertex, such terms proportional to $\frac{1}{m_K^2}$ would arise out of the diagrams shown in Fig. 7. To compute these we note that from Eq. (2.31),

$$\frac{3}{m_K^2} = - \frac{1}{m_K^2 - m_8^2} \tag{2.31}$$

and from Eq. (4.4),

$$(\pi_0 Z) \text{ vertex} = \sqrt{3} (\eta_8 Z) \text{ vertex}$$

and, therefore, the sum of the diagrams in Fig. 7 is proportional to $(\Sigma_{\pi_0} - \sqrt{3} \Sigma_8) \frac{1}{m_K^2}$. The diagrams that contribute to Σ are already shown in Fig. 6(b) - (f). It is easy to verify that at $p^2 = 0$, the

contribution of each of these diagrams to Σ_{π_0} is equal and opposite to the contribution to $-\sqrt{3} \Sigma_8$. Hence,

$$(\Sigma_{\pi_0} - \sqrt{3} \Sigma_8) = 0 \text{ at } p^2 = 0$$

showing that there are no terms proportional to $\frac{1}{m_K^2}$ in this part of the amplitude.

[For the sake of completeness, we comment on letting $m_\pi^2 \neq 0$.

It is evident that the additional terms that this will generate will be of $0\left(\frac{m_\pi^2}{m_K}\right)$ or of $0\left(\frac{m_\pi^2}{m_c}\right)$ lower than the ones that we have computed. They can be neglected provided they have a finite limit as $\mu^2 \rightarrow \infty$. This has been verified to be the case.]

Thus it is evident that the contribution of the Z and χ reducible diagrams to the $K_0 \rightarrow \mu\bar{\mu}$ amplitude is of $0\left(\frac{m_K^2}{M^2 \sin^2 \theta_W} \cdot G_F \alpha\right)$.

(IV-B) IPI Diagrams

Next we consider the one particle irreducible diagrams. These are shown in Fig. 8.

The diagrams in Fig. 8(a) and 8(b), with the intermediate states K_c^+ and π_c^- are of $0\left(\frac{m_K^2}{M^2} G_F \alpha\right)$, when the intermediate states are κ_c^+ and ϕ_c^- , they vanish as $\mu^2 \rightarrow \infty$. The two intermediate states that contribute to the diagrams in Fig. 8(c) are such that their sum is of $0\left(\frac{m^2}{M^2} G_F \alpha\right)$, thus is again negligible.

(IV-C) Higgs Exchange Diagrams

Finally, we consider the Higgs-exchange diagrams. They are shown in Fig. 9.

The diagram in Fig. 9(a) is of $O\left(G_F \alpha \frac{M_K^2}{M^2} \frac{m_c^2}{\mu^2} \text{Higgs}\right)$. The two intermediate states in Fig. 9(b) cancel between themselves as $\mu^2 \rightarrow \infty$. The diagrams in Fig. 9(c), 9(d) and 9(f) are of $O(\mu^{-2})$ and they vanish as $\mu^2 \rightarrow \infty$. The $K_0^2 \xi_c$ self-energy part in the diagram of Fig. 9(e) is apparently of $O(\mu^2)$. However, we have evaluated it later [see Eq. (6.8)] in a different context and have found that the terms of $O(\mu^2)$ cancel between the two intermediate states. So that the diagram in Fig. 9(d) is also of $O(\mu^{-2})$ and vanishes as $\mu^2 \rightarrow \infty$. Thus the total of the Higgs exchange is of $O\left(G_F \alpha \frac{m_K^2}{M^2} \frac{m_c^2}{\mu_{\text{Higgs}}^2}\right)$. Therefore so long as $\mu_{\text{Higgs}}^2 \gtrsim m_c^2$, this contribution is also at most that of the other diagrams [i. e., of $O\left(\frac{m_K^2}{M^2} G_F \alpha\right)$].

The conclusion is therefore that the contribution to the amplitude for $K_{L,S} \rightarrow \mu\bar{\mu}$ from this set of diagrams is much smaller than would be naively expected [i. e., of $O\left(G_F \alpha \frac{m_c^2}{M^2}\right)$] due to the perhaps accidental cancellation of the terms of $O\left(\frac{m_c^2}{M^2} G_F \alpha\right)$. In Sec. X, we have compared the amplitude of $O\left(\frac{m_K^2}{M^2 \sin^2 \theta_W} G_F \alpha\right)$ with the total amplitude for the $K_L \rightarrow \mu\bar{\mu}$ decay as determined from the experimental result and found that it is two orders of magnitude smaller than the total amplitude for

$K_L \rightarrow \mu\bar{\mu}$. Thus the main contribution to the $K_L \rightarrow \mu\bar{\mu}$ amplitude arises out of the process $K_L \rightarrow \gamma\gamma \rightarrow \mu\bar{\mu}$. [That this is the main contribution can be seen from the fact that the unitarity bound obtained from the absorptive part of the process $K_L \rightarrow \gamma\gamma \rightarrow \mu\bar{\mu}$ is close to the experimental result.²¹ An identical conclusion was reached in the free quark model calculation of Ref. (5)].

V. $K^+ \rightarrow \pi^+ \nu\bar{\nu}$

Diagrams that contribute to this process consist of Z exchange diagrams and diagrams in which the leptons couple to W^\pm and s^\pm (box diagrams). We shall first consider the Z-exchange diagrams.

Diagrammatic representation for the total $K^+ \rightarrow \pi^+ Z$ vertex is shown in Fig. 10. [We note here that there are no $\phi^+ \rightarrow \pi^+ Z$ and $K^+ \rightarrow \kappa^+ Z$ vertices.]

The diagrams in Fig. 10(b), 10(e), 10(f) and 10(g) are proportional to q_μ , the momentum of Z, and hence do not contribute when contracted with the neutrino current (on mass shell).

The calculation of the sum of the diagrams in Fig. 10(a), 10(c) and 10(d) can be simplified through the use of the Ward-Takahashi identity derived in the Appendix B. [See Eq. (B.11).] The WT identity states:

$$q_\mu \Gamma_Z^\mu(p, q) - i M_Z \Gamma_\chi(p, q) = - \frac{i}{2} \sum_i G f_i t_{3i} \Gamma_i^{(3)}(p, q) - \frac{g^2 - g'^2}{2G} \left[\Sigma_+(p) - \Sigma_+(p-q) \right] \quad (5.1)$$

$\Gamma_Z^\mu(p, q) =$ the $K^+(p) \rightarrow \pi^+(p-q) Z^\mu(q)$ proper vertex

$\Sigma_+(p) = K^+ \rightarrow \pi^+$ self energy

$\Gamma_\chi(p, q) =$ the $K^+ \pi^- \chi$ proper vertex

$\Gamma_i^{(3)}(p, q) =$ the proper vertex consisting of $K^+ \pi^-$ and Π_{ii} , the diagonal elements of Π .

$t_{3i} = 1$ for $i = 1, 2$

$= -1$ for $i = 3, 4$.

The diagrammatic representation for Eq. (5.1) is shown in Fig. 11.

Now, from Lorentz invariance,

$$\Gamma_Z^\mu(p, q) = A p^\mu + B q^\mu \quad (5.2)$$

where A and B are functions of the Lorentz invariants. To the order we shall be interested in,

$$\Sigma_+(p) = a + b p^2 \quad (5.3)$$

where a and b are constants. We note that the terms proportional to q_μ in $\Gamma_2^\mu(p, q)$ need not be computed.

We expand A in powers of external momenta:

$$A = A_0 + A_1 p \cdot q + A_2 p^2 + A_3 q^2 + \dots \quad (5.4)$$

The leading contribution will come from A_0 .

The sum of the diagrams in Fig. 10(c) and 10(d) when K^+ and π^+ are on mass shell is,

$$\begin{aligned}
 & -i(2p-q)_\mu \left(\frac{g^2 - g'^2}{2G} \right) \left[\Sigma_+(p) \frac{i}{m_K^2 - m_\pi^2} + \Sigma_+(p-q) \frac{i}{m_\pi^2 - m_K^2} \right]_{\text{mass shell}} \\
 & = \frac{g^2 - g'^2}{2G} (2p)_\mu \frac{[\Sigma_+(p) - \Sigma_+(p-q)]_{\text{mass shell}}}{m_K^2 - m_\pi^2} + \text{terms in } q_\mu
 \end{aligned}$$

using Eq. (5.3)

$$= p_\mu \left(\frac{g^2 - g'^2}{G} \right) b + \text{terms in } q_\mu . \quad (5.5)$$

Thus the terms proportional to p_μ in the sum of the diagrams in Fig. 10(a), 10(c), and 10(d) (with K^+ and π^+ on mass shell) is,

$$\left[A_0 + \frac{g^2 - g'^2}{G} b \right] p_\mu + \dots \quad (5.6)$$

which is what we need to compute.

On the other hand, if we substitute the expressions for $\Gamma_Z^\mu(p, q)$ and $\Sigma(p)$ from Eqs. (5.2) - (5.4) in the WT identity of Eq. (5.1), we obtain,

$$\begin{aligned}
 & \left[(A_0 p \cdot q + \dots) + Bq^2 \right] - i M_Z \Gamma_\chi(p, q) \\
 & = \frac{i}{2} G \sum_i f_i t_{3i} \Gamma_i^{(3)}(p, q) - \frac{g^2 - g'^2}{2G} \cdot b \cdot [2p \cdot q - q^2]
 \end{aligned}$$

i. e. ,

$$\begin{aligned}
 & \left[\left(A_0 + \frac{g^2 - g'^2}{G} b \right) p \cdot q + Bq^2 \right] \\
 & = i M_Z \Gamma_\chi(p, q) - \frac{i}{2} G \sum_i f_i t_{3i} \Gamma_i^{(3)}(p, q) - \frac{g^2 - g'^2}{2G} bq^2 + \dots \quad (5.7)
 \end{aligned}$$

Thus, we see that $\left(A_0 + \frac{g^2 - g'^2}{G} b\right)$ is given by the terms proportional to $p \cdot q$ in

$$i M_Z \Gamma_\chi(p, q) - \frac{i}{2} G \sum_i f_i t_{3i} \Gamma_i^{(3)}(p, q) . \quad (5.8)$$

First, consider $\Gamma_\chi(p, q)$. The diagrams that contribute to $\Gamma_\chi(p, q)$ are shown in Fig. 12. The four diagrams in Fig. 12 [two intermediate states in each of the Fig. 12(a) and 12(b)] contribute equally to the terms proportional to $p \cdot q$. Their sum is,

$$\Gamma_\chi(p, q) = -(p \cdot q) \frac{3\pi^2}{4(2\pi)^4} g^3 \sin \theta \cos \theta \frac{m_c^2}{M^2} \ln \frac{M^2}{m_c^2} + \text{other terms} \quad (5.9)$$

and thus, its contribution to terms proportional to p_μ in $E_Z^\mu(p, q)$ is given by,

$$-i p_\mu \frac{3\pi^2}{4(2\pi)^4} g^2 G \sin \theta \cos \theta \frac{m_c^2}{M^2} \ln \frac{M^2}{m_c^2} . \quad (5.10)$$

In the Appendix G, we shall deal with the term

$-i \frac{G}{2} \sum_k f_k t_{3k} \Gamma_k^{(3)}(p, q)$. [The diagrams that contribute to $\Gamma_k^{(3)}(p, q)$ are shown in Fig. 13.] There, we have shown that, only the diagrams in Fig. 13(h), 13(i), 13(j) contribute to the $p \cdot q$ terms of $O\left(\frac{m_c^2}{M^2}\right)$. Their total contribution is,

$$\begin{aligned} & \mathcal{M}(h) + \mathcal{M}(i) + \mathcal{M}(j) \\ & = -(p \cdot q) \frac{1}{4} \frac{\pi^2}{(2\pi)^4} g^2 \sin \theta \cos \theta \frac{m_c^2}{M^2} + \text{other terms} \end{aligned} \quad (5.11)$$

and thus, their contribution to the terms proportional to p_μ in $E_Z^\mu(p, q)$

is given by

$$ip_{\mu} \frac{\pi^2}{8(2\pi)^4} g^2 G \sin \theta \cos \theta \frac{m_c^2}{M^2} + 0 \left(\frac{m_c^2}{M^2} \right) . \quad (5.12)$$

We note that this contribution in (5.12) is very small numerically as compared to the one in (5.10) $\left[\text{smaller by a factor of } \frac{1}{12 \ln(M/mc)} \right]$. Thus, it is interesting to note that by the use of the WT identity of Eq. (5.1), we have been able to obtain the major contribution through only one independent diagram calculation.

In the Appendix E, we have shown that the box diagrams for this process contribute to $0 \left(\frac{m_K^2}{M^2} \right)$ and hence will be neglected. Hence, the amplitude for $K^+ \rightarrow \pi^+ \nu \bar{\nu}$ is given by

$$\begin{aligned} \mathcal{M}(K^+ \rightarrow \pi^+ \nu \bar{\nu}) &= E_Z^{\mu} (p, q) \frac{-i}{-M_Z^2} \frac{iG}{2} \bar{u}(k) \gamma_{\mu} \gamma_L v(\bar{k}) \\ &= i \frac{3}{4} \frac{G_F}{\sqrt{2}} \frac{\alpha}{\pi} \sin \theta \cos \theta \frac{m_c^2}{M^2 \sin^2 \theta_W} \left\{ \ln \frac{M^2}{m_c^2} + \frac{1}{6} \right\} \\ &\quad \times \bar{u}(k) \gamma_{\mu} \gamma_L v(\bar{k}) \end{aligned} \quad (5.13)$$

$$\left[\gamma_L = \frac{1-\gamma_5}{2}, \quad k = 4\text{-momentum of } \nu \right.$$

$$\left. \bar{k} = 4\text{-momentum of } \bar{\nu} \right] .$$

Using Eq. (5.13), we shall estimate the branching ratio $\Gamma(K^+ \rightarrow \pi^+ \nu \bar{\nu}) / \Gamma(K^+ \rightarrow \text{all})$ in Sec. X.

VI. $K^0 \rightarrow \pi^0 \nu \bar{\nu}$

The calculation of the amplitude for $K^0 \rightarrow \pi^0 \nu \bar{\nu}$ is similar to that of $K^+ \rightarrow \pi^+ \nu \bar{\nu}$. Here, too, there are two kinds of diagrams: the Z-exchange diagrams and the diagrams in which the leptons couple to $W^\pm s^\pm$ (\equiv Box diagrams).

Let us first consider the Z-exchange diagrams. They are shown in Fig. 14. The diagrams in Fig. 14(b), 14(c), 14(d) and 14(g) are proportional to q_μ , the momentum of Z_μ and hence do not contribute with $\nu\bar{\nu}$ on mass shell. The calculation of the diagrams in Fig. 14(a), namely the proper $K^0 \pi^0 Z$ vertex, is simplified through the use of the WT identity of Eq. (B+13), which reads:

$$q_\mu \Gamma_{0Z}^\mu(p, q) = i M_Z \Gamma_{0\chi}(p, q) - \frac{iG}{2} \sum_k f_k t_{3k} \Gamma_{0k}^{(3)}(p, q) + \frac{iG}{2} \left\{ \frac{1}{\sqrt{3}} \Sigma'_0(p) + \frac{\sqrt{2}}{\sqrt{3}} \Sigma_0(p) - \Sigma'_0(p-q) \right\} \quad (6.1)$$

where

$$\Gamma_{0Z}^\mu(p, q) = \text{the proper vertex for } K^0(p) \rightarrow \pi^0(p-q) Z^\mu(q)$$

$$\Gamma_{0\chi}(p, q) = \text{the } K^0 \pi^0 \chi \text{ proper vertex}$$

$$\Sigma_0(p) = K_0 \xi_8 \text{ self energy}$$

$$\Sigma'_0(p) = K_0 \xi_0 \text{ self energy}$$

$$\Sigma'_0(p-q) = \kappa_0 \pi_0 \text{ self energy}$$

$$\Gamma_{0k}^{(3)}(p, q) = \text{the proper vertex consisting of } K_0 \pi_0 \text{ and } \Pi_{kk}.$$

$$\begin{aligned}
 t_{3k} &= 1 & k &= 1, 2 \\
 &= -1 & k &= 3, 4.
 \end{aligned}$$

The diagrammatic representation for Eq. (6.1) is shown in Fig. 15.

Let us first consider the diagrams that contribute to $\Gamma_{0\chi}(p, q)$. They are shown in Fig. 16. These diagrams are, in fact, very similar to those for $\Gamma_{\chi}(p, q)$ of Fig. 12 in Sec. V. The $p \cdot q$ terms in $\Gamma_{0\chi}(p, q)$ are given by

$$\begin{aligned}
 i M_Z \Gamma_{0\chi}(p, q) &= \frac{1}{\sqrt{2}} \Gamma_{\chi}(p, q) (i M_Z) \\
 &= -\frac{i}{\sqrt{2}} (p \cdot q) \frac{3\pi^2}{4(2\pi)^4} g^2 G \sin \theta \cos \theta \left(\frac{m_c^2}{M^2} \ln \frac{M^2}{m_c^2} \right) \\
 &\quad + \text{other terms} .
 \end{aligned} \tag{6.2}$$

Next, let us consider the other two terms in the right-hand side of the Eq. (6.1). The analysis of these terms is a little complicated and hence we shall deal with them in the Appendix F. The diagrams that contribute to these terms are shown in Fig. 17 and Fig. 18 respectively. In the Appendix F, we have shown that the contributions come only out of the diagrams in Fig. 17(a), 17(c) and Fig. 18(f).

The diagrams in Fig. 17(a) and 17(c) are equal and their contribution to the $p \cdot q$ terms in $-\frac{iG}{2} \sum_k f_k t_{3k} \Gamma_{0k}^{(3)}(p, q)$ is given by

$$\begin{aligned}
17(a) + 17(c) &= \frac{-i}{2\sqrt{2}} (p \cdot q) \frac{3\pi^2}{4(2\pi)^4} g^2 G \sin\theta \cos\theta \left(\frac{m_c^2}{M^2} \ln \frac{M^2}{m_c^2} \right) \\
&\quad + \text{other terms} .
\end{aligned} \tag{6.3}$$

The contribution of the diagram in Fig. 18(f) is finite and finite as $\mu^2 \rightarrow \infty$. The contribution of Fig. 18(f) to the $p \cdot q$ terms in $-\frac{i}{2} G \Sigma_0''(p-q)$ is given by,

$$\begin{aligned}
18(f) &= \frac{-i}{2\sqrt{2}} (p \cdot q) \frac{3\pi^2}{4(2\pi)^4} g^2 G \sin\theta \cos\theta \left(\frac{m_c^2}{M^2} \ln \frac{M^2}{m_c^2} \right) \\
&\quad + \text{other terms} .
\end{aligned} \tag{6.4}$$

Thus, using Eqs. (6.2) - (6.4) in the WT identity of Eq. (6.1), we obtain the terms proportional to p_μ in $\Gamma_{0Z}^\mu(p, q)$:

$$\begin{aligned}
\Gamma_{0Z}^\mu(p, q) &= -p_\mu \left[\frac{i}{\sqrt{2}} \cdot \frac{3\pi^2}{4(2\pi)^4} \cdot g^2 G \sin\theta \cos\theta \frac{m_c^2}{M^2} \ln \frac{M^2}{m_c^2} + O\left(\frac{1}{M^4}\right) \right] \\
&\quad + \text{terms proportional to } q_\mu .
\end{aligned} \tag{6.5}$$

Finally, we shall compute the one particle reducible diagrams in Fig. 14(e) and 14(f). Referring to the Feynman rules in the Appendix A, we find that their contribution to $E_{0Z}^\mu(p, q)$, (the total $K^0 \pi^0 Z^\mu$ vertex) is:

$$\begin{aligned}
&\mathcal{M}(e) + \mathcal{M}(f) \\
&= \frac{i^2 G}{2} (2p - q)_\mu \left[\frac{i}{m_\pi^2 - \mu^2} \Sigma_0''(p-q) + \frac{i}{m_K^2 - \mu^2} \left(\frac{\Sigma_0(p)}{\sqrt{3}} - \frac{\Sigma_{02}(p)}{2\sqrt{6}} \right) \right. \\
&\quad \left. + \frac{i}{m_k^2 - \mu_1^2} \frac{\Sigma_{01}(p)}{2\sqrt{2}} \right]
\end{aligned} \tag{6.6}$$

where

$$\Sigma_{0i}(p) = K_0 \xi_i \text{ self energy}$$

and $\xi_{i's}$ are the two eigenstates of the (mass)² matrix and are defined in Eq. (2.26b). μ_1 is the mass of ξ_1 [see Eq. (2.26b)]. We thus need to compute the terms of $O\left(\mu^2 \frac{m_c^2}{M^2}\right)$ in the self-energies. The diagrams that contribute to the self-energies Σ_{01} , Σ_{02} and are of $O(\mu^2)$ are shown in Fig. 19.

The K_0 -tadpole diagram is identically zero (when summed over both the intermediate states). In Σ_{01} and Σ_{02} , the diagram in Fig. 19(b) cancels that in Fig. 19(a). This can be seen from the Feynman rules for the meson- S^+ vertices and the interaction terms describing the trilinear vertices:

$$- \left\{ \left[2\alpha \mu_0^2 \left(f \xi_c + f \frac{\xi_0}{\sqrt{3}} \right) + 4\beta f \mu_0^2 \left(\xi_c + \sqrt{3} \xi_0 \right) - \frac{4}{\sqrt{3}} \gamma \mu_0^2 f \xi_0 \right] \right. \\ \left. \times \left[\underline{K_c^+ K_c^- + \pi_c^+ \pi_c^-} \right] \right\} - \frac{\mu_c^2}{2f} K_0 \left(\underline{\kappa_c^+ \pi_c^- + \phi_c^+ K_c^-} \right) . \quad (6.7)$$

Thus,

$$\Sigma_{0i}(p=0) = O(\mu^0) . \quad (6.8)$$

Referring to the Eq. (F.10) in the Appendix F, we obtain [and this has been verified directly] :

$$\Sigma_0'(0) = \frac{1}{\sqrt{3}} \Sigma_0(0) + O(\mu^0) . \quad (6.9)$$

Thus the leading contribution [of $O\left(\frac{m_c^2}{M^2}\right)$] of the diagrams in Figs. 14(e) and 14(f) is given by:

$$\mathcal{M}(e) + \mathcal{M}(f) = \frac{(i)^2 G}{2} \frac{(2p-q)_\mu}{-2} \cdot 2i\Sigma'_0(0). \quad (6.10)$$

The contribution to $\Sigma'_0(0)$ of $O(\mu^2)$ comes from the diagram in Fig. 20. It is easily shown to be,

$$\Sigma'_0(0) = \frac{\pi^2}{(2\pi)^4} \frac{g^2 m_c^2 \mu^2}{8\sqrt{2} M^2} \sin\theta \cos\theta + O(\mu^0) \quad (6.11)$$

and hence its contribution to the terms proportional to p_μ in $E_{0Z}^\mu(p, q)$ is:

$$p_\mu \frac{i}{\sqrt{2}} \frac{\pi^2}{4(2\pi)^4} g^2 G \sin\theta \cos\theta \frac{m_c^2}{M^2} + O\left(\frac{1}{M^4}\right) + \text{terms in } q_\mu. \quad (6.12)$$

Hence, from Eqs. (6.5) and (6.12), the terms in $E_{0Z}^\mu(p, q)$ which are proportional to p_μ are given by

$$E_{0Z}^\mu(p, q) = -p_\mu \cdot \frac{i}{\sqrt{2}} \frac{\pi^2}{(2\pi)^4} g^2 G \sin\theta \cos\theta \frac{m_c^2}{M^2} \left\{ \frac{3}{2} \ln \frac{M^2}{m_c^2} - \frac{1}{4} \right\} + \text{terms in } q_\mu. \quad (6.13)$$

As in the case of the $K^+ \rightarrow \pi^+ \nu \bar{\nu}$ amplitude, the box diagrams for this process are of $O\left(\frac{m_K^2}{M^2}\right)$ and therefore will be neglected. Hence the total amplitude for $K_0^0 \rightarrow \pi^0 \nu \bar{\nu}$ is given by:

$$\mathcal{M}(K_0^0 \rightarrow \pi^0 \nu \bar{\nu}) = \frac{i}{\sqrt{2}} \frac{G_F}{\sqrt{2}} \frac{\alpha}{\pi} \sin\theta \cos\theta \frac{m_c^2}{M^2 \sin^2\theta_W} \left\{ \frac{3}{2} \ln \frac{M^2}{m_c^2} - \frac{1}{4} \right\}$$

$$\times p^\mu u(k) \gamma_\mu \gamma_L v(\bar{k}) + O\left(\frac{m_K^2}{M^4}\right) . \quad (6.14)$$

It is easy to verify directly that for this amplitude that

$$\mathcal{M}(K^0 \rightarrow \pi^0 \nu \bar{\nu}) = -\mathcal{M}(\bar{K}_0 \rightarrow \pi^0 \nu \bar{\nu}) \quad (6.15)$$

and hence,

$$\begin{aligned} \mathcal{M}(K_S^0 \rightarrow \pi^0 \nu \bar{\nu}) &= \sqrt{2} \mathcal{M}(K_0 \rightarrow \pi^0 \nu \bar{\nu}) \\ &= \frac{iG_F}{\sqrt{2}} \cdot \frac{3\alpha}{2\pi} \sin \theta \cos \theta \frac{m_c^2}{M^2 \sin^2 \theta_W} \left\{ \ln \frac{M^2}{m_c^2} - \frac{1}{6} \right\} \\ &\quad \times p^\mu \bar{u}(k) \gamma_\mu \gamma_L v(\bar{k}) \end{aligned} \quad (6.16)$$

and

$$\mathcal{M}(K_L^0 \rightarrow \pi^0 \nu \bar{\nu}) = 0 .$$

The branching ratio,

$$\frac{\Gamma(K_S^0 \rightarrow \pi^0 \nu \bar{\nu})}{\Gamma(K_S^0 \rightarrow \text{all})}$$

is estimated in Sec. X.

VII. $K^+ \rightarrow \pi^+ e \bar{e}$

The diagrams contributing to this process consist of (i) the photon exchange diagrams, (ii) the Higgs scalar (ψ_0) exchange diagrams (iii) the Z - χ exchange diagrams, (iv) the 'box' diagrams. We shall

show that the photon exchange diagrams are of $O(G_F \alpha)$. We have already evaluated the $K^+ \rightarrow \pi^+ Z$ vertex in Sec. V, and we know that its contribution to the amplitude is of $O\left(G_F \alpha \frac{m_c^2}{M^2}\right)$. Therefore, we shall neglect it. The box diagrams for this process are similar to those for the process $K^+ \rightarrow \pi^+ \nu \bar{\nu}$. They will be of the order $\lesssim O\left(G_F \alpha \frac{m_c^2}{M^2}\right)$ and hence can be neglected.

Let us first consider the photon exchange diagrams. The $K^+ \pi^- \gamma$ truncated Green's function is shown in Fig. 31. [See Appendix B.] It is shown in the Appendix B that $E_Y^\mu(p, q)$, the full $K^+ \pi^- \gamma$ vertex, on mass shell is given by.

$$E_Y^\mu(p, q) = C_3 q^2 p^\mu + \text{terms proportional to } q^\mu \quad (\text{B. 23})$$

where C_3 is the coefficient of the $q^2 p^\mu$ terms in the proper vertex $\Gamma_Y^\mu(p, q)$ evaluated on mass shell [i.e., $p^2 = m_K^2$, $(p-q)^2 = m_\pi^2$].

The diagrams that contribute to the proper vertex $\Gamma_Y^\mu(p, q)$ are shown in the Fig. 21. First consider the set of diagrams in Fig. 21(a) - 21(n).

In the diagram of Fig. 21(a), the two intermediate states contribute, with opposite signs and the resulting amplitude is of $O\left(\frac{1}{M^4}\right)$ and hence will be neglected. The diagram in Fig. 21(i) is independent of q and hence do not contribute to terms proportional to $q^2 p_\mu$. The diagrams in Fig. 21(h) are proportional to q_μ . The diagram in Fig. 21(j) depends only on $(p-q)^2$. Since we have chosen $(p-q)^2$, q^2 and p^2 as the three independent

Lorentz invariants, it does not contribute to terms proportional to $q^2 p_\mu$ either. All the rest of the diagrams contribute to the terms proportional to $q^2 p_\mu$. The results upto $O\left(\frac{1}{M^2}\right)$ are:

$$\mathcal{M}(b) = -q^2 p_\mu \frac{\pi^2 i}{(2\pi)^4} \frac{g^2 e \sin \theta \cos \theta}{4M^2} \times \left\{ \frac{1}{2} \int d\epsilon \epsilon(1-\epsilon) \ln \left[\frac{-\epsilon(1-\epsilon)q^2}{m_c^2} \right] - \frac{1}{72} \right\} \quad (7.6)$$

$$\mathcal{M}(c) = -q^2 p_\mu \frac{\pi^2 i}{(2\pi)^4} \frac{g^2 e \sin \theta \cos \theta}{4M^2} \cdot \frac{1}{2} + \mathcal{M}(b) \quad (7.7)$$

$$\mathcal{M}(d) = \mathcal{M}(b) \quad (7.8)$$

$$\mathcal{M}(e) = -q^2 p_\mu \frac{\pi^2 i}{(2\pi)^4} \frac{g^2 e \sin \theta \cos \theta}{4M^2} \cdot \frac{1}{3} + \mathcal{M}(b) \quad (7.9)$$

$$\mathcal{M}(f) = \mathcal{M}(g) = -g^2 p_\mu \frac{\pi^2 i}{(2\pi)^4} \left\{ - \int d\epsilon \epsilon(1-\epsilon) \ln \left[\frac{-\epsilon(1-\epsilon)q^2}{m_c^2} \right] - \frac{5}{36} \right\}. \quad (7.10)$$

[Note that the logarithmic singularity $\ln(-q^2)$ in these amplitudes arises from the fact that the W^\pm and s^\pm propagators have a singularity at $k^2 = 0$. However, this singularity cancels when we add up $\mathcal{M}(b) + \dots + \mathcal{M}(g)$.]

Adding Eqs. (7.6) - (7.10), we obtain

$$\mathcal{M}(b) + \dots + \mathcal{M}(g) = -g^2 p_\mu \frac{\pi^2 i}{(2\pi)^4} \frac{g^2 e \sin \theta \cos \theta}{4M^2} \cdot \frac{1}{2}. \quad (7.11)$$

Summing over all intermediate states in the diagrams of Fig. 21(k) and 21(l), we obtain:

$$\begin{aligned} \mathcal{M}(k) &= -q^2 p_\mu \frac{\pi^2 i}{(2\pi)^4} \frac{g^2 e \sin \theta \cos \theta}{4M^2} \\ &\times \left\{ \frac{1}{2} \int d\beta \beta (1-\beta) \ln \frac{m_c^2}{m_K^2 - \beta q^2} + \frac{1}{6} \right\} \end{aligned} \quad (7.12)$$

and

$$\begin{aligned} \mathcal{M}(l) &= -q^2 p_\mu \frac{\pi^2 i}{(2\pi)^4} \frac{g^2 e \sin \theta \cos \theta}{4M^2} \\ &\times \left\{ \frac{1}{2} \int d\beta \beta (1-\beta) \ln \frac{m_c^2}{m_\pi^2 - \beta q^2} + \frac{2}{9} \right\} . \end{aligned} \quad (7.13)$$

The contributions of the diagrams in Fig. 21(m) and 21(n) to terms proportional to $q^2 p_\mu$ are equal and their sum is given by

$$\mathcal{M}(m) + \mathcal{M}(n) = -q^2 p_\mu \frac{\pi^2 i}{(2\pi)^4} \frac{g^2 e \sin \theta \cos \theta}{4M^2} \cdot \frac{1}{9} . \quad (7.14)$$

[Here, we note that $\phi^\pm W^\mp \gamma$ and $\chi^\pm W^\mp \gamma$ coupling is of the order $0\left(\frac{m_c^2}{\mu^2}\right)$. Hence the diagrams with intermediate states (ϕ^+, ϕ_c^+) in Fig. 21(l) and (χ^+, χ_c^+) in Fig. 21(k) do not contribute as $\mu^2 \rightarrow \infty$. Also the diagrams with the intermediate states κ^+, κ_c^+ in Fig. 21(m) and ϕ^+, ϕ_c^+ in Fig. 21(n) are of order $0\left(\frac{1}{\mu^2}\right)$ and hence they do not contribute as $\mu^2 \rightarrow \infty$.]

Further, we note that the $q^2 p_\mu$ terms in the diagrams in Figs. 21(b) -

21(g) and in Figs. 21(k) - 21(n) are not proportional to m_c^2 and thus are of zeroth order in the SU(4) symmetry breaking. Hence we must also consider the diagrams with intermediate states $K^+, \kappa^+, \pi^-, \phi^-$ etc., shown in Figs. 21(o) - 21(v) which may have terms proportional to $q_\mu^2 p_\mu$ which will not vanish in the SU(3) limit being of zeroth order in the SU(3) symmetry breaking.

In the diagrams of Fig. 21(u) and 21(v) when the intermediate states to which photon couples are scalars, the contribution to the terms proportional to $q_\mu^2 p_\mu$ is of $O\left(\frac{1}{2}\right)$ and hence will be neglected. We quote the results for the diagrams in Figs. 21(o) - 21(v):

$$\begin{aligned} \mathcal{M}(0) &= -q_\mu^2 p_\mu \frac{\pi^2 i}{(2\pi)^4} \frac{g^2 e \sin \theta \cos \theta}{4M^2} \\ &\times \frac{1}{2} \int d\gamma \gamma(1-\gamma) \ln \left(\frac{m_\pi^2 - \gamma q^2}{-\gamma q^2} \right) \end{aligned} \quad (7.15)$$

$\mathcal{M}(p) = 0$, since the $\phi^+ s^-$ coupling is zero. [This is so because from gauge invariance, this coupling has to be proportional to $m_\pi^2 - m_0^2 = 0$]

$$(7.16)$$

$$\begin{aligned} \mathcal{M}(q) &= -q_\mu^2 p_\mu \frac{\pi^2 i}{(2\pi)^4} \frac{g^2 e \sin \theta \cos \theta}{4M^2} \\ &\times \frac{1}{2} \int d\gamma \gamma(1-\gamma) \ln \left(\frac{m_K^2 - \gamma q^2}{-\gamma q^2} \right) . \end{aligned} \quad (7.17)$$

$\mathcal{M}(r)$ vanishes in the SU(3) limit . (7.18)

$$\begin{aligned} \mathcal{M}(s) &= g^2 p_\mu \frac{\pi^2 i}{(2\pi)^4} \frac{g^2 e \sin \theta \cos \theta}{4M^2} \\ &\times \left\{ \int d\gamma \gamma(1-\gamma) \ln \frac{m_\pi^2 - \gamma q^2}{-\gamma q^2} - \int d\gamma \gamma(1-\gamma) \ln \left[\frac{(1-\gamma)m_K^2 + \gamma m_\pi^2 - \gamma(1-\gamma)q^2}{(1-\gamma)(m_K^2 - \gamma q^2)} \right] \right\} \end{aligned} \quad (7.19)$$

$$\mathcal{M}(t) = 0 \quad (7.20)$$

$$\begin{aligned} \mathcal{M}(u) &= q^2 p_\mu \frac{\pi^2 i}{(2\pi)^4} \frac{g^2 e \sin \theta \cos \theta}{4M^2} \\ &\times \int d\gamma \gamma(1-\gamma) \ln \left[\frac{(1-\gamma)m_K^2 + \gamma m_\pi^2 - \gamma(1-\gamma)q^2}{(1-\gamma)m_K^2 - \gamma q^2} \right] \end{aligned} \quad (7.21)$$

$$\begin{aligned} \mathcal{M}(v) &= q^2 p_\mu \frac{\pi^2 i}{(2\pi)^4} \frac{g^2 e \sin \theta \cos \theta}{4M^2} \\ &\times \int d\gamma \gamma(1-\gamma) \ln \left[\frac{m_\pi^2 - \gamma(1-\gamma)q^2}{(1-\gamma)(m_\pi^2 - \gamma q^2)} \right] \end{aligned} \quad (7.22)$$

The singularities in the above amplitude of the type $\int d\gamma \ln(m_\pi^2 - \gamma q^2)$, etc. (a cut $q^2 \geq m_\pi^2$) are unphysical and arise solely because of our choice of the Landau gauge for the W^\pm, s^\pm propagators. We note the cancellation of such singularities between the amplitudes $[\mathcal{M}(l) + \mathcal{M}(o)]$, $[\mathcal{M}(k) + \mathcal{M}(q)]$ and $[\mathcal{M}(s) + \mathcal{M}(n) + \mathcal{M}(v)]$. The singularities which are cuts in $q^2 \geq 4m_\pi^2$ and

$q^2 \geq (m_K + m_\pi)^2$ are physical and they may stay.

Adding Eqs. (7.12), (7.13) and Eqs. (7.15) - (7.22), we obtain

$$\begin{aligned}
 & [\mathcal{M}(l) + \mathcal{M}(k)] + \mathcal{M}(o) + \dots + \mathcal{M}(v) = \\
 & = -q^2 p_\mu \frac{\pi^2 i}{(2\pi)^4} \frac{g^2 e \sin \theta \cos \theta}{4M^2} \left\{ \frac{1}{4} + \int d\beta \beta (1-\beta) \ln \left[\frac{m_c^2}{m_\pi^2 - \beta(1-\beta)q^2} \right] \right\}.
 \end{aligned} \tag{7.23}$$

Thus, from Eq. (7.11), (7.14) and (7.23), we obtain the terms proportional to $q^2 p_\mu$ in $\Gamma_Y^\mu(p, q)$ and hence $E_Y^\mu(p, q)$ as,

$$\begin{aligned}
 E_Y^\mu(p, q) &= -q^2 p^\mu \frac{\pi^2 i}{(2\pi)^4} \frac{g^2 e \sin \theta \cos \theta}{4M^2} \\
 &\times \left\{ \frac{31}{36} + \int d\beta \beta (1-\beta) \ln \frac{m_c^2}{m_\pi^2 - \beta(1-\beta)q^2} \right\} \\
 &+ \text{terms proportional to } q_\mu.
 \end{aligned} \tag{7.24}$$

Thus, the contribution of the photon exchange diagrams to the $K^+ \rightarrow \pi^+ e e^-$ amplitude is given by

$$\begin{aligned}
 & -\frac{i}{q} (-ie) \bar{u}(k) \gamma_\mu v(\bar{k}) E_Y^\mu(p, q) \\
 &= \frac{iG_F}{\sqrt{2}} \frac{\alpha}{2\pi} \sin \theta \cos \theta p^\mu \bar{u}(k) \gamma_\mu v(\bar{k}) \\
 &\times \left\{ \frac{31}{36} + \int d\beta \beta (1-\beta) \ln \frac{m_c^2}{m_\pi^2 - \beta(1-\beta)q^2} \right\}.
 \end{aligned} \tag{7.25}$$

In the Appendix H, we shall show that the contribution due to the Higgs exchange is negligible. Hence Eq. (7.25) describes the full amplitude to $O(G_F \alpha)$.

As a crude approximation, we may let:

$$\int d\beta \beta(1-\beta) \ln \frac{m_c^2}{m_\pi^2 - \beta(1-\beta)q^2 + i\epsilon} \approx \frac{1}{6} \ln \frac{m_c^2}{m_\pi^2} .$$

Then,

$$\begin{aligned} \mathcal{M}(K^+ \rightarrow \pi^+ e\bar{e}) &= \frac{iG_F}{\sqrt{2}} \frac{\alpha}{2\pi} \sin\theta \cos\theta \left\{ \frac{1}{6} \ln \frac{m_c^2}{m_\pi^2} + \frac{31}{36} \right\} \\ &\times p^\mu \bar{u}(k) \gamma_\mu v(\bar{k}) . \end{aligned} \quad (7.26)$$

We have computed the branching ratio for this process in Sec. X and it is found to be close to the recent experimental results.¹⁵

VIII. $K^0 \rightarrow \pi^0 e\bar{e}$

This calculation is similar to the calculation of the decay amplitude for $K^+ \rightarrow \pi^+ e\bar{e}$. Here, too, the leading contribution comes from the photon exchange amplitude. All other contributions are of the same order of magnitude as the corresponding amplitudes for the process $K^+ \rightarrow \pi^+ e\bar{e}$, and therefore, can be neglected as compared to the photon exchange amplitude.

As mentioned in the Appendix B, we need to compute the terms proportional to $q^2 p_\mu$ from the diagrams that contribute to the proper $K^0 \pi^0 \gamma$ vertex. The set of diagrams that contribute to the $K^0 \rightarrow \pi^0 \gamma$

proper vertex are shown in Fig. 22.

The terms proportional to $q^2 p_\mu$ in the diagrams of Fig. 22(a) are given by

$$\begin{aligned} \mathcal{M}(a) = & -q^2 p_\mu \frac{\pi^2 i}{(2\pi)^4} \frac{g^2 e \sin \theta \cos \theta}{2\sqrt{2} M^2} \\ & \times \left[2 \int d\beta d\gamma \gamma \ln \left(\frac{m_c^2}{m_\pi^2 (\beta + \beta\gamma + \gamma^2) - \beta\gamma q^2 - \beta(1-\beta-\gamma)m_K^2} \right) \right. \\ & \left. - \int d\beta d\gamma \gamma \ln \frac{m_c^2}{m_K^2 (\gamma + \beta\gamma + \beta^2) - \beta\gamma q^2 - \gamma(1-\beta-\gamma)m_\pi^2} - \frac{1}{18} \right]. \quad (8.1) \end{aligned}$$

The $q^2 p_\mu$ terms in the diagrams of Fig. 22(b) are given by,

$$\mathcal{M}(b) = -q^2 p_\mu \frac{\pi^2 i}{(2\pi)^4} \cdot \frac{7}{72} \cdot \frac{g^2 e \sin \theta \cos \theta}{\sqrt{2} M^2}. \quad (8.2)$$

The diagrams in Fig. 22(c) and 22(d) do not contribute to $q^2 p_\mu$ terms as $\mu^2 \rightarrow \infty$. The diagrams in Figs. 22(i) and 22(j) are functions only of p^2 and $(p-q)^2$ respectively, and hence, do not contribute to the terms proportional to $q^2 p_\mu$. The diagrams in Fig. 22(k) are proportional to q_μ .

The diagrams in Figs. 22(e) - 22(h) are very similar to the diagrams in Fig. 21(a) - 21(g) and 21(o) - 21(t). The diagrams in Figs. 22(l) - 22(o) are similar to the diagrams in Figs. 21(k) - 21(n) and 21(u), 21(v). In fact there is a one-to-one correspondence between the diagrams. The total contribution of the rest of these diagrams to the

$q^2 p_\mu$ terms is given by,

$$\begin{aligned}
& \mathcal{M}(e) + \dots + \mathcal{M}(h) + \mathcal{M}(l) + \dots + \mathcal{M}(o) \\
&= \left(-\frac{1}{\sqrt{2}}\right)(-)q^2 p_\mu \frac{\pi^2 i}{(2\pi)^4} \frac{g^2 e \sin \theta \cos \theta}{4M^2} \\
&\times \left\{ \frac{31}{36} + \int d\beta \beta (1-\beta) \ln \frac{m_c^2}{m_\pi^2 - \beta(1-\beta)q^2} \right\} . \quad (8.3)
\end{aligned}$$

The total amplitude for $K^0 \rightarrow \pi^0 \gamma$ is obtained by adding Eqs. (8.1) - (8.3). As a rough approximation, if we approximate the integrals in Eq. (8.1) by $\frac{1}{6} \ln \frac{m_c^2}{m_\pi^2}$ and $\frac{1}{6} \ln \frac{m_c^2}{m_K^2}$ respectively, then we find that the terms proportional to $q^2 p_\mu$ in the $K^0 \rightarrow \pi^0 \gamma$ vertex, $E_{0\gamma}^\mu(p, q)$ are given by:

$$\begin{aligned}
E_{0\gamma}^\mu(p, q) &= -\frac{1}{\sqrt{2}} q^2 p_\mu \frac{\pi^2 i}{(2\pi)^4} \frac{g^2 e \sin \theta \cos \theta}{4M^2} \\
&\times \left\{ \frac{1}{2} \ln \frac{m_c^2}{m_\pi^2} - \frac{1}{3} \ln \frac{m_c^2}{m_K^2} - \frac{21}{36} \right\} \\
&+ \text{terms in } q_\mu . \quad (8.4)
\end{aligned}$$

Hence,

$$\begin{aligned}
(K^0 \rightarrow \pi^0 e \bar{e}) &= \frac{i}{\sqrt{2}} \frac{G_F}{\sqrt{2}} \frac{\alpha}{2\pi} \sin \theta \cos \theta p_\mu \bar{u}(k) \gamma^\mu v(\bar{k}) \\
&\times \left\{ \frac{1}{6} \ln \frac{m_c^2}{m_\pi^2} + \frac{1}{3} \ln \frac{m_K^2}{m_\pi^2} - \frac{21}{36} \right\} . \quad (8.5)
\end{aligned}$$

It is easy to verify that this photon exchange amplitude satisfies:

$$\mathcal{M}(K^0 \rightarrow \pi^0 e\bar{e}) = -\mathcal{M}(\bar{K}^0 \rightarrow \pi^0 e\bar{e}) \quad (8.6)$$

so that we have

$$\begin{aligned} \mathcal{M}(K_S \rightarrow \pi^0 e\bar{e}) &= \sqrt{2} \mathcal{M}(K^0 \rightarrow \pi^0 e\bar{e}) \\ &= i \frac{G_F}{\sqrt{2}} \frac{\alpha}{2\pi} \sin \theta \cos \theta \left\{ \frac{1}{6} \ln \frac{m_c^2}{m_\pi^2} + \frac{1}{3} \ln \frac{m_K^2}{m_\pi^2} - \frac{21}{36} \right\} \\ &\quad \times p_\mu \bar{u}(k) \gamma^\mu v(\bar{k}) . \end{aligned} \quad (8.7)$$

The amplitude for the process $K_L \rightarrow \pi^0 e\bar{e}$ is highly suppressed.

IX. $\underline{K_L - K_S}$ MASS DIFFERENCE

$K_L - K_S$ mass difference arises because of the weak $K_0 \leftrightarrow \bar{K}_0$ transition. $K_0 \rightarrow \bar{K}_0$ transition is a $\Delta S = 2$, $\Delta Q = 0$ process and therefore must proceed through a minimum of four steps: two of which are $\Delta S = \Delta Q = \pm 1$ processes and the two other $\Delta S = 0$, $\Delta Q = \pm 1$ processes. Thus the lowest order $K_0 - \bar{K}_0$ transition amplitude is of $O(g^4)$ and the diagrams for this $O(g^4)$ do not contain either (i) internal Z, χ, γ lines or (ii) a vertex involving two or more gauge bosons (like 2 mesons - W^+W^- , W^+W^-Z , etc.) since either of them add additional factors of g without accomplishing any additional steps of the four mentioned above.

Thus, the diagrams contributing to the $K_0 - \bar{K}_0$ transition amplitude involve 2 internal W lines (and the corresponding diagrams in which one or more W 's are replaced by the associated unphysical scalars.

These fall into two categories. When the two W lines are opened, the corresponding Green's function $K_0 K_0 \rightarrow W^+ W^- W^+ W^-$ is disconnected for the diagrams of the first category and connected for the diagrams of the second category. The diagrams of the first category contain one loop while those of the second category contain two loops. This is shown schematically in Fig. 23.

First let us consider the one loop diagrams. The one-loop diagrams that contribute in the Landau gauge are shown in Fig. 24. The two possible intermediate states in the diagram of Fig. 24(a) contribute equally. Their sum is given by,

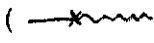
$$\begin{aligned} \mathcal{M}(a) &= -\frac{i\pi^2}{(2\pi)^4} \cdot \frac{3}{8} \cdot m_K^2 \cdot \frac{g^4 f^2 m_c^2}{M^4} \sin^2 \theta \cos^2 \theta \\ &= -i m_K^2 f_K^2 \left(\frac{G_F}{\sqrt{2}} \frac{3\alpha}{16\pi} \right) \sin^2 \theta \cos^2 \theta \frac{m_c^2}{M^2 \sin^2 \theta_W} . \end{aligned} \quad (9.1)$$

There are four possible intermediate states in the diagram of Fig. 24(b). They are such that at $p = 0$, (p being the 4-momentum of K^0) their sum would be identically zero. [In other words, for $m_K = 0$, the diagrams in Fig. 24(b) would vanish. The amplitude in Fig. 24(a) also obviously vanishes at $m_K = 0$.] The sum of the diagrams in Fig. 24(b) is given by,

$$\mathcal{M}(b) = +i m_K^2 f_K^2 \frac{G_F}{\sqrt{2}} \frac{7\alpha}{96\pi} \sin^2 \theta \cos^2 \theta \frac{m_c^2}{M^2 \sin^2 \theta_W} \quad (9.2)$$

so that the total contribution of the one-loop diagrams to the $K_0 \rightarrow \bar{K}_0$ transition amplitude is given by

$$\mathcal{M}(a) + \mathcal{M}(b) = -i m_K^2 f_K^2 \frac{G_F}{\sqrt{2}} \frac{11\alpha}{96\pi} \sin^2 \theta \cos^2 \theta \frac{m_c^2}{M^2 \sin^2 \theta_W}. \quad (9.3)$$

Next, consider the two-loop diagrams. The number of the two-loop diagrams that may contribute is large. Again, we shall choose the Landau gauge. In any other gauge, the number of the contributing diagrams is tremendously large because of the presence of the meson-W () vertex. Further, many of the diagrams are more convergent in the Landau gauge. Figure 25 shows the diagrams that contribute in the Landau gauge. In Fig. 25 we have shown the diagrams collectively and have not shown the intermediate states explicitly. We shall draw the diagrams in more details where we shall deal with them individually.

The diagrams can be classified according to the number of the W-propagators they contain. The diagrams in Class 1 contain two W propagators while those in Class 2 contain one W^\pm and one s^\mp propagators. The diagrams in Class 3 are obtained by first constructing the Green's function for $K_0 K_0 \rightarrow 4$ charged charmed mesons ($4p$ or $2p + 2s$ or $4s$) and then closing it with s^+ and s^- propagators. The diagrams contributing to this Green's function are classified in Fig. 25(n), 25(o) and 25(p)

according to whether they contain a p. s. neutral intermediate state, a scalar intermediate state, or no neutral intermediate state at all respectively.

We shall compute only those terms which make a non-zero contribution to $\left\{ \lim_{m_K \rightarrow 0} \frac{m_L - m_S}{m_K} \right\}$, in other words, we shall drop the terms proportional to m^4 and higher powers of m_K^2 in the $K_0 - \bar{K}_0$ transition amplitude.

It is found that each of these diagrams, separately, may contain terms which grow like $(\ln \mu^2)$ multiplied by various powers [i. e., 0, 1, 2, ...] of $\frac{m_c^2}{M^2}$ and upto one power of $\ln M^2$ or $\ln m_c^2$ and terms which grow like $(\ln \mu^2)^2$ multiplied by various powers of $\frac{m_c^2}{M^2}$. Each kind of these terms must cancel separately, in order that the amplitude has a finite limit as $\mu^2 \rightarrow \infty$. Furthermore, it is not obvious here that the diagrams of Class 3 do not contain terms that grow like μ^2 as $\mu^2 \rightarrow \infty$. Also, each diagram in Classes 1 and 2 may contain terms that are proportional to M^0 or M^{-2} . Unless these terms cancel the amplitude will not be of $O(G_F^2)$, which it experimentally is. Finally, it is far from obvious that the two loop contribution to the $K^0 \rightarrow \bar{K}_0$ amplitude vanishes at $m_K^2 = 0$. Therefore, we shall show by direct calculation or otherwise that,

- (i) the two loop contribution vanishes at $m_K^2 = 0$,
- (ii) the amplitude has a finite limit as $\mu^2 \rightarrow \infty$,
- (iii) the amplitude is of $O\left(\frac{m_c^4}{M^4}\right)$ in the leading order, and then

compute the terms of the leading order.

(i) First, consider the amplitude at $m_K^2 = 0$. Any diagram whose left-most and/or right-most vertex is a meson-meson-W vertex is proportional to p^2 ($= m_K^2$ on mass shell) because such a vertex is proportional to p_μ in the Landau gauge (and because of the Lorentz invariance). Thus all the diagrams in Class 1 and all the diagrams in Class 2, except 25(f), 25(g), 25(h) and 25(l) are proportional to m_K^2 .

At $p = 0$, the diagrams in Fig. 25(f) cancel among themselves. For example, consider the subset of intermediate states contributing to Fig. 25(f) as shown in Fig. 26(a). Then we find the cancellation at $p = 0$ as shown in Figs. 26(b) and 26(c), when summed over all the unlabeled intermediate states. One can verify similar cancellations among the intermediate states in Fig. 25(g) and 25(l) taken together.

The fact that the sum of the diagrams of the class 3 vanishes at $p = 0$ is not so easy to see. We have given the proof in the Appendix I. We shall only outline the proof here. The sum of the diagrams can be shown to be proportional to the Green's function for the process

$$(\kappa_c^- + iK_c^-), (\kappa_c^- + iK_c^-), (\phi_c^+ - i\pi_c^+) (\phi_c^+ - i\pi_c^+) \rightarrow \bar{K}_0(p) \bar{K}_0(-p) \quad (9.4)$$

[which is defined to be the derivative of the generating functional of Green's function $Z[J]$, with respect to appropriate sources, e.g., $(J_{\kappa_c^-} + iJ_{K_c^-}), (J_{\phi_c^+} - iJ_{\pi_c^+}), J_{K_0}$ etc.] when $\underline{p} = 0$, the Green's function can be related to 4-point Green's functions not involving K_0 's through

the Ward identities that follow from the broken chiral $SU(4) \times SU(4)$ (global) symmetry of the strong interaction Lagrangian. These 4-point functions are much easier to evaluate directly than the original 6-point functions. Then one can easily verify that the Green's function of Eq. (9.4) vanishes at $p = 0$.²³ Thus, we have shown that the $K_0 - \bar{K}_0$ on mass shell amplitude is proportional to m_K^2 .

Now, consider the diagrams of Class 3 in Fig. 25. To examine their behavior for $|k^2|, |q^2|, |(k+q)^2| < \mu^2$ we may expand the scalar propagator,

$$\frac{1}{k^2 - \mu^2} = -\frac{1}{\mu^2} - \frac{k^2}{\mu^4} - \dots, \text{ etc.} \quad (9.5)$$

When this is done, there are contributions which behave as $\mu^4, \mu^2, \mu^0, \frac{1}{\mu^2} \dots$ and higher powers of $(\frac{1}{\mu^2})$. We shall show that the terms which grow as μ^4, μ^2 cancel among themselves. To this end, we note that in a 4-point function with 4 pseudoscalar external lines (not involving the $SU(4)$ singlet $\frac{1}{2} \text{tr } \Pi$), the terms proportional to μ^2 must cancel. This can be seen as follows: the terms proportional to μ^2 are independent of external momenta, hence they are the same if the external lines are on mass shell. But the on-mass shell 4-point function is equal to the corresponding on-mass shell 4-point function of the related nonlinear model which is independent of μ^2 , etc. We will use this to show the cancellation of the terms proportional to μ^2 and μ^4 in the diagrams for B.

The diagrams which may contain terms proportional to μ^2 and μ^4

and their cancellation are shown in Fig. 27. [Note that, here we are considering the Green's functions, i. e. , external propagators of mesons except those of K_0, \bar{K}_0 are included.] Figure 27(a) is just the statement made about the 4-point function of pseudoscalars. Because of this the terms proportional to μ^2 and μ^4 in the diagrams of Fig. 27(b) and Fig. 27(c) cancel. The diagrams in Fig. 27(d) together with those in Fig. 27(b) form a 6-point pseudoscalar Green's function, which must not have terms in μ^2 and μ^4 at least on mass shell, (as in the case of the four-point function). As shown above, the sum of the diagrams in Fig. 27(b) does not have them, while the terms proportional to μ^2 are independent of the external momenta. Hence, the terms proportional to μ^2 in the sum of diagrams in Fig. 27(d) must also cancel, etc.

Now consider the diagrams of Class 1, viz., those in Figs. 25(a) - (c). In Fig. 25(a), the π^0 and the η_8 pole diagrams can be summed together using

$$-\frac{3}{m_K^2 - m_\pi^2} = \frac{1}{m_K^2 - m_8^2} .$$

In the sum, the pole $\frac{1}{m_K^2 - m_\pi^2}$ cancels and the resulting amplitude is proportional to m_K^4 ; therefore, will not contribute to $\lim_{m_K \rightarrow 0} \frac{m_L - m_S}{m_K}$.

The diagram with the η'_c pole is also proportional to m_K^4 . The other pole diagrams are of $O\left(\frac{1}{\mu^2}\right)$, therefore we neglect them. The diagrams in Fig. 25(b) and (25(c) are redrawn with details in Figs. 28 and 29 respectively.

The sum of all the diagrams in Fig. 28 is given by

$$\begin{aligned}
\mathcal{M}(28) = & 2 \left[2A(000) - A(00m) - A(m00) + \frac{2}{3}A(m0m) + \frac{4}{3}A(mm'm) \right. \\
& \left. - A(0mm) - A(mm0) \right] \\
& + 2 \left[-A(\mu 00) - A(00\mu) + \frac{1}{3}A(m0\mu) + \frac{1}{3}A(\mu 0m) - \frac{4}{3}A(\mu m'm) \right. \\
& - \frac{4}{3}A(mm\mu) + A(0m\mu) + A(\mu m0) + A(mm\mu) + A(\mu mm) \\
& + \frac{2}{3}A(\mu 0\mu) + \frac{4}{3}A(\mu m'm) - 2A(\mu m\mu) \\
& \left. - A(0\mu 0) - A(m\mu m) + A(0\mu m) + A(m\mu 0) \right] \quad (9.6)
\end{aligned}$$

where

$$\begin{aligned}
A(m_1 m_2 m_3) = & \frac{ig^4 p^\mu p^\nu}{4(2\pi)^8} \sin^2 \theta \cos^2 \theta \\
& \times \int \frac{d^4 k d^4 q}{(k^2 - m_1^2)} \frac{k^\beta q^\alpha \mathcal{D}_{\mu\alpha}(k) \mathcal{D}_{\nu\beta}(q)}{[(k+q)^2 - m_2^2](q^2 - m_3^2)(k^2 - M^2)(q^2 - M^2)} \quad (9.7)
\end{aligned}$$

$$p^2 = m_K^2, \quad m \equiv m_c, \quad m' \equiv m'_c.$$

It is easy to show, by appropriately grouping the terms in the second bracket, that these terms vanish as $\mu^2 \rightarrow \infty$. For example,

$[A(0\mu m) - A(m\mu m)]$ is finite and is proportional to (m^2/μ^2) . The terms in the first square bracket contribute to the amplitude. To see that their contribution is of $O\left(\frac{m_c^4}{M^4}\right)$, we regroup the terms in the first bracket as:

$$\begin{aligned}
& 4 \left[A(000) - A(m00) - A(00m) + A(m0m) \right] \\
& + \frac{8}{3} \left[A(mm'm) - A(m0m) \right] - 4 \left[A(mm0) - A(m00) \right].
\end{aligned}$$

The first square bracket in the above is in the form of a second derivative. It can be easily shown to be of $O\left(\frac{m_c^4}{M^4}\right)$. The second and the third square brackets contain terms of $O\left(\frac{m_c^2}{M^2}\right)$ each. However, these terms cancel between them. This can be seen by using $m_c'^2 = \frac{3}{2} m_c^2$ [i. e., $\frac{8}{3} m_c'^2 = 4 m_c^2$].

A similar discussion applies to the diagrams in Fig. 29. We shall only write those terms which are analogous to the first square bracket in Eq. (9.6):

$$\mathcal{M}(29) = 2 \left[B(000) - B(0m0) + \frac{4}{3} B(mm'm) - \frac{1}{3} B(m0m) - B(mmm) \right] \quad (9.8)$$

where

$$B(m_1 m_2 m_3) = \frac{ig^4 p^\mu p^\nu}{4(2\pi)^4} \sin^2 \theta \cos^2 \theta \times \int \frac{d^4 k d^4 q k^\alpha k^\beta \mathcal{D}_{\mu\nu}(k) \mathcal{D}_{\alpha\beta}(q)}{(k^2 - m_1^2)(k^2 - m_3^2) [(k+q)^2 - m_2^2] (k^2 - M^2)(q^2 - M^2)} \quad (9.9)$$

By an appropriate regrouping of the terms in Eq. (9.8), we can show, as above, that $\mathcal{M}(29)$ is also of $O\left(\frac{m_c^4}{M^4}\right)$.

Finally, consider the diagrams of Class 2. [Figures 25(d) - (m)]. These are obviously proportional to $\frac{1}{M^2}$ due to the couplings of s^\pm with the mesons. In each of the Figs. 25(d) - 25(m), there are intermediate states

for which the amplitude may be of $O\left(\frac{m_c^2}{M^2}\right)$. However, we have verified that such terms cancel between different intermediate states of the same diagram. Thus the total result for the diagrams of Class 2 is of $O\left(\frac{1}{M^4}\right)$. The diagrams of Class 3 are clear of $O\left(\frac{1}{M^4}\right)$.

We have computed the terms which are proportional to $\frac{m_c^4}{M^4} \ln \frac{M^2}{m_c^2}$. (There are no terms of the type $\frac{m_c^4}{M^4} \left(\ln \frac{M^2}{m_c^2}\right)^2$) These come from the diagrams of Class 1 and 2. Because of the factor $\ln \frac{M^2}{m_c^2} \gtrsim 6$, these are assumed to dominate over the terms not containing this factor [i. e., proportional to $\frac{m_c^4}{M^4}$]. The result is

$$\begin{aligned} \mathcal{M}(2\text{-loop}) = & -i m_K^2 \cdot \frac{\pi^4}{(2\pi)^8} \cdot \frac{9}{8} \cdot g^4 \sin^2 \theta \cos^2 \theta \cdot \frac{m_c^4}{M^4} \ln \frac{M^2}{m_c^2} \\ & + \text{terms of } O\left(\frac{m_c^4}{M^4}\right) . \end{aligned} \quad (9.10)$$

The contributions of both the one loop and the two loop diagrams to $(m_L - m_S)$ are separately positive. Their sum is,

$$\begin{aligned} \mathcal{M}(K_0 \rightarrow \bar{K}_0) = & -i m_K^2 \frac{G_F}{\sqrt{2}} \frac{\alpha}{\pi} \sin^2 \theta \cos^2 \theta \frac{m_c^2}{M^2 \sin^2 \theta_W} \\ & \left\{ \frac{11}{96} f_K^2 + \frac{9m_c^2}{64\pi^2} \ln \frac{M^2}{m_c^2} \right\} . \end{aligned} \quad (9.11)$$

The $K_L - K_S$ mass difference is given by,

$$\frac{m_L - m_S}{m_K} = - \frac{1}{i m_K^2} \mathcal{M}(K^0 \rightarrow \bar{K}^0) \approx 0.7 \times 10^{-14} \quad (9.12)$$

experimentally.

Using Eqs. (9.11) and (9.12) and $f_K \sin \theta = 33 \text{ Mev}$, we obtain

$$\Delta m_c \approx 0.7 \text{ GeV.}$$

It should be noted that we have computed the results as $m_K \rightarrow 0$ and therefore it is appropriate to think of the result as an estimate of the difference between the masses of the charmed and uncharmed mesons.

We also note that with this value of m_c , the two loop contribution is about three times larger than the one loop contribution.

It should be pointed out that in the quark model calculation of Ref. 4, the procedure of evaluating the matrix element of the effective $\Delta S = 2$ Lagrangian by inserting only the vacuum intermediate states is, in a sense, equivalent to only computing our one loop diagrams. The contribution of the two -loop diagrams is large and helps restrict the bound on m_c .

X. NUMERICAL ESTIMATES AND CONCLUSIONS

In this section we shall compute the branching ratios and compare them with the experimental data. We shall also compare our results with the results of the free quark model calculation of Ref. 5.

(A) $K_L \rightarrow \mu\bar{\mu}$

As remarked earlier in Sec. IV, we have found that there is a cancellation among the terms of the leading order: $O\left(G_F \alpha \frac{m_c^2}{M^2} \ln \frac{M^2}{m_c^2}\right)$.

The resulting amplitude from this set of diagrams is expected to be of $O\left(\frac{m_K^2}{M^2} G_F \alpha\right)$. In addition, the amplitude $K_L \rightarrow \gamma\gamma \rightarrow \mu\bar{\mu}$ also contributes to this process. To see the relative orders of magnitude, we note that if we parametrize the total amplitude for $K_L \rightarrow \mu\bar{\mu}$ as,

$$\mathcal{M}(K_L \rightarrow \mu\bar{\mu}) = \frac{G_F \alpha}{\sqrt{2} \pi} f_K \sin \theta \cos \theta \cdot \mathcal{A} \quad (10.1)$$

then we find, from the experimental decay rate for this process that

$$|\mathcal{A}| \approx \frac{1}{50} . \quad (10.2)$$

This is to be compared with

$$\frac{m_K^2}{M^2 \sin^2 \theta_W} \approx \frac{1}{5500} . \quad (10.3)$$

Furthermore, we know that the unitarity bound from the absorptive part of the amplitude $K_L \rightarrow \gamma\gamma \rightarrow \mu\bar{\mu}$ is of the same order as the experimental result.²¹ We thus conclude that the main contribution to the $K_L \rightarrow \mu\bar{\mu}$ amplitude comes from the two photon intermediate states. The same conclusion was reached in the free quark model calculation of Ref. 5. We have demonstrated that the result still holds even when strong interactions are taken into account.

(B) $K^+ \rightarrow \pi^+ e \bar{e}$

This process is of more interest because the result for the branching ratio in the free quark model was found to be close to the experimental bound. Recently, the result (not bound) has been reported for this branching ratio.¹⁵

From Eq. (7.26) we have

$$\begin{aligned} \mathcal{M}(K^+(p) \rightarrow \pi^+(r) e(k) \bar{e}(k)) \\ = + \frac{iG_F}{\sqrt{2}} \frac{\alpha}{4\pi} \sin \theta \cos \theta \left[\frac{1}{6} \ln \frac{m_c^2}{m_\pi^2} + \frac{31}{36} \right] \\ \times (p+r)^\mu \bar{u}(k) \gamma_\mu \nu(\bar{k}) + O(G_F^2). \end{aligned} \quad (7.26)$$

The result is of the same order of magnitude as the quark model estimate, in fact, same except for the replacement:

$$\ln \frac{m_c^2}{m_{\text{had}}^2} \rightarrow \left(\frac{3}{32} \ln \frac{m_c^2}{m_\pi^2} + \frac{31}{64} \right)$$

in the case of the fractionally charged quarks.

To obtain the branching ratio, the result is to be compared with the first order decay $K^+ \rightarrow \pi^0 e \nu$ which has the same phase space. We parametrize the amplitude for $K^+ \rightarrow \pi^0 e \nu$ as

$$\begin{aligned} \mathcal{M}[K^+(p) \rightarrow \pi^0(r) e \nu] = i 2 \frac{G_F}{\sqrt{2}} \sin \theta \left[(p+r)_\mu f_+(q^2) + (p-r)_\mu f_-(q^2) \right] \\ \times \bar{\nu}(k) \gamma^\mu \gamma_L e(\bar{k}) \end{aligned} \quad (10.4)$$

where $q^2 = (p - r)^2$. The contribution due to the term $f_-(q^2)(p - r)_\mu$ is small. Therefore, we shall neglect it. Also, we approximate:

$$f_+(q^2) \simeq f_+(0) \simeq 1/\sqrt{2} \quad . \quad (10.5)$$

We, then, find from Eqs. (7.26) and (10.4) that

$$\begin{aligned} \frac{\Gamma(K^+ \rightarrow \pi^+ e e^-)}{\Gamma(K^+ \rightarrow \pi^0 e \nu)} &= \frac{2 \cdot \left\{ \frac{\alpha}{4\pi} \left(\frac{1}{6} \ln \frac{m_c^2}{m_\pi^2} + \frac{31}{36} \right) \cos \theta \right\}^2}{(2f_+)^2} \\ &= \left\{ \frac{\alpha}{4\pi} \left(\frac{1}{6} \ln \frac{m_c^2}{m_\pi^2} + \frac{31}{36} \right) \cos \theta \right\}^2 \quad . \end{aligned} \quad (10.6)$$

Clearly, the result is not very sensitive to the value of m_c . As an example, let $m_c = 2, (5) \text{ GeV}$. Then using the experimental branching ratio for $K^+ \rightarrow \pi^0 e \nu$, we obtain,

$$\frac{\Gamma(K^+ \rightarrow \pi^+ e e^-)}{\Gamma(K^+ \rightarrow \text{all})} \simeq 0.75, (1.0) \times 10^{-7} \quad . \quad (10.7)$$

This is to be compared with the recent experimental result¹⁵ for the branching ratio

$$\left. \frac{\Gamma(K^+ \rightarrow \pi^+ e e^-)}{\Gamma(K^+ \rightarrow \text{all})} \right|_{\text{expt.}} = (2.3 \pm 0.8) \times 10^{-7} \quad . \quad (10.8)$$

Our result is in reasonable agreement with the experimental branching ratio. Of course, since the branching ratio is not very sensitive to the value of m_c , we cannot obtain a bound on m_c .

(C) $K_S \rightarrow \pi^0 e \bar{e}$

Equation (8.7) gives the amplitude for $K_S \rightarrow \pi^0 e \bar{e}$:

$$\begin{aligned} & \mathcal{M}(K_S(p) \rightarrow \pi^0(r) e(k) \bar{e}(\bar{k})) \\ &= i \frac{G_F}{\sqrt{2}} \frac{\alpha}{4\pi} \sin \theta \cos \theta \left\{ \frac{1}{6} \ln \frac{m_c^2}{m_\pi^2} + \frac{1}{3} \ln \frac{m_K^2}{m_\pi^2} - \frac{21}{36} \right\} \\ & \quad \times (p+r)_\mu \bar{u}(k) \gamma^\mu(\bar{k}) . \end{aligned} \quad (8.7)$$

We compared this with the branching ratio for the process

$K_L^0 \rightarrow \pi^+ e^- \bar{\nu}$, $\pi^- e^+ \nu$. As before, we find that,

$$\frac{2\Gamma(K_S \rightarrow \pi^0 e \bar{e})}{\Gamma(K_L \rightarrow \pi^+ e \bar{\nu}) + \Gamma(K_L \rightarrow \pi^- e \nu)} = \left\{ \frac{\alpha}{4\pi} \cos \theta \left(\frac{1}{6} \ln \frac{m_c^2}{m_\pi^2} + 0.27 \right) \right\}^2 \quad (10.9)$$

and thus

$$\frac{\Gamma(K_S \rightarrow \pi^0 e \bar{e})}{\Gamma(K_S \rightarrow \text{all})} = 3.2 \times 10^{-4} \left\{ \frac{\alpha}{4\pi} \cos \theta \left(\frac{1}{6} \ln \frac{m_c^2}{m_\pi^2} + 0.27 \right) \right\}^2 . \quad (10.9a)$$

Thus for $m_c = 2.0, 5.0$ Gev,

$$\frac{\Gamma(K_S \rightarrow \pi^0 e \bar{e})}{\Gamma(K_S \rightarrow \text{all})} = 1.4 \times 10^{-10}, 2.2 \times 10^{-10} \quad (10.10)$$

(D) $K^+ \rightarrow \pi^+ \nu \bar{\nu}$

We compare the decay rates for $K^+ \rightarrow \pi^+ \nu_e \bar{\nu}_e$, $\pi^+ \nu_\mu \bar{\nu}_\mu$ with that for $K^+ \rightarrow \pi^0 e \nu$. The decay amplitude for the process $K^+ \rightarrow \pi^+ \nu \bar{\nu}$ is given in Eq. (5.13):

$$\begin{aligned}
& \mathcal{M}(K^+(p) \rightarrow \pi^+(r) \nu(k) \bar{\nu}(\bar{k})) \\
&= -i \frac{3}{4} \frac{G_F}{\sqrt{2}} \frac{\alpha}{\pi} \sin \theta \cos \theta \frac{m_c^2}{M^2 \sin^2 \theta_W} \left\{ \ln \frac{M^2}{m_c^2} + \frac{1}{6} \right\} \\
&\quad \times (p+r)^\mu \bar{u}(k) \gamma_\mu \gamma_L \nu(\bar{k}) + 0 \left(G_F \alpha \frac{m_K^2}{M^2} \right). \quad (5.13)
\end{aligned}$$

From Eqs. (5.13) and (10.4), we obtain,

$$\frac{\Gamma(K^+ \rightarrow \pi^+ \nu_\mu \bar{\nu}_\mu) + \Gamma(\pi^+ \nu_e \bar{\nu}_e)}{\Gamma(K^+ \rightarrow \pi^0 e \nu_e)} = \left[\frac{3\alpha}{4\pi} \frac{m_c^2 \cos^2 \theta_c}{(38 \text{ GeV})^2} \left(\ln \frac{M^2}{m_c^2} + \frac{1}{6} \right) \right]^2 \quad (10.11)$$

from which, we find:

$$\frac{\Gamma(K^+ \rightarrow \pi^+ \nu_\mu \bar{\nu}_\mu) + \Gamma(\pi^+ \nu_e \bar{\nu}_e)}{\Gamma(K^+ \rightarrow \text{all})} = 0.8 \times 10^{-6} \left\{ \frac{m_c^2}{(38 \text{ GeV})^2} \ln \frac{M}{m_c} \right\}^2. \quad (10.12)$$

The present experimental bound on this branching ratio is

$$\frac{\Gamma(K^+ \rightarrow \pi^+ \nu \bar{\nu})}{\Gamma(K^+ \rightarrow \text{all})} < 0.6 \times 10^{-6} \quad (10.13)$$

and it does not allow us to place a meaningful bound on m_c . Our result is in close agreement with the result of the free quark model calculation.

$$(E) \quad K_S^0 \rightarrow \pi^0 \nu \bar{\nu}$$

The decay amplitude for the process $K_S^0 \rightarrow \pi^0 \nu \bar{\nu}$ is given by

Eq. (6.16):

$$\begin{aligned}
& \mathcal{M}(K_S(p) \rightarrow \pi^0(r) \nu(k) \bar{\nu}(\bar{k})) \\
&= i \frac{G_F}{\sqrt{2}} \frac{\alpha}{2\pi} \sin \theta \cos \theta \frac{m_c^2}{M^2 \sin^2 \theta_W} \left\{ \frac{3}{2} \ln \frac{M^2}{m_c^2} - \frac{1}{4} \right\} \\
&\quad \times (p+r)_\mu \bar{u}(k) \gamma^\mu \gamma_L v(\bar{k}) . \tag{6.14}
\end{aligned}$$

Comparing this with the decay width for the process $K_L \rightarrow \pi^\pm e^\mp \nu$,

we obtain

$$\frac{\Gamma(K_S \rightarrow \pi^0 \nu_\mu \bar{\nu}_\mu) + \Gamma(K_S \rightarrow \pi^0 \nu_e \bar{\nu}_e)}{\Gamma(K_L \rightarrow \pi^+ e^- \bar{\nu}_e) + \Gamma(K_L \rightarrow \pi^- e^+ \nu_e)} = \left\{ \frac{3\alpha}{2\pi} \cos \theta \frac{m_c^2}{(38 \text{ GeV})^2} \left(\ln \frac{M^2}{m_c^2} - \frac{1}{6} \right) \right\}^2 \tag{6.15}$$

and thus

$$\frac{\Gamma(K_S \rightarrow \pi^0 \nu_\mu \bar{\nu}_\mu) + \Gamma(K_S \rightarrow \pi^0 \nu_e \bar{\nu}_e)}{\Gamma(K_S \rightarrow \text{all})} \simeq 0.5 \times 10^{-8} \left\{ \frac{m_c^2}{(38 \text{ GeV})^2} \ln \frac{M}{m_c} \right\}^2 \tag{6.16}$$

In conclusion, we have, here, constructed a phenomenological model unifying strong, weak and electromagnetic interactions. The model of strong interactions is constructed to incorporate the results of $SU(4) \times SU(4)$ current algebra and PCAC; thus incorporating the low energy phenomenology.

We have found that our results are in qualitative agreement with the quark model estimates of Ref. 5. We have also found that the amplitude for $K_0 \rightarrow \mu\bar{\mu}$ which proceeds via exchange of only the heavy vector

bosons (W^\pm, Z) is unexpectedly small due to the cancellation of the leading order terms i. e., $O\left(G_F \propto \frac{m_c^2}{M^2}\right)$. The experimental knowledge of this process does not allow us to infer about the average mass of the charmed mesons therefore. Our results for the $K^+ \rightarrow \pi^+ e\bar{e}$ branching ratio is in reasonably good agreement with the recent experimental result.¹⁵ The experimental bound on the $K^+ \rightarrow \pi^+ \nu\bar{\nu}$ branching ratio is not stringent enough to allow us to obtain a bound on m_c , at present, via this decay. However, calculation of the $K_L - K_S$ mass difference in the model puts a strong bound on the average mass of the charmed mesons. Our estimates of m_c are strongly indicative that the charmed mesons must lie in the few GeV range.

ACKNOWLEDGMENTS

I would like to thank Professor B. W. Lee for suggesting the problem and reading the manuscript. I would also like to thank Professor M. K. Gaillard and Professor B. W. Lee for discussions on this subject.

APPENDIX A

Feynman Rules

In this Appendix, we shall give some of the Feynman rules (or interaction terms) relevant in our calculation.

(1) Vector meson and Higgs' scalar interactions: [See the Lagrangian of Eq. (2.4)]

$$W_{\mu}^{\pm} = \frac{B_{1\mu} \mp iB_{2\mu}}{\sqrt{2}} \quad Z_{\mu} = \frac{gB_{3\mu} - g'B_{0\mu}}{G}$$

$$A_{\mu} = \frac{g'B_{3\mu} + gB_{0\mu}}{G} \quad G = \sqrt{g^2 + g'^2}$$

$$e = -gg'/G \quad \cos \theta_W = g/G \quad \sin \theta_W = g'/G.$$

The relevant interaction terms are:

$$s^+ s^- A_{\mu} : \quad ie A_{\mu} (s^+ \partial_{\mu} s^- - s^- \partial_{\mu} s^+)$$

$$s^+ s^- Z_{\mu} : \quad -i \left(\frac{g^2 - g'^2}{G} \right) Z_{\mu} (s^+ \partial_{\mu} s^- - s^- \partial_{\mu} s^+)$$

$$s^+ W^{-} \chi : \quad -\frac{1}{2} g W^{-\mu} (\partial_{\mu} \chi s^+ - \chi \partial_{\mu} s^+) + \text{h.c.}$$

$$s^+ W^{-} A : \quad -e M_{\chi} A^{\mu} (W_{\mu}^{+} s^- + s^+ W_{\mu}^{-})$$

$$s^+ W^{-} Z : \quad G \cos^2 \theta_W M_{\chi} Z_{\mu} (W_{\mu}^{+} s^- + W_{\mu}^{-} s^+).$$

The Feynman rules for the $W^+ W^- A$ and the $W^+ W^- Z$ vertices

are:

$$W_{\alpha}^{+}(p) W_{\beta}^{-}(q) A_{\mu}(r): \quad -ie \left\{ (p-q)_{\mu} g_{\alpha\beta} + (q-r)_{\alpha} g_{\mu\beta} + (r-p)_{\beta} g_{\mu\alpha} \right\}$$

$$W_{\alpha}^{+}(p) W_{\beta}^{-}(q) Z_{\mu}(r): \quad i G \cos^2 \theta_W \left\{ (p-q)_{\mu} g_{\alpha\beta} + (q-r)_{\alpha} g_{\mu\beta} + (r-p)_{\beta} g_{\mu\alpha} \right\}$$

where the fields and the momenta p, q, r enter the vertex.

(2) Leptonic Interactions:

Here, we shall give the interaction terms for the μ -leptons.

[The interaction terms for the e -leptons can be obtained by $(\mu, \nu) \rightarrow (e, \nu_e)$.] They are

$$\left\{ \frac{G}{2} \bar{\nu} \gamma_{\mu} \gamma_L \nu + \bar{\mu} \gamma_{\mu} \left(\frac{g^2 - g'^2}{G} \gamma_L - \frac{g'^2}{G} \gamma_R \right) \mu \right\} Z^{\mu} + \frac{g}{2} (\bar{\nu} \gamma_{\mu} \gamma_L \mu W^{+\mu} + \text{h.c.})$$

$$+ e \bar{\mu} \gamma_{\mu} \mu A^{\mu} + \frac{gm_{\mu}}{2M} \left[2(\bar{\nu} \gamma_R s^{+} + \text{h.c.}) + \bar{\mu} \mu \psi_0 + \bar{\mu} i \gamma_5 \mu \chi \right].$$

(3) Meson (Σ, Π), Vector meson (W, Z, A) Interactions

These are obtained from the Lagrangian of Eq. (2.14). We shall use Π, Σ and B to collectively denote the pseudoscalar, the scalar and the gauge bosons respectively. Also, wherever applicable, we shall write the Feynman rules only in the case of the exact $SU(3)$ symmetry (and $m_K^2 = m_{\pi}^2 = 0$, etc.). Changes due to the $SU(3)$ breaking can be obtained easily from these.

(a) ΠB Couplings:

These can be obtained from: $-\text{tr} \left\{ \left[g(T_{+} W_{+\mu} + T_{-} W_{-\mu}) + G T_3 Z \right] F \partial^{\mu} \Pi \right\}$.

(i) Feynman rules for $\Pi^{\pm}(q) \rightarrow W_{\mu}^{\pm}(q)$: unit $\frac{-gf}{\sqrt{2}} q_{\mu}$

Field II	π	K	π_c	K_c
Vertex	$-\cos \theta$	$-\sin \theta$	$\sin \theta(1+\epsilon)$	$-\cos \theta(1+\epsilon)$

(ii) Feynman rules for $\Pi^0(q) \rightarrow Z_\mu(q)$: unit $\frac{igf}{2\sqrt{2}} q_\mu$

Field II	η_c	π_0	η_8	η_0
Vertex	$(1+\epsilon)$	$\sqrt{2}$	$\frac{2}{\sqrt{6}}$	$-\frac{1}{\sqrt{3}}$

(b) Σ B Couplings:

These are obtained from: $-\frac{i}{2} \text{tr} \left[F, \partial_\mu \tilde{\Sigma} \right] (T_+ W_+^\mu + T_- W_-^\mu)$

Feynman rules for $\Sigma^\pm(q) \rightarrow W_\mu^\pm(q)$; unit: $\frac{ig\epsilon}{2\sqrt{2}} q_\mu$

Field Σ	ϕ_c^+	ϕ_c^-	κ_c^+	κ_c^-
Vertex	$\sin \theta$	$-\sin \theta$	$-\cos \theta$	$\cos \theta$

There are no ΣZ vertices.

(c) $\Sigma^\pm \rightarrow s^\pm$ and $\Pi^\pm \rightarrow s^\pm$ and $\Pi^\pm \rightarrow s^\pm$ Eq. (2.16)

unit: $-\frac{igf}{\sqrt{2}} \frac{m_c^2}{M}$

Field	π_c^+	π_c^-	K_c^+	K_c^-	ϕ_c	κ_c
Vertex	$i \sin \theta$	$-i \sin \theta$	$-i \cos \theta$	$i \cos \theta$	$-\sin \theta$	$\cos \theta$

(d) $\Pi \Pi W$ Couplings:

We tabulate below the Feynman rules for

$$\Pi^-(p) \rightarrow W_\mu^-(p-q) \Pi^0(q) .$$

For brevity, we shall omit a factor of $+\cos \theta$ or $+\sin \theta$ which can be easily supplied by observation. The Feynman rules for

$\Sigma^-(p) \rightarrow \Sigma^0(q) W_\mu^-(p-q)$ are given by the same table with appropriate

replacements $\Pi \rightarrow \Sigma$. The Feynman rules for the process $\Pi^+(p) \rightarrow \Pi^0(q) W_\mu^-(p-q)$ need only a sign change.

Feynman rules for $\Pi^-(p) \rightarrow \Pi^0(q) W_\mu^-(p-q)$

$$\text{unit: } \frac{ig}{2\sqrt{2}} (p+q)_\mu \left[\sin \theta / \cos \theta \right]$$

	π^-	K^-	π^-	K_c^-
π_0	$-\sqrt{2}$	$-1/\sqrt{2}$	$1/\sqrt{2}$	0
\bar{K}_0	1	1	1	-1
\bar{X}_{0c}	1	-1	-1	-1
η_8	0	$-3/\sqrt{6}$	$-1/\sqrt{6}$	$-2/\sqrt{6}$
η_0	0	0	$-1/\sqrt{3}$	$1/\sqrt{3}$
η_c	0	0	1	-1

(e) $\Pi \Sigma W$ Couplings:

Feynman rules for $\Pi^\pm(p) \rightarrow \Sigma^0(q) W_\mu^\pm(q)$

$$\text{unit: } \frac{g}{2\sqrt{2}} (p+q)_\mu \left[\sin \theta / \cos \theta \right]$$

	π^\pm	K^\pm	π_c^\pm	K_c^\pm
ϕ_0	0	$1/\sqrt{2}$	$1/\sqrt{2}$	0
$\kappa_0 (\bar{\kappa}_0)$	1	1	1	-1
$Y_{0c} (\bar{Y}_{0c})$	-1	1	1	1
ξ_8	$2\sqrt{6}$	$-1\sqrt{6}$	$-1\sqrt{6}$	$-2\sqrt{6}$

ξ_0	$2/\sqrt{3}$	$2/\sqrt{3}$	$-1/\sqrt{3}$	$1/\sqrt{3}$
ξ_c	0	0	-1	1

The Feynman rules for $\Sigma^+(p) \rightarrow \Pi^0(q) W_\mu^\pm(p-q)$ are obtained by replacements $\Sigma \leftrightarrow \Pi$ and a change in sign.

(f) $\Pi \chi$ Vertex:

$$\eta_c \chi = \frac{-igf m_c^2}{M} .$$

(g) $\Pi \Pi Z$ Interaction Terms: These can be obtained from,

$$-\frac{i}{2} \text{tr} \left\{ G Z_\mu T_3 \left[\Pi, \partial^\mu \Pi \right] + g' B_{0\mu} \left[(C\Pi) \partial^\mu \Pi + \partial^\mu \Pi (C\Pi) \right] \right\}$$

where,

$$(C\Pi)_{ij} = e_{ij} \Pi_{ij} ; \quad e_{ij} = \text{electric charge of } \Pi_{ij} (1, 0, -1) .$$

We shall write only those couplings which we have used:

$$-i Z^\mu \left(\frac{g^2 - g'^2}{2} \right) \left\{ (K^+ \partial_\mu K^- - K^- \partial_\mu K^+) + (\pi^+ \partial_\mu \pi^- - \pi^- \partial_\mu \pi^+) \right\} .$$

(h) $\Pi \Sigma Z$ Interaction Terms:

Only the neutral mesons have such vertices. They are obtained from,

$$\mathcal{L}_{\Pi \Sigma Z} = \frac{1}{2} G Z_\mu \text{tr} \left\{ T_3 (\Pi \partial^\mu \tilde{\Sigma} - \tilde{\Sigma} \partial^\mu \Pi + \partial^\mu \tilde{\Sigma} \Pi - \partial \Pi \tilde{\Sigma}) \right\} .$$

We shall write down those vertices which we have used:

$$\mathcal{L}_{\Pi\Sigma Z} = \frac{GZ^\mu}{2} \left\{ \sqrt{2} \pi_0 \overleftrightarrow{\partial}_\mu \left(\frac{\xi_8}{\sqrt{6}} + \frac{\xi_0}{\sqrt{3}} \right) - \left(\frac{2\eta_8}{\sqrt{6}} - \frac{\eta_0}{\sqrt{3}} \right) \overleftrightarrow{\partial} \left(\frac{2\xi_8}{\sqrt{6}} - \frac{\xi_0}{\sqrt{3}} \right) + \dots \right. \\ \left. + \bar{X}_c^0 \overleftrightarrow{\partial}_\mu Y_{0c} + X_c^0 \overleftrightarrow{\partial}_\mu \bar{Y}_{0c} - K_0 \overleftrightarrow{\partial}_0 \bar{\kappa}_0 - \bar{K}_0 \overleftrightarrow{\partial}_\mu \bar{\kappa}_0 \right\} + \dots$$

(g) W^\pm_γ II Interaction Terms:

These are given by

$$\frac{-igf}{2} \left[-\pi_c^- \sin \theta \left(1 + \frac{\epsilon}{2} \right) + K_c^- \cos \theta \left(1 + \frac{\epsilon}{2} \right) + K^- \sin \theta + K_c^- \cos \theta \right] W_\mu^+ A^\mu$$

+ h. c.

APPENDIX B

The Ward-Takahashi Identities for Proper Vertices

Since the use of the Ward-Takahashi (WT) identities simplify the calculations considerably, we shall explain them briefly.

WT identity for proper vertices in arbitrary gauge field theories have been derived in Ref. (25). We shall only quote the result and express it for the Lagrangian \mathcal{L} of Eq. (2.14). In the notation of Ref. 25, the WT identity for the generating functional of proper vertices $\Gamma[\Phi]$ is,

$$L_i^\alpha \frac{\delta \Gamma_0}{\delta \Phi_i} = 0 \quad (\text{B. 1})$$

where, the subscript i runs over all fields in the Lagrangian and over the space time; and

$$L_i^\alpha = \partial_i^\alpha + g^\alpha t_{ij}^\alpha \Phi_j + \gamma_i^\alpha[\Phi] \quad (\text{B. 2})$$

$$\Gamma_0[\Phi] = \Gamma[\Phi] + \frac{1}{2} \left\{ F_\alpha[\Phi] \right\}^2$$

$$\gamma_i^\alpha[\Phi] = -i t_{ij}^\beta \Delta_{jk}[\Phi] G_{\beta\gamma}[\Phi] \left(\frac{\delta}{\delta \Phi_k} G_{\gamma\alpha}^{-1}[\Phi] \right).$$

In one loop approximation, $\gamma_i^\alpha[\Phi]$ does not contribute to the processes that we shall use WT identities for, essentially because the pseudoscalar and the scalar mesons (Σ, Π) do not couple to the Faddeev-Popov ghosts directly in the gauge we have chosen [see Eq. (2.7).]

When $\gamma_i^\alpha[\Phi]$ is dropped $\left\{ - \sum_\alpha \frac{\theta^\alpha}{g_\alpha} L_i^\alpha \frac{\delta}{\delta \Phi_i} \right\}$ becomes the operator

which produces the change in a functional under an infinitesimal gauge transformation of the gauge group described by parameters $\{\theta_\alpha\}$.

In this Appendix only, we shall, for the lack of symbols, use M, Σ, Π , etc., etc., to denote the expectation value of the meson fields, etc., etc., in the presence of the external sources (instead of the fields themselves). Σ_k, Π_k are 4×4 matrices and k refers to the space time point x_k of the fields in Σ and Π . [The notation used here will be somewhat different from the usual (e.g., in Ref.25). We have separated the space time index and the field index for the meson fields. The field index is identical to the matrix indices of the fields in Σ and Π .]

Then, dropping $\gamma_i^\alpha[\Phi]$, the WT identity in our notation becomes,

$$\delta^\alpha B_i \frac{\delta \Gamma_0}{\delta B_i} + \text{tr} \left\{ \delta^\alpha M_k \frac{\delta \Gamma_0^T}{\delta M_k} + \delta^\alpha M_k \frac{\delta \Gamma_0^T}{\delta M_k} \right\} + \delta^\alpha s_n \frac{\delta \Gamma_0}{\delta s_n} = 0 \quad (\text{B.4})$$

where,

$$-\delta^\alpha B_i = \frac{1}{g_\alpha} \partial_i^\alpha + \epsilon_{ij}^\alpha B_j$$

$$\delta^\alpha M_k = -i T_L^\alpha M_k + i M_k T_R^\alpha$$

$$\delta^\alpha M_k^\dagger = i M_k^\dagger T_L^\alpha - i T_R^\alpha M_k^\dagger$$

$$\delta^\alpha s_n = \frac{-i}{2} \tau_{nm}^\alpha s_m$$

[$\tau^0 = 1$, $\tau^\alpha (\alpha = 1, 2, 3)$ are the Pauli matrices]

$$\left(\frac{\delta \Gamma_0^T}{\delta M} \right)_{\beta \gamma} \equiv \frac{\delta \Gamma_0}{\delta M_{\gamma \beta}} \quad . \quad (B.5)$$

[For the sake of notational simplicity, here too, we have made some changes as compared to the usual summation integration convention. For example, $\delta^\alpha M_k$ is a 4×4 matrix with two space-time arguments x_α, x_k . Its $(\xi, \eta)^{th}$ matrix element is given by,

$$(\delta^\alpha M_k)_{\xi \eta} = -i(T_L^\alpha)_{\xi \sigma, kj} (M_j)_{\sigma \eta} + i(M_j)_{\xi \sigma} (T_R^\alpha)_{\sigma \eta, jk}$$

where jk refer to x_j and x_k ; ξ, σ, η are matrix indices; and $(T_L^\alpha)_{\xi \sigma, kj} \sim (T_L^\alpha)_{\xi \sigma} \delta^4(x_\alpha - x_k) \delta^4(x_\alpha - x_j)$ etc. So long as one keeps this in mind, the simplified notation used here, will not cause confusion.]

We shall not differentiate the WT identity with respect to the gauge fields nor with respect to the Higgs fields (s_n) in our applications. Hence, in our applications, we may put $B_i = \langle B_i \rangle_{vac} \equiv 0$ and $s^\pm = \langle s^\pm \rangle_{vac} \equiv 0$ and $\chi = \langle \chi \rangle_{vac} \equiv 0$ in Eq. (B.4). Therefore, we may replace Γ_0 by Γ [See Eq. (B.3)] and drop the second term in $\delta^\alpha B_i$ of Eq. (B.5).

Then the WT identity becomes,

$$-\frac{1}{g_\alpha} \partial_i^\alpha \frac{\delta \Gamma}{\delta B_i} + \text{tr} \left\{ (-i T_L^\alpha M_k + i M_k T_R^\alpha) \frac{\delta \Gamma^T}{\delta M_k} + (i M_k^\dagger T_L^\alpha - i T_R^\alpha M_k^\dagger) \frac{\delta \Gamma^T}{\delta M_k^\dagger} \right\} + \delta^\alpha s_n \frac{\delta \Gamma}{\delta s_n} = 0 \quad . \quad (B.6)$$

Expressing Eq. (B.6) in terms of Σ and Π , we obtain after some simplifications:

$$\begin{aligned}
& -\frac{1}{\alpha} \partial_i^\alpha \frac{\delta \Gamma}{\delta B_i} + \frac{i}{2} \text{tr} \left\{ \left[\left(\frac{\delta \Gamma^T}{\delta \Sigma_k} \Sigma_k - \Sigma_k \frac{\delta \Gamma^T}{\delta \Sigma_k} \right) + \left(\frac{\delta \Gamma^T}{\delta \Pi_k} \Pi_k - \Pi_k \frac{\delta \Gamma^T}{\delta \Pi_k} \right) \right] (T_L^\alpha + T_R^\alpha) \right\} \\
& + \frac{1}{2} \text{tr} \left\{ \left[\left(\frac{\delta \Gamma^T}{\delta \Pi_k} \Sigma_k + \Sigma_k \frac{\delta \Gamma^T}{\delta \Pi_k} \right) - \left(\frac{\delta \Gamma^T}{\delta \Sigma_k} \Pi_k + \Pi_k \frac{\delta \Gamma^T}{\delta \Sigma_k} \right) \right] (T_R^\alpha - T_L^\alpha) \right\} \\
& + \delta^\alpha_s \frac{\delta \Gamma}{\delta s_n} = 0 \quad . \quad (B.7)
\end{aligned}$$

From Eq. (B.7) we shall derive the desired WT identities in special cases successively.

$$(1) \quad \underline{K^+ \rightarrow \pi^+ \nu \bar{\nu}}$$

Here, we shall derive the WT identity of Eq. (5.1) for the $K^+ \pi^- Z$ vertex.

We first note that,

$$\begin{aligned}
\frac{\delta}{\delta Z_\mu} &= \frac{g}{G} \frac{\delta}{\delta B_{3\mu}} - \frac{g'}{G} \frac{\delta}{\delta B_{0\mu}} \\
&= \frac{g^2}{G} \frac{1}{g} \frac{\delta}{\delta B_{3\mu}} - \frac{g^2}{2G} \frac{1}{(g'/2)} \frac{\delta}{\delta B_{0\mu}} \quad . \quad (B.8)
\end{aligned}$$

With the help of Eq. (B.8), the WT identity of Eq. (B.7) can be written, for the special case, as

$$\begin{aligned}
& -\partial_{\mu} \frac{\delta \Gamma}{\delta Z_{\mu}} + \frac{i}{2} \text{tr} \left\{ \left[\frac{\delta \Gamma^T}{\delta \Sigma_k} \Sigma_k - \Sigma_k \frac{\delta \Gamma^T}{\delta \Sigma_k} \right] + \left(\frac{\delta \Gamma^T}{\delta \Pi_k} \Pi_k - \Pi_k \frac{\delta \Gamma^T}{\delta \Pi_k} \right) \left(\frac{g^2}{G} T_3 - \frac{g^2}{2G} (Y_L + Y_R) \right) \right\} \\
& + \frac{1}{2} \text{tr} \left\{ \left[\frac{\delta \Gamma^T}{\delta \Pi_k} \Sigma_k + \Sigma_k \frac{\delta \Gamma^T}{\delta \Pi_k} \right] - \left(\frac{\delta \Gamma^T}{\delta \Sigma_k} \Pi_k + \Pi_k \frac{\delta \Gamma^T}{\delta \Sigma_k} \right) \left(-\frac{g^2}{G} T_3 - \frac{g^2}{2G} (Y_R - Y_L) \right) \right\} \\
& + \frac{1}{2} G v \frac{\delta \Gamma}{\delta \chi} = 0 \quad . \quad (B.9)
\end{aligned}$$

Here, we have used,

$$\delta^{(3)} \chi \Big|_{\text{vac}} = \frac{v}{2} \quad \delta^{(0)} \chi \Big|_{\text{vac}} = -\frac{v}{2} \quad .$$

We differentiate the WT identity with respect to K_m^+ and π_n^- and set $\Sigma = F$, $\Pi = 0$. We note:

(i) The diagonal elements of $\frac{\delta^2}{\delta K_m^+ \delta \pi_n^-} \left(\frac{\delta \Gamma^T}{\delta \Sigma_k} \Sigma_k - \Sigma_k \frac{\delta \Gamma^T}{\delta \Sigma_k} \right)$ are zero. $\Sigma = F$,
 $\Pi = 0$

$$(ii) \quad \frac{-g^2}{G} T_3 - \frac{g^2}{2G} (Y_L - Y_R) = -G T_3$$

$$(iii) \quad \frac{g^2}{G} T_3 - \frac{g^2}{2G} (Y_L + Y_R) = \text{Diag} \left(\frac{1}{2} \frac{g^2}{G} - \frac{5}{6} \frac{g^2}{G}, \frac{1}{2} \frac{g^2}{G} - \frac{5}{6} \frac{g^2}{G}, \right. \\ \left. -\frac{1}{2} \frac{g^2}{G} + \frac{1}{6} \frac{g^2}{G}, -\frac{1}{2} \frac{g^2}{G} + \frac{1}{6} \frac{g^2}{G} \right)$$

$$(iv) \quad \frac{\delta^2}{\delta K_m^+ \delta \pi_n^-} \text{tr} \left\{ \left(\frac{\delta \Gamma^T}{\delta \Sigma_k} \Pi_k + \Pi_k \frac{\delta \Gamma^T}{\delta \Sigma_k} \right) \left(\frac{g^2}{G} T_3 + \frac{g^2}{G} (Y_R - Y_L) \right) \right\} = 0.$$

Using these, we obtain,

$$\begin{aligned}
& -\partial^\mu \frac{\delta^3 \Gamma}{\delta Z_\mu \delta K_m^+ \delta \pi_n^-} + \frac{i}{2} \left(\frac{\delta^2 \Gamma}{\delta K_m^+ \delta \pi_n^-} \delta_{kn} - \frac{\delta^2 \Gamma}{\delta K_k^+ \delta \pi_n^-} \delta_{km} \right) \left(\frac{g^2 - g'^2}{G} \right) \\
& - \frac{1}{2} \sum_k 2 \cdot \frac{\delta^3 \Gamma}{\delta K_m^+ \delta \pi_n^- \delta \Pi_{kk}} f_k G(T_3)_{kk} + \frac{Gv}{2} \frac{\delta^3 \Gamma}{\delta \chi \delta K_m^+ \delta \pi_n^-} = 0 \quad .
\end{aligned} \tag{B.10}$$

Writing Eq. (B.10) in momentum space (see also Fig. 11), we obtain,

$$\begin{aligned}
q_\mu \Gamma_Z^\mu(p, q) - i M_Z \Gamma_\chi(p, q) &= - \frac{i}{2} G \sum_k f_k t_{3k} \Gamma_k^{(3)}(p, q) \\
&= \frac{-(g^2 - g'^2)}{2G} \left[\Sigma_+(p) - \Sigma_+(p-q) \right]
\end{aligned} \tag{B.11}$$

where,

$\Gamma_Z^\mu(p, q)$ is the $K^+(p) \rightarrow \pi^+(p-q) Z^\mu(q)$ proper vertex.

$\Gamma_\chi(p, q) = K^+ \pi^- \chi$ proper vertex

$\Sigma_+ = K^+ \pi^-$ self energy

$i\Gamma_k^{(3)}(p, q) = \text{F. T.} \left\{ \frac{\delta^3 \Gamma}{\delta K_m^+ \delta \pi_n^- \delta \Pi_{kk}} \right\}$

$t_{3i} = 1 \quad i = 1, 2$
 $\quad = -1 \quad i = 3, 4 .$

(2) $K^0 \rightarrow \pi^0 \nu \bar{\nu}$

Here, we shall derive the WT identity of Eq. (6.1) for the $K^0 \pi^0 Z$ proper vertex. This derivation is similar to that for the $K^+ \pi^- Z$

proper vertex, hence we shall be brief. We differentiate Eq. (B.9) with respect to K_m^0 and π_n^0 and set $\Sigma = F$, $\Pi = 0$. We note that the second term in Eq. (B.9) does not contribute. We shall only give the final result. It is

$$\begin{aligned}
& -\partial_\mu \frac{\delta^3 \Gamma}{\delta Z_\mu \delta K_m^0 \delta \pi_n^0} - \frac{1}{2} \sum_k 2G(T_3)_{kk} f_k \frac{\delta^3 \Gamma}{\delta \Pi_{kk} \delta K_m^0 \delta \pi_n^0} \\
& - \frac{G}{2} \left[\frac{\delta^2 \Gamma}{\delta \kappa_k^0 \delta \pi_n^0} \delta_{km} - \frac{1}{\sqrt{3}} \frac{\delta^2 \Gamma}{\delta \xi_8^0 \delta K_m^0} \delta_{kn} - \frac{\sqrt{2}}{\sqrt{3}} \frac{\delta^2 \Gamma}{\delta \xi_0^0 \delta K_m^0} \delta_{kn} \right] \\
& + \frac{Gv}{2} \frac{\delta^3 \Gamma}{\delta \Pi_{kk} \delta K_m^0 \delta \pi_n^0} = 0 \quad . \quad (B.12)
\end{aligned}$$

Writing Eq. (B.12) in momentum space, (also see Fig. 15), we obtain,

$$\begin{aligned}
q_\mu \Gamma_{0z}^\mu(p, q) &= iM_z \Gamma_{0\chi}(p, q) - \frac{iG}{2} \sum_k f_k t_{3k} \Gamma_k^{(3)}(p, q) \\
&+ \frac{iG}{2} \left\{ \frac{1}{\sqrt{3}} \Sigma_0(p) + \frac{\sqrt{2}}{\sqrt{3}} \Sigma_0'(p) - \Sigma_0''(p-q) \right\} \quad (B.13)
\end{aligned}$$

where

$$\Gamma_{0z}^\mu(p, q) = K_0(p) \rightarrow \pi^0(p-q) Z^\mu(q) \text{ proper vertex}$$

$$\Gamma_{0k}^{(3)}(p, q) = K_0 \pi_0 \Pi_{kk} \text{ proper vertex}$$

$$\Gamma_{0\chi}(p, q) = K_0 \pi^0 \chi \text{ proper vertex}$$

$$\Sigma_0(p) = \xi_8 K_0 \text{ self energy}, \quad \Sigma_0'(p-q) = \kappa_0 \pi_0 \text{ self energy}$$

$$\Sigma_0'(p) = \xi_8 K_0 \text{ self energy.}$$

$$(3) \underline{K^+ \rightarrow \pi^+ \gamma}$$

Here, we shall derive the WT identity for the $K^+ \pi^- \gamma$ proper vertex, and show how the terms of our interest can be obtained with the use of it. We note,

$$\frac{\delta}{\delta A_\mu} = \frac{g'}{G} \frac{\delta}{\delta B_{3\mu}} + \frac{g}{G} \frac{\delta}{\delta B_{0\mu}} = -e \left(\frac{1}{g} \frac{\delta}{\delta B_{3\mu}} + \frac{1}{2} \frac{1}{(g'/2)} \frac{\delta}{\delta B_{0\mu}} \right). \quad (\text{B. 14})$$

Using Eq. (B. 14) in Eq. (B. 7) we obtain,

$$-\partial_\mu \frac{\delta \Gamma}{\delta A_\mu} + \frac{ie}{2} \text{tr} \left\{ Q' \left[\frac{\delta \Gamma^T}{\delta \Sigma_k} \Sigma_k - \Sigma_k \frac{\delta \Gamma^T}{\delta \Sigma_k} + \frac{\delta \Gamma^T}{\delta \Pi_k} \Pi_k - \Pi_k \frac{\delta \Gamma^T}{\delta \Pi_k} \right] \right\} = 0, \quad (\text{B. 15})$$

where

$$Q' = T_3 + \frac{1}{2}(Y_L + Y_R) = \text{diag} \left(\frac{4}{3}, \frac{4}{3}, -\frac{2}{3}, -\frac{2}{3} \right).$$

Then, differentiating Eq. (B. 15) with respect to $K_m^+ \pi_n^-$ and setting $\Sigma = F$, $\Pi = 0$, we obtain the WT identity, which may be written in the momentum space as,

$$q_\mu \Gamma_Y^\mu(p, q) = e \left[\Sigma_+(p) - \Sigma_+(p-q) \right], \quad (\text{B. 16})$$

where,

$$\Gamma_Y^\mu(p, q) = K^+(p) \rightarrow \pi^+(p-q) \gamma(q) \text{ proper vertex.}$$

$$\Sigma_+(p) = K^+ \pi^- \text{ self energy, as before.}$$

Equation (B. 16) is shown diagrammatically in Fig. 30.

On the other hand, the truncated $K^+ \pi^- \gamma$ Green's function $E_Y^\mu(p, q)$

is given by (See Fig. 31),

$$\begin{aligned}
 E_Y^\mu(p, q) \Big|_{\text{mass shell}} &\equiv \left\{ \Gamma_\mu(p, q) + \frac{(i)^2 e(2p-q)_\mu}{m_K^2 - m_\pi^2} \Sigma_+(p) \right. \\
 &\quad \left. + \frac{(i)^2 e(2p-q)_\mu}{m_\pi^2 - m_k^2} \Sigma_+(p-q) \right\}_{\text{mass shell}} \\
 &= \left\{ \Gamma_\mu(p, q) - \frac{e(2p-q)_\mu}{m_k^2 - m_\pi^2} \left[\Sigma_+(p) - \Sigma_+(p-q) \right] \right\}_{\text{mass shell}} . \quad (\text{B. 17})
 \end{aligned}$$

As far as terms of our interest are concerned [i. e., upto the terms of $O\left(\frac{1}{M^2}\right)$] $\Sigma_+(p)$ can be expressed as,

$$\Sigma_+(p) = \alpha + \beta p^2 + \gamma p^4 . \quad (\text{B. 18})$$

From the Lorentz transformation property of $\Gamma_\mu(p, q)$, we write,

$$\Gamma_\mu(p, q) = Cp^\mu + Dq^\mu \quad (\text{B. 19})$$

where C and D are functions of Lorentz invariants. We shall choose the three independent Lorentz invariants to be p^2 , q^2 and $(p-q)^2$.

We expand C and D in powers of the external momenta: e. g., as

$$C = C_0 + C_1 p^2 + C_2 (p-q)^2 + C_3 q^2 + \dots \quad (\text{B. 20})$$

where the C_i 's can possibly have (only) a logarithmic dependence on the Lorentz invariants.

Substituting Eqs. (B. 18), (B. 19) and (B. 20) in the WT identity of

Eq. (B.16) and compare the coefficients of the powers of the independent Lorentz invariants, we get:

$$\begin{aligned} C_0 &= 2e\beta + 0\left(\frac{1}{M^4}\right) \\ C_1 &= 2e\gamma \\ C_2 &= 2e\gamma \quad . \end{aligned} \quad (\text{B.21})$$

Now,

$$\begin{aligned} E_Y^\mu(p, q) &= p_\mu \left\{ C_0 + C_1 p^2 + C_2 (p-q)^2 + C_3 q^2 + \dots \right. \\ &\quad \left. - \frac{e[\alpha + \beta p^2 + \gamma p^4]}{p^2 - m_\pi^2} - \frac{e[\alpha + \beta(p-q)^2 + \gamma(p-q)^2]}{(p-q)^2 - m_K^2} \right\} \\ &\quad + \text{terms proportional to } q_\mu \quad . \end{aligned} \quad (\text{B.22})$$

The terms proportional to q_μ do not contribute. $E_Y^\mu(p, q)$ has terms proportional to $p^2 p_\mu$, $(p-q)^2 p_\mu$ and p_μ in addition to the terms proportional to $q^2 p_\mu$. However, using Eq. (B.21) on mass shell, we find

$$E_Y^\mu(p, q) \Big|_{\text{mass shell}} = C_3 q^2 p^\mu + \text{terms proportional to } q^\mu \quad (\text{B.23})$$

Hence, we need to compute C_3 only. This can be done by computing $\Gamma_Y^\mu(p, q)$ on mass shell and picking terms proportional to $q^2 p^\mu$.

(4) $K^0 \rightarrow \pi^0 \gamma$ Vertex

The only one particle reducible diagram for the $K^0 \rightarrow \pi^0 \gamma$ vertex

consists of $K_0 \pi^0 \rightarrow \kappa^0 \rightarrow \gamma$. This diagram is clearly proportional to q_μ , the photon 4-momentum. The WT identity for the total $K^0 \rightarrow \pi^0 \gamma$ vertex $E_{0\gamma}^\mu(p, q)$ can be shown to be,

$$q_\mu E_{0\gamma}^\mu(p, q) = 0 \quad \text{for arbitrary } p, q. \quad (\text{B. 24})$$

Writing,

$$E_{0\gamma}^\mu(p, q) = F p_\mu + G q_\mu,$$

it follows from Eq. (B. 24) that F is proportional to q^2 . Hence, we need to compute the terms proportional to $q^2 p_\mu$ from the $K_0 \pi^0 \gamma$ total vertex (terms proportional to q_μ do not contribute) and these terms come from the IPI diagrams.

(5) $K^0 Z$ vertex

Here, we shall prove the WT identity relating the $K^0 Z$ and the $K^0 \chi$ vertices; which is given in Sec. (IV. 1).

Differentiate Eq. (B. 9) with respect to K_{0m} and set $\Sigma = F$, $\Pi = 0$.

We obtain,

$$-\partial_\mu \frac{\delta^2 \Gamma}{\delta K_m^0 \delta Z_\mu} + M_Z \frac{\delta^2 \Gamma}{\delta K_{0m} \delta \chi} - \frac{G}{2} \sum_k \frac{\delta^2 \Gamma}{\delta K_{0m} \delta \Pi_{kk}} f_k t_{3k} = 0. \quad (\text{B. 25})$$

Writing Eq. (B. 25) in momentum space, in obvious notation, we get

$$i p_\mu \Gamma_Z^\mu(p) + M_Z \Gamma_\chi(p) - \frac{G}{2} \sum_k f_k t_{3k} \Sigma(K_0 \rightarrow \Pi_{kk}, p) = 0. \quad (\text{B. 26})$$

Next, we shall show that

$$\begin{aligned}
 & - \frac{G}{2} \sum_k f_k t_{3k} \Sigma(K^0 \rightarrow \Pi_{kk}, p) \\
 & = (i p_\mu) (\text{pole diagrams for } K_0 \rightarrow Z^\mu) + M_Z (\text{pole diagrams for } K_0 \rightarrow \chi).
 \end{aligned}
 \tag{B.27}$$

The right-hand side is

$$i p_\mu \sum_k \Sigma_k(p) \frac{i}{p^2 - m_k^2} a_k(i) p^\mu + M_Z \sum_k \Sigma_k(p) \frac{i}{p^2 - m_k^2} i a_k m_k^2 / M_Z$$

where a_i 's are defined in Eq. (4.5) and the sum over k runs over

$$\pi_0, \eta_8', \eta_c', \eta_0'$$

$$\begin{aligned}
 & = \sum_{\pi_0 \eta_c \eta_c' \eta_0'} \Sigma_k(p) a_k \\
 & = \sum_k \left(- \frac{G}{2} f_k t_{3k} \right) \Sigma(K^0 \rightarrow \Pi_{kk}, p)
 \end{aligned}$$

changing the basis to Π_{kk} ($k = 1, 2, 3, 4$).

Thus, from Eqs. (B.26) and (B.27), we obtain,

$$i p_\mu E^\mu(p) + M_Z F(p) = 0
 \tag{B.28}$$

where

$$E^\mu(p) = \text{truncated } K_0 Z \text{ Green's function}$$

$$F(p) = \text{truncated } K_0 \chi \text{ Green's function.}$$

APPENDIX C

Finiteness of the Results

In this Appendix, we shall make a brief comment which will make it more transparent the fact that all the results are finite.

Nothing that we are using the Landau gauge for the W propagator, we find that among all the diagrams that have appeared so far, only the diagrams which are divergent are the self-energy diagrams with W -exchange. As an example, we may consider the $K^+\pi^-$ diagrams shown in Fig. 25(a). In the Landau gauge such a diagram with a single intermediate state (say π^0) is logarithmically divergent. However, when one sums over all the intermediate states, the logarithmic divergence cancels. That this must happen can be seen as follows.

Consider the tree diagrams for the process $K^+\pi^- \rightarrow W^+W^-$. (See Fig. 25.) There is no direct $K^+\pi^-W^+W^-$ vertex. [The direct meson-meson W^+W^- vertices are always $\Delta S = \Delta Q = 0$. The self-energy diagrams we shall be dealing with are always be $\Delta S \neq 0$. There are more diagrams for this process but these vanish when the W^\pm are on mass shell.] Then the fact that the sum of all the diagrams with longitudinal polarizations of the W^+ and W^- must not grow like a positive power of the CM energy necessarily requires that the sum of the products of the coupling constants $\sum_i h_i p_i$ must vanish. Due to this condition, the logarithmic divergences must cancel in the self-energy diagrams of the Fig. 25(a).

APPENDIX D

The 3 meson (2p, 1s or 3s) couplings can be directly obtained from the interaction terms of Eq. (2.3). However, it is instructive and easier in some cases to obtain them via the WT identity. It makes many considerations simpler.

As an example consider the $K_c^+ \bar{\kappa}_0^- \pi_c^-$ vertex. We use the WT identity of Eq. (B.7) in the tree approximation. Differentiate Eq. (B.7) with respect to κ_0^- and π_c^- and set $\Sigma = F$, $\Pi = 0$. Then we obtain,

$$-\frac{1}{g} \partial_\mu \frac{\delta^3 \Gamma}{\delta W_\mu^+ \delta \bar{\kappa}_0^- \delta \pi_c^-} = \frac{1}{2\sqrt{2}} (f + f') \frac{\delta^3 \Gamma}{\delta K_c^+ \delta \bar{\kappa}_0^- \delta \pi_c^-} \cos \theta$$

+ terms that vanish when π_c^- and κ_0^0 are on mass shell. (D.1)

The first term when $\bar{\kappa}_0^0$ and π_c^- are on mass shell is $\frac{1}{2\sqrt{2}} (m_c^2 - \mu_c^2) \cos \theta$. Therefore, the three point $\chi^0 \pi_c^- K_c^+$ vertex is:

$$\Gamma_{K_c^+ \chi^0 \pi_c^-}^{(3)} = \frac{-\mu_c^2 + m_c^2}{f + f'} = \left(-\frac{\mu_c^2}{2f} + 0(1) \right). \quad (D.2)$$

The conclusions from this simple exercise is that in the three meson vertex the parameters $\mu_0^2, \alpha, \beta, \gamma$ [which enter the strong interaction phenomenological Lagrangian] enter only in such combinations that they can be expressed in terms of the masses of the mesons. Since the Feynman integrals also depend only upon the masses

(through propagators), it becomes easier to understand the fact that the results are independent of the parameters α, β, γ as $\mu_0^2 \rightarrow \infty$.

The fact that the 4-meson vertices (with 4 external pseudoscalar mesons) has similar property can be seen easily as follows: As an example, consider the $K^+ \pi^- \rightarrow K_c^+ \pi_c^-$ tree diagrams. These are shown in Fig. 26. We know that the sum of these diagrams must vanish when the external momenta vanish and $m_c = m_K = 0$. [Exact $SU(4) \times SU(4)$ symmetry of strong interactions Lagrangian.] This relates the 4-point function (c) to the diagrams 26(a) and 26(b) which themselves can be expressed in terms of μ^2 (up to $SU(4)$ breaking corrections).

APPENDIX E

The 'Box' Diagrams for $K^+ \rightarrow \pi^+ \nu \bar{\nu}$

These are the diagrams that arise out of the direct coupling of W^+W^- (or s^+s^-), [from the $K^+\pi^-W^+(s^+)W^-(s^-)$ vertex] to leptons.

They are shown in the Fig. 27.

In the diagrams of Fig. 27(a), when the intermediate states are scalars, (ξ_8, ξ_0, Y_{0c}) the diagrams vanish as $\mu^2 \rightarrow \infty$. The two intermediate states (π_0, X_c^0) contribute with the opposite signs. Their sum is of order $< 0 \left(\frac{m_K^2}{M^4} \ln \frac{m_c^2}{m_K^2} \right)$, thus smaller by a factor $\frac{m_K^2}{m_c^2} \ln \frac{m_c^2}{m_K^2}$ as compared to the Z-exchange diagrams. The diagrams in Figs. 27(b) and 27(c) are also of order $\leq 0 \left(\frac{m_K^2}{M^4} \right)$. The diagrams in the Figs. 27(d), 27(e) and 27(f) can grow as μ^2 individually, but their sum is finite as $\mu^2 \rightarrow \infty$. The cancellation of the terms proportional to μ^2 is related to fact mentioned in the Appendix D (see Fig. 26), that the sum of the $K^+\pi^- \rightarrow K_c^+\pi_c^-$ scattering diagrams vanishes at zero external momenta and $m_c = 0$. Hence, their sum is found to be of order $0 \left(\frac{m^2}{M^4} \right)$. The diagrams in Figs. 27(g), 27(h) and 27(i) are also found to be of order $0 \left(\frac{m^2}{M^4} \right)$. Hence, all box diagrams can be neglected as compared to the Z-exchange diagrams.

APPENDIX F

Here we shall deal with the terms $-\frac{iG}{2} \sum_k f_k t_{3k} \Gamma_{0k}^{(3)}(p, q)$ + $\frac{i}{2} G \left[\frac{1}{\sqrt{3}} \Sigma_0(p) + \frac{\sqrt{2}}{\sqrt{3}} \Sigma'_0(p) - \Sigma'_0(p-q) \right]$ in the right-hand side of Eq. (B.13). We need the terms proportional to $p \cdot q$ from these, which will contribute to the terms proportional to p_μ in the proper vertex.

First, let us consider $\Gamma_{0k}^{(3)}(p, q)$. The diagrams that contribute to $\Gamma_{0k}^{(3)}(p, q)$ are shown in Fig. 17.

We are going to show that none of the diagrams in Fig. 17 except those in Figs. 17(a), 17(c) and 17(q) contribute to the $p \cdot q$ terms of $0 \left(\frac{1}{M^2} \right) \sum_k f_k t_{3k} \Gamma_{0k}^{(3)}(p, q)$ and that the contribution of the diagram in Fig. 17(q) to $-\frac{i}{2} G \sum_k f_k t_{3k} \Gamma_{0k}^{(3)}$ is equal and opposite to the contribution of the diagram in Fig. 18(b) to $-\frac{iG}{2} \Sigma'_0(p-q)$; so that they together do not contribute to the sum of the terms in the right-hand side of Eq. (B.13) that we are considering.

Let us first note the following:

(i) Let C_k be the Feynman rule for the vertex of a scalar $\rightarrow W_\mu^\pm \Pi_{kk}$. [The scalar may be $\kappa^\pm, \kappa_c^\pm, \phi^\pm, \phi_c^\pm$.] Then from the Feynman rules in the Appendix A, we find that

$$\sum_k t_{3k} C_k = 0. \quad (F.1)$$

(ii) We compute all the trilinear couplings involving Π_{kk} and two charged fields. The result is:

$$\begin{aligned}
& - (K_c^+ \chi_c^- + K_c^- \chi_c^+) \left\{ 4\alpha \mu_0^2 (f \Pi_{11} + f' \Pi_{44}) + 2\gamma \mu_0^2 f (\Pi_{22} + \Pi_{44}) \right\} \\
& - (\pi_c^+ \phi_c^- + \pi_c^- \phi_c^+) \left\{ 4\alpha \mu_0^2 (f \Pi_{11} + f' \Pi_{33}) + 2\gamma \mu_0^2 f (\Pi_{22} + \Pi_{44}) \right\} \\
& - (K^+ \kappa^- + K^- \kappa^+) \left\{ 4\alpha \mu_0^2 f (\Pi_{22} + \Pi_{44}) + 2\gamma \mu_0^2 (f' \Pi_{33} + f \Pi_{11}) \right\} \\
& - (\pi^+ \phi^- + \pi^- \phi^+) \left\{ 4\alpha \mu_0^2 f (\Pi_{22} + \Pi_{33}) + 2\gamma \mu_0^2 (f' \Pi_{44} + f \Pi_{11}) \right\} . \quad (F. 2)
\end{aligned}$$

Thus, if we define the $\Pi^\pm \rightarrow \Sigma^\pm \Pi_{kk}$ vertex as b_k , where Π^\pm and Σ^\pm are some charged pseudoscalar fields, then we find:

$$\sum_k f_k t_{3k} b_k = 0 . \quad (F. 3)$$

[Equation (F. 3) can also be alternately derived from the WT identity for the tree diagrams. (See Eq. B. 9). It essentially follows from the fact that there are no vertices of the kind $\Pi^\pm \rightarrow \Sigma^\pm Z_\mu$ (e.g., $K^+ \rightarrow \kappa^+ Z_\mu$).

(iii) In particular, we note from Eq. (F. 2) that the interaction of π^0 with charged fields are given by,

$$\begin{aligned}
& \frac{\pi^0}{\sqrt{2}} (\pi_c^+ \phi_c^- + \pi_c^- \phi_c^+) \left\{ 2f \mu_0^2 (2\alpha - \gamma) - 4\alpha f \epsilon \mu_0^2 \right\} \\
& - \frac{\pi^0}{\sqrt{2}} (K^+ \kappa^- + K^- \kappa^+) \left\{ 2f \mu_0^2 (2\alpha - \gamma) - 2\gamma f \epsilon \mu_0^2 \right\} \\
& = \frac{\pi^0}{\sqrt{2}} \frac{\mu_c^2}{2f} \left\{ \phi_c^+ \pi_c^- + \pi_c^+ \phi_c^- - \kappa^+ K^- - \kappa^- K^+ \right\} + 0(\mu^0) . \quad (F. 4)
\end{aligned}$$

(iv) The trilinear interactions of K_0 with the charged fields are given by,

$$-\frac{\mu_c^2}{2f} K^0 \left\{ \kappa^- \pi^+ + K^- \phi^+ + K_c^- \phi_c^+ + \kappa_c^- \pi_c^+ \right\} + 0(\mu^0) . \quad (F.5)$$

Now, consider the diagrams of Figs. 17(b) and 17(d). They are of $0(\mu^0)$ and therefore in their contribution to $\sum_k f_k t_{3k} \Gamma_{0k}^{(3)}$, we may put $f_k = f$ (i. e., $\epsilon = 0$). Then due to Eq. (F.1), the contribution of the diagrams in Figs. 17(b) and 17(d) to $\sum_k f_k t_{3k} \Gamma_{0k}^{(3)}$ vanishes identically.

Further, on account of Eq. (F.3), the contribution of the diagrams in Figs. 17(e), 17(f), 17(h) and 17(i) to $\sum_k f_k t_{3k} \Gamma_{0k}^{(3)}(p, q)$ is zero. The diagrams in Fig. 16(g) do not have terms proportional to $p \cdot q$ since it depends on p^2 only. In Fig. 16(j), each diagram is of $0\left(\frac{1}{M^2}\right)$. However, when summed over all k , for each intermediate state, the contribution to $\sum_k f_k t_{3k} \Gamma_{0k}^{(3)}(p, q)$ vanishes. This is so, because the $\Pi_k W^+ W^-$ vertex is described by,

$$(\text{const}) W_\mu^+ W^{-\mu} \sum_k (\Pi_{kk}) ,$$

and since each diagram is of $0(\mu^0)$, we may put $f_k = f$. The diagrams in Fig. 17(k), 17(l) are of $0\frac{1}{M^4}$. The contribution of the diagrams in Fig. 17(m), 17(n) to $\sum_k f_k t_{3k} \Gamma_{0k}^{(3)}$ vanishes because of Eq. (F.3). The diagrams in Fig. 17(p) are of $0(\mu^0)$; however, the $p \cdot q$ terms in them are of $0(\mu^{-2})$ and hence can be neglected as $\mu^2 \rightarrow \infty$.

This leaves us with the diagrams in Fig. 17(a), 17(c) and 17(q). Let us first consider the $p \cdot q$ terms in Fig. 17(q) together with the $p \cdot q$ terms from $\Sigma_0'(p-q)$. We shall redraw Fig. 17(q), for convenience,

with the diagrams for $\Sigma_0''(p-q)$ in Fig. 18. [Figure 17(q) \equiv Fig. 18(a)].

The diagrams in Figs. 18(d) and 18(e) are independent of the external momenta. The diagram in Fig. 18(c) is of $O(\mu^0)$; however, the terms proportional to $p \cdot q$ are of $O(\mu^{-2})$ and hence will be neglected. The two diagrams in the Fig. 18(a) and 18(b) are identical except for the left bottom vertex in each. We find that the $\kappa_0 K_c^- \pi_c^+$ vertex in Fig. 18(b) is described by,

$$\mathcal{L}_{\kappa_0 K_c^- \pi_c^+} = \kappa_0 K_c^- \pi_c^+ \left\{ -2(2\alpha - \gamma) f \mu_0^2 + 4\alpha f \epsilon \mu_0^2 \right\} + \text{h.c.} , \quad (\text{F.6})$$

while the $K_c^0 K_c^- \pi_c^+ \Pi_{kk}$ vertex in the diagram of Fig. 18(a) is described by,

$$\mathcal{L}_{K_c^0 K_c^- \pi_c^+ \Pi_{kk}} = \left[-4\alpha \mu_0^2 (\Pi_{11} + \Pi_{33} + \Pi_{44}) - 2\gamma \mu_0^2 \Pi_{22} \right] K_c^0 K_c^- \pi_c^+ . \quad (\text{F.7})$$

Thus, the contribution of the diagrams in Fig. 18(a) to $\sum_k f_k t_{3k} \Gamma_{0k}^{(3)}$ is described by an "effective" vertex (Feynman rule)

$$\begin{aligned} &= \left[-4\alpha \mu_0^2 (f' - 2f) - 2\gamma \mu_0^2 f \right] \\ &= 2(2\alpha - \gamma) \mu_0^2 f - 4\alpha f \epsilon \mu_0^2 \end{aligned} \quad (\text{F.8})$$

which is exactly equal and opposite to the $\chi_0 K_c^- \pi_c^+$ vertex in Eq. (F.7).

Hence, the total contribution of the diagrams in Fig. 18(a) and 18(b) to $\{ \sum_k f_k t_{3k} \Gamma_{0k}^{(3)}(p,q) + \Sigma_0''(p-q) \}$ is zero.

We have computed the terms proportional to $p \cdot q$ in the diagrams of Figs. 17(a) and 17(c) and of Fig. 18(f). The results are already

quoted in Eqs. (6.3) and (6.4).

Finally, let us consider the WT identity of Eq. (B.13) at $p = q = 0$. $q_\mu \Gamma_{0Z}^\mu$ vanishes at $p = q = 0$; so does the $K^0 \pi^0 \chi$ proper vertex $\Gamma_{0\chi}(p, q)$. (See the diagrams of Fig. 16.) Therefore, we obtain

$$\Sigma_{3k} t_{3k} f_k \Gamma_{0k}^{(3)}(0, 0) + \Sigma \tau(0) - \frac{1}{\sqrt{3}} \Sigma_0(0) - \frac{\sqrt{2}}{\sqrt{3}} \Sigma_0'(0) = 0. \quad (\text{F.9})$$

As remarked in Sec. VI, the contribution of the one particle reducible diagrams to $K^0 \pi^0 Z$ total vertex depends on the terms in $\Sigma_0, \Sigma_0', \Sigma_0''$ which are proportional to μ^2 . Let us therefore consider the terms of $O\left(\mu^2 \frac{1}{M^2}\right)$ in Eq. (F.9).

From all the above discussion, it is clear that the contribution to $\Sigma_{3k} t_{3k} f_k \Gamma_{0k}^{(3)}(0, 0)$ which is of $O(\mu^2)$ comes from only two diagrams: (i) the diagram in Fig. 17(q), (ii) the diagram in Fig. 17(g) with the intermediate state $(\kappa^+, \pi_c^-, \pi_c^+)$. The contribution of these are found to be equal and opposite in sign, hence, they cancel. Thus we obtain

$$\Sigma_0''(0) - \frac{1}{\sqrt{3}} \Sigma_0(0) - \frac{\sqrt{2}}{\sqrt{3}} \Sigma_0'(0) = O(\mu^0). \quad (\text{F.10})$$

We shall use Eq. (F.10) in Sec. VI.

APPENDIX G

In this Appendix, we shall deal with the term $-\frac{iG}{2} \sum_k f_k t_{3k} \Gamma_k^{(3)}(p, q)$ in the WT identity for the proper $K^+ \pi^- Z$ vertex of Eq. (B.11). We need to find the terms which are of $O\left(\frac{1}{M^2}\right)$ and are proportional to $p \cdot q$. This appendix is similar to the Appendix F.

The diagrams that contribute to this vertex are shown in Fig. 13.

On account of Eq. (F.1), the contribution of the diagrams in Fig. 13(b) and 13(d) to $\sum_k f_k t_{3k} \Gamma_k^{(3)}(p, q)$ vanishes. On account of Eq. (F.3), the diagrams in Fig. 13(e) and 13(f) do not contribute to $\sum_k f_k t_{3k} \Gamma_k^{(3)}(p, q)$. The diagrams in Fig. 13(g) do not have terms proportional to $p \cdot q$. The diagrams in Fig. 13(k) is of $O(\mu^0)$ as such, but the $p \cdot q$ terms in them are of $O(\mu^{-2})$ and hence they vanish as $\mu^2 \rightarrow \infty$. The diagrams in Figs. 13(m) - 13(q) are similar to the diagrams in Figs. 17(j) - 17(n), (which we have discussed in the Appendix F) and can be neglected for identical reasons. The diagrams in Fig. 13(h), 13(i), and 13(j) contribute to the terms proportional to $p \cdot q$ and their contribution is already stated in Eq. (5.11). This leaves us with the diagrams in Figs. 13(a), 13(c) and 13(l). The following, we shall show that the terms in their sum which are proportional to $p \cdot q$ are of $O\left(\frac{m_K^2}{M^2}\right)$ as against the terms of the leading order $O\left(\frac{m_c^2}{M^2}\right)$ and thus negligible.

Consider the diagrams in Fig. 13(1). To compute these, we need

"effective vertices" such as $\sum_k f_k t_{3k} \left(\begin{array}{c} \xi_8 \\ \pi_0 \end{array} \right) \Pi_{kk}$. These can be

most easily obtained through the use of the WT identity of Eq. (B.9) in the tree approximation and the knowledge of the meson-meson-Z vertices. As an example, consider the WT identity of Eq. (B.9) differentiated with respect to ξ_8 and π_0 (at $\Sigma = F$, $\Pi = 0$) on mass shells (of ξ_8 and π_0) in the tree approximation. The result is,

$$-\partial_\mu \left. \frac{\delta^3 \Gamma}{\delta Z_\mu \delta \xi_8 \delta \pi_0} \right|_{\text{mass shell}} + \sum_k f_k \left(-\frac{G}{2} t_{3k} \right) \frac{\delta^3 \Gamma}{\delta \xi_8 \delta \pi_0 \delta \Pi_{kk}} = 0. \quad (\text{G.1})$$

Reading the $\xi_8 \pi_0 Z$ vertex from the Appendix A, it is easily seen that

$$\begin{aligned} \sum_k t_{3k} f_k \left(\begin{array}{c} \xi_8 \\ \pi_0 \end{array} \right) \Pi_{kk} &= -\frac{2}{G} \frac{G\mu^2}{2\sqrt{3}} + 0(\mu^0) \\ &= -\frac{\mu^2}{\sqrt{3}} + 0(\mu^0). \end{aligned} \quad (\text{G.2})$$

In other words, the effective vertices are described by, $\frac{2}{G} \times$ (the divergence of the ps-scalar current that couples to Z_μ). These effective vertices are, thus, described by,

$$-\mu^2 \left[\frac{\pi_0 \xi_8}{\sqrt{3}} - \frac{\pi_0 \xi_2}{\sqrt{6}} - \frac{2}{3} \xi_8 \eta_8 - \frac{\xi_2 \eta_8}{3\sqrt{2}} + X_c^0 \bar{Y}_c^0 + \bar{X}_c^0 Y_c^0 \right]$$

$$+ \mu_1^2 \xi_1 \left(\frac{\pi_0}{\sqrt{2}} + \frac{\eta_8}{\sqrt{6}} \right) + 0(\mu^0) \quad (\text{G. 3})$$

with the help of Eq. (G. 3) and the Feynman rules in the Appendix A,

it is easy to show that the total contribution of the diagrams in

Fig. 13(1) to $\sum_k f_k t_{3k} \Gamma_k^{(3)}(p, q)$ is given by

$$m(1) = (-p \cdot q) \left\{ 2B(\mu_1, 0) - 2B(\mu, m_c) + 0\left(\frac{m_K^2}{M^2}\right) + 0(\mu^{-2}) \right\} \\ + \text{other terms,} \quad (\text{G. 4})$$

where,

$$B(\lambda, \rho) = \frac{3ig^2}{8} \frac{\lambda^2}{(2\pi)^4} \int \frac{d^4k}{(k^2 - \lambda^2)(k^2 - \rho^2)(k^2 - M^2)}. \quad (\text{G. 5})$$

[The contribution proportional to $B(\mu, m_c)$ comes from the X_c^0, Y_c^0 intermediate states. The contribution proportional to $B(\mu_1, 0)$ comes from the $(\xi_1; \pi_0, \eta_8)$ intermediate states. The contribution from the $(\xi_8; \pi_0, \eta_8)$ intermediate states cancels the contribution from the (ξ_2, π_0, η_8) intermediate states. Hence, there is no term proportional to $B(\mu, 0)$ in Eq. (G. 4).]

Next the strong vertices in the diagrams of Fig. 13(a) and 13(c)

are described by

$$\frac{1}{2f} (K^+ K^-) \left[\frac{\mu^2 \xi_8}{\sqrt{6}} + \frac{\mu^2 \xi_2}{\sqrt{3}} - \mu_1^2 \xi_1 \right] - \frac{1}{2} (\pi^+ \pi^-) \left[\mu^2 \left(\frac{2\xi_8}{\sqrt{6}} - \frac{\xi_2}{\sqrt{3}} \right) + \mu_1^2 \xi_1 \right] \\ - \frac{\mu^2}{2f} Y_c^0 (K_c^+ K_c^- + \pi_c^+ \pi_c^-) + 0(\mu^0). \quad (\text{G. 6})$$

With the help of Eq. (G.6), we have computed the contribution of the diagrams in Fig. 13(a) and 13(c) to the $p \cdot q$ terms in $\sum_k f_k t_{3k} \Gamma_k^{(3)}(p, q)$.

The results are:

$$m(a) = m(c) = (p \cdot q) \left[B(\mu_1, 0) - B(\mu, m_c) + O\left(\frac{m_K^2}{M^2}\right) + O(\mu^{-2}) \right] + \text{other terms} . \tag{G.7}$$

Thus, from Eqs. (G.4) and (G.7) we find,

$$m(a) + m(c) + m(e) = (p \cdot q) \times O\left(\frac{m_K^2}{M}\right) + \text{other terms} . \tag{G.8}$$

Hence, the contribution of these diagrams in Figs. 13(a), 13(b) and 13(l) to the terms proportional to p_μ of $O\left(\frac{m_c^2}{M^2}\right)$ in $E_Z^\mu(p, q)$ is zero.

This cancellation will become less mysterious if one notes that each diagram is proportional to $\left[B(\mu_1, 0) - B(\mu, m_c) \right]$ which, among other

things, contains a term proportional to $\ln \frac{\mu}{2} \sim \ln(2\alpha - \gamma)$ which

depends on the parameters α and γ which enter the strong interaction phenomenological Lagrangian. While, if one draws all diagrams for

$E_Z^\mu(p, q)$ it is easy to see (with the help of the Appendix D) that it should not depend on α and γ .

APPENDIX H

Higgs' Exchange Diagrams for $K^+ \rightarrow \pi^+ e e^-$

These diagrams are proportional to the lepton mass, therefore, we shall estimate them for the process $K^+ \rightarrow \pi^+ \mu \mu^-$ to see whether they are significant. The Higgs exchange diagrams that contribute to this process fall into two categories. They are shown in Fig. 36(a) and 36(b).

The diagrams that contribute to the proper $K^+ \pi^- \psi_0$ vertex are shown in Fig. 37. The diagrams in Fig. 37(a) are of $O\left(m_\mu \cdot \frac{m_K^2}{M^2} \times \frac{1}{2} \right)$ for each of the intermediate states. However, their μ_{Higgs} sum is of $O\left(m_\mu \frac{m_K^2}{M^4} \frac{m_c^2}{2} \right)$. The diagrams in Figs. 37(b) and 37(c) are of $O\left(m_\mu \frac{m_c^2}{M^2} \frac{1}{2} \right)$. The diagrams in Fig. 37(d) are of $O\left(m_\mu \frac{m_c^2}{M^4} \right)$.

One can convince oneself that the weak $K^+ \pi^- \xi_c$ vertex itself is of $O\left(\frac{m_c^2}{M^2} \right)$. Hence, Fig. 36(b) is of $O\left(m_\mu \frac{m_c^2}{M^4} \frac{m_c^2}{2} \right)$. Thus, all the Higgs' exchange diagrams can be neglected.

APPENDIX I

The Contributions of the Diagrams in Class 3 in Fig. 25 at $p = 0$

We shall show that this contribution at $p = 0$ is zero with the help of the WT identities that follow from the broken chiral $SU(4) \times SU(4)$ symmetry of the Lagrangian of the strong interactions with known symmetry breaking. [This Lagrangian is just \mathcal{L}_0 of Eq. (2.3) + the symmetry breaking terms, $\mathcal{L}_{M\Phi} \Big|_{\Phi = v}$. Let $W[J]$ be the generating functional of the Green's functions for this Lagrangian. $W[J]$ is defined by

$$W[J] = \int [dM dM^\dagger] \exp i \int d^4x [\mathcal{L}_0 + \text{tr} \{ A(M + M^\dagger) + J^+ M + J^{*T} M^\dagger \}]. \quad (\text{I. 1})$$

\mathcal{L}_0 is invariant under the global $SU(4) \times SU(4)$ group transformations. J and J^* are 4×4 complex matrices corresponding to the sources of M and M^\dagger . A is a diagonal matrix proportional to v , which in the exact $SU(3)$ symmetry limit, (with the $SU(3)$ octet of pseudoscalar mesons being massive) has the form:

$$A = (\text{const}) \times \text{Diag} (f^2 m_c^2, f m_K^2, f m_K^2, f m_K^2) . \quad (\text{I. 2})$$

Now, under a left-handed $SU(4)$ transformation, M and M^\dagger transform according to Eq. (2.2), viz:

$$\begin{aligned} \delta M(x) &= - \frac{i}{2} \theta^i \lambda_i M(x) \\ \delta M^\dagger(x) &= \frac{i}{2} \theta^i M^\dagger(x) \lambda_i . \end{aligned} \quad (\text{I. 3})$$

Such a transformation is just a change of variables of integration which must leave $W[J]$ invariant. Further, the transformation has a unit Jacobian. Using these, one can write down the WT identities for $Z[J] = -i \ln W[J]$ in the usual manner. The result is,

$$0 = \int d^4x \operatorname{tr} \left\{ \lambda_i \left[\frac{\delta Z}{\delta J(x)} J^T(x) - J^{*T}(x) \frac{\delta Z}{\delta J^*(x)} \right] - \lambda_i \left[A \frac{\delta Z}{\delta J^*(x)} - \frac{\delta Z}{\delta J(x)} A \right] \right\} . \quad (I.4)$$

Equation (I.4) holds for each generator λ_i , in general for any complex linear combination of λ_i 's, and since complex linear combinations of λ_i 's span the space of 4×4 traceless matrices, it follows, in particular, that

$$0 = \int d^4x \left\{ \frac{\delta Z}{\delta J(x)} J^T(x) - J^{*T}(x) \frac{\delta Z}{\delta J^*(x)} - A \frac{\delta Z}{\delta J^*(x)} + \frac{\delta Z}{\delta J(x)} A \right\} \text{off diagonal element} . \quad (I.5)$$

Now, consider the contribution of the diagrams of Class 3, in Fig. 25. They can be obtained by constructing the Green's functions for the processes

$$\begin{aligned} K_0 K_0 &\rightarrow 4p \\ &\rightarrow 2p + 2s && p = \text{pseudoscalar meson} \\ &\rightarrow 4s && s = \text{scalar meson.} \end{aligned}$$

[where the final state involves charged charmed mesons carrying two units of strangeness and no charge] and by closing them with s^\pm propagators. The Feynman rules at the vertices involving s^\pm are such that the contribution is proportional to the sum of the above Green's functions. This sum is in turn proportional to the (hermitian part of the) Green's function:

$$K_0 K_0 \rightarrow (\kappa_c^+ + iK_c^+), (\kappa_c^+ + iK_c^+), (\phi_c^- - i\pi_c^-), (\phi_c^- - i\pi_c^-) .$$

Thus, at $p = 0$, we need to compute the Green's function for,

$$M_{41} M_{41} M_{13}^+ M_{13}^+ \rightarrow 2 \text{ 'soft' [i.e., } p = 0, \text{ but massive] } \bar{K}_0 \text{'s. (I.6)}$$

[where,

$$M_{41} = (\kappa_c^- + iK_c^-), M_{13}^+ = (\phi_c^+ - i\pi_c^+), M_{34} = \kappa_0 + iK_0] .$$

Differentiate the Ward identity of Eq. (I.5) with respect to $J_{41}(y)$, $J_{41}(z)$, $J_{13}^*(w)$, $J_{13}^*(v)$ and set $J = J^* = 0$ except,

$$J_{34} = -J_{34}^* = -ic, \quad c \equiv J_{K_0}$$

(c is a real constant). Then take the (3,4)th element of the resulting matrix equation. We obtain

$$A_{44} \int d^4x \frac{\delta^5 Z}{\delta J_{K_0}(x) \delta J_{41}(y) \delta J_{41}(z) \delta J_{13}^*(w) \delta J_{13}^*(v)} \Bigg|_{J_{34} = -ic}$$

$$\begin{aligned}
 &= - \frac{\delta^4 Z}{\delta J_{31}(y) \delta J_{41}(z) \delta J_{13}^*(w) \delta J_{13}^*(v)} \Bigg|_{J_{34} = -ic} + (y \leftrightarrow z) \\
 &+ \frac{\delta^4 J}{\delta J_{14}^*(w) \delta J_{41}(y) \delta J_{41}(z) \delta J_{13}^*(v)} \Bigg|_{J_{34} = -ic} + (w \leftrightarrow v) \quad (I.7)
 \end{aligned}$$

where, we note,

$$A_{33} = A_{44}, \quad i \frac{\delta}{\delta J_{K_0}(x)} = \frac{\delta}{\delta J_{34}(x)} - \frac{\delta}{\delta J_{34}^*(x)}.$$

The external source is such that it conserves charge and creates (positive) strangeness. Then the left-hand side of Eq. (I.7) corresponds to the Green's function containing 2 'soft' K_0 's, while each term on the right-hand side contains only one 'soft' K_0 . In the same manner the Green's functions on the right-hand side can be related to 4-point Green's functions containing no K_0 's. The result is

$$\begin{aligned}
 A_{44} &\int d^4x \frac{\delta^5 Z}{\delta J_{31}(y) \delta J_{41}(z) \delta J_{13}^*(w) \delta J_{13}^*(v) \delta J_{K_0}(x)} \\
 &= \left\{ \frac{\delta^4 Z}{\delta J_{31}(y) \delta J_{41}(z) \delta J_{14}^*(w) \delta J_{13}^*(v)} + (w \leftrightarrow v) \right\} \\
 &\quad - \frac{\delta^4 Z}{\delta J_{31}(y) \delta J_{31}(z) \delta J_{13}^*(w) \delta J_{13}^*(v)} \quad (I.8)
 \end{aligned}$$

etc. Using Eq. (I.8) and a similar equation in Eq. (I.7) we obtain the

final result which is shown diagrammatically in Fig. 38. The sum of the 4-point Green's functions is much easier to deal with directly. For example, one component of the right-hand side of Fig. 38 is shown in Fig. 9. That this vanishes at least on mass shell can be seen easily. For, then, it is the corresponding sum of the Green's functions of the related nonlinear model;^{23, 24} which has the interaction terms:

$$\begin{aligned} \mathcal{L}_{(K_c \pi_c)} &= (\text{const}) [(K_c^+ \partial K_c^-)^2 + (\pi_c^+ \partial \pi_c^-)^2 + 2(K_c^+ \partial K_c^-)(\pi_c^+ \partial \pi_c^-)] \\ &+ (\text{const}) [(K_c^+ K_c^-)^2 + (\pi_c^+ \pi_c^-)^2 + 2(K_c^+ K_c^- \pi_c^+ \pi_c^-)] . \end{aligned}$$

REFERENCES AND FOOTNOTES

- ¹For a review of the subject, see e. g., B. W. Lee, "Perspectives in the Theory of Weak Interactions" in Proceedings of the XVI International Conference on High Energy Physics (NAL 1972) Vol. V; S. Weinberg, "Recent Progress in Gauge Theories of Weak, Electromagnetic and Strong Interactions," Rev. Mod. Phys. 46, 255 (1974).
- ²For a discussion of several specific models see, B. D. Bjorken and C. H. Llewellyn-Smith, Phys. Rev. D7, 887 (1973).
- ³S. L. Glashow, J. Iliopoulos and L. Maiani, Phys. Rev. D2, 1285 (1970).
- ⁴It should be noted that the modification of the charged weak current to $J_{\mu}^{+} = \bar{p} \gamma_{\mu} (1 - \gamma_5) n_c + \bar{p}' \gamma_{\mu} (1 - \gamma_5) \lambda_c$, where $\lambda_c = \lambda \cos \theta - n \sin \theta$, suppresses these $\Delta S = 1$, $\Delta Q = 0$ processes at the level G_F . Such a suppression alone may not be enough as these processes may proceed via induced neutral currents at the level $G_F \alpha$. However, one notes that the processes we shall consider are all forbidden in the exact SU(4) limit; i. e., if $m_{\text{charmed}}^2 = m_{\text{uncharmed}}^2 = \Delta m_c^2 = 0$. This leads to an additional suppression of $(\Delta m_c^2 / M^2)$.
- ⁵M. K. Gaillard and B. W. Lee, Phys. Rev. D10, 897 (1974). This paper lists several references related to this subject.

⁶S. Weinberg, Phys. Rev. Lett. 19, 1264 (1967); A. Salam in Proceedings of the Eighth Nobel Symposium (Almqvist and Wiksell, Stockholm, 1968).

The scheme which incorporates hadrons is discussed in: S. Weinberg, Phys. Rev. Lett. 27, 1688 (1971). Also see Ref. 2.

⁷Except in context of specific models, see for example: "Search for Charm", M.K. Gaillard, B.W. Lee and J. Rosner, FERMILAB-Pub-74/86-THY, to be published.

⁸This model is an $SU(4) \times SU(4)$ version of the model discussed in W.A. Bardeen and B.W. Lee, Phys. Rev. 177, 2389 (1969).

⁹For a detailed discussion of the σ -model see "Chiral Dynamics", B.W. Lee (Gorden and Breach, NY 1972).

¹⁰The $SU(3)$ σ -model is discussed in M. Levy, Nuovo Cimento 52, 23 (1967). See also Ref. 8.

¹¹See for example: C.H. Albright, Phys. Rev. D8, 3162 (1973); B. Aubert et al., Phys. Rev. Lett. 32, 1457 (1974).

¹²As discussed in Ref. 8, if we let $\mu_0^2 \rightarrow -\infty$ [see Eq. (2.3)] in such a phenomenological model of strong interactions alone, we recover one of the nonlinear realizations of the $SU(4) \times SU(4)$ group containing only the 15 pseudoscalar (independent) fields. One may compute weak processes in such a model. However, there are divergences in such a theory. In keeping μ_0^2 large but finite, we are in a sense regularizing

the nonlinear model. In any case, one should note that the model of strong interactions incorporates current algebra and PCAC for any μ_0^2 .

¹³ Whenever the result is proportional to the SU(4) breaking, we may do this since SU(4) breaking is assumed to be large as compared to SU(3) breaking.

¹⁴ This process, therefore, does not allow us to infer about m_c .

¹⁵ "Observation of $K^+ \rightarrow \pi^+ e \bar{e}$ Decay," P. Bloch et al., Reported at the London Conference, July 1974.

¹⁶ For some range of parameters α, β, γ .

¹⁷ As a result of the interaction $\frac{1}{2} \text{tr} (D_\mu M^\dagger D^\mu M)$ of Eq. (2.14) M_W^2 and M_Z^2 will acquire additional contribution due to the vacuum expectation value of M. This change in M_W^2 and M_Z^2 is of $0 \left(\frac{f^2}{v^2} \right) \lesssim 10^{-6}$, thus numerically small and therefore negligible. What enter the gauge condition of Eq. (2.7) are however $\frac{1}{2} gv$ and $\frac{1}{2} Gv$ rather than M_W and M_Z .

¹⁸ K. Fujikawa, B. W. Lee and A. I. Sanda, Phys. Rev. D6, 2923 (1972).

¹⁹ The reason for choosing only quadratic terms in $\mathcal{L}_{M\Phi}$ is as follows: $\mathcal{L}_{M\Phi}$ has a contribution to the phenomenological Lagrangian of strong interactions defined by $\lim_{g \rightarrow 0} \mathcal{L}_{M\Phi}$. When $\mathcal{L}_{M\Phi}$ is chosen as we have done, $\lim_{g \rightarrow 0} \mathcal{L}_{M\Phi} = \mathcal{L}_{M\Phi} \Big|_{\Phi=v}^{g \rightarrow 0}$ has the form $\text{tr} A(M + M^\dagger)$. With this

SU(4) \times SU(4) symmetry breaking term, the "PCAC equations" are incorporated.

²⁰See for example, B. W. Lee and H. T. Nieh, Phys. Rev. 166, 1507 (1968) and references quoted therein.

²¹W. C. Carruthers et al., Phys. Rev. Lett. 31, 1025 (1973) ;
B. Martin, E. DeRafael and J. Smith, Phys. Rev. D2, 179 (1970).
This paper lists earlier works on the unitarity bound.

²²The number of diagrams contributing to $\Gamma_{0k}^{(3)}$ is comparable to that contributing to Γ_{0Z}^{μ} . The WT identity of Eq. (6.1) would not have been of particular use were it not the fact that most of the diagrams contributing to $\Gamma_{0k}^{(3)}$ do not contribute to the combination $\sum_k f_k t_{3k} \Gamma_{0k}^{(3)}$.

²³We need to consider only that part which has a nonzero limit as $\mu^2 \rightarrow \infty$ after the loop integrations are performed.

²⁴See discussion of Ref. 8.

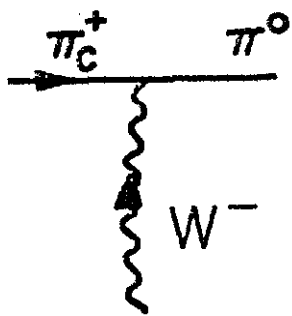
²⁵B. W. Lee, Phys. Rev. D9, 933 (1974).

FIGURE CAPTIONS

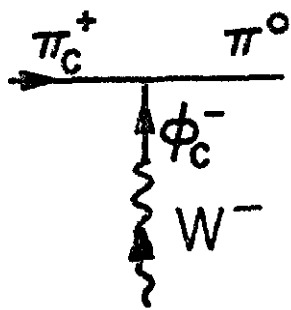
- Fig. 1 $\pi_c^+ \pi^0 W^- (s^-)$ vertex
- Fig. 2 A possible one loop diagram for $\pi_c^+ \pi^0 W^-$ vertex.
- Fig. 3 Some of the diagrams for $K^0 \rightarrow \mu\bar{\mu}$.
- Fig. 4 Diagrams for $K^0 \rightarrow W^+ W^-$ vertex.
- Fig. 5 $K^0 \pi^0$ self-energy diagrams.
- Fig. 6 Diagrams for the $K^0 \chi$ vertex.
- Fig. 7 Diagrams contributing to $K^0 Z$ vertex which may be proportional to $\frac{1}{m_K^2}$ for K^0 on mass shell (and $m_\pi^2 = 0$).
- Fig. 8 IPI graphs for $K^0 \rightarrow \mu\bar{\mu}$.
- Fig. 9 Higgs exchange diagrams for $K^0 \rightarrow \mu\bar{\mu}$.
- Fig. 10 Diagrams for the $K^+ \pi^- Z_\mu$ vertex.
- Fig. 11 WT identity for the $K^+ \pi^- Z_\mu$ proper vertex.
- Fig. 12 Diagrams for the $K^+ \pi^- \chi$ vertex.
- Fig. 13 Diagrams for the $K^+ \pi^- \Pi_{ii}$ proper vertex.
- Fig. 14 Diagrams for the $K^0 \pi^0 Z_\mu$ vertex.
- Fig. 15 WT identity for the $K^0 \pi^0 Z_\mu$ proper vertex.
- Fig. 16 Diagrams for the $K^0 \pi^0 \chi$ proper vertex.
- Fig. 17 Diagrams for the $K^0 \pi^0 \Pi_{kk}$ proper vertex.
- Fig. 18 The diagram of Fig. 17(q) and the $\kappa^0 \pi^0$ self-energy diagrams.

- Fig. 19 $K_{\xi_1}^0(\xi_2)$ self-energy diagrams.
- Fig. 20 The diagram of $O(\mu^2)$ which contributes to K_{π}^{00} self-energy.
- Fig. 21 Diagrams for the $K^+\pi^-\gamma$ proper vertex.
- Fig. 22 Diagrams for the $K^0\pi^0\gamma$ proper vertex.
- Fig. 23 The two kinds of diagrams contributing to $K^0 \rightarrow \bar{K}^0$ transition.
- Fig. 24 One-loop diagrams for $K^0 \rightarrow \bar{K}^0$ transition.
- Fig. 25 Two-loop diagrams for the $K_0 \rightarrow \bar{K}_0$ transition.
- Fig. 26 The cancellations among diagrams of Class 2 at $p = 0$.
- Fig. 27 The cancellations of terms proportional to μ^2 and μ^4 in the diagrams of Class 3.
- Fig. 28 The diagram of Fig. 25(b) shown with all intermediate states.
- Fig. 29 The diagram in Fig. 25(c) shown with all intermediate states.
- Fig. 30 WT identity for the $K^+\pi^-\gamma$ proper vertex.
- Fig. 31 Contributions to the total $K^+\pi^-\gamma$ vertex.
- Fig. 32 Contributions to the total $K^0\pi^0\gamma$ vertex.
- Fig. 33 The diagrams for the $K^+ \rightarrow \pi^+$ transition involving a W propagator (Landau gauge) and for the $K^+\pi^- \rightarrow W^+W^-$ amplitude which do not vanish when W^\pm are on mass shell.
- Fig. 34 Diagrams for $K^+\pi^- \rightarrow K_c^+\pi_c^-$.

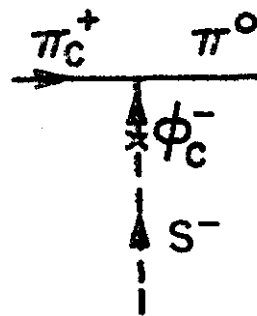
- Fig. 35 'Box' diagrams for $K^+ \rightarrow \pi^+ \nu \bar{\nu}$.
- Fig. 36 Higgs exchange diagrams for $K^+ \rightarrow \pi^+ \mu \bar{\mu}$.
- Fig. 37 Diagrams contributing to Fig. 36(a).
- Fig. 38 The equation used in showing that the sum of the diagrams of Class 3 vanish at $p = 0$.
- Fig. 39 A contribution to the right-hand side of the equation in Fig. 38.



(a)



(b)



(c)

FIG. 1

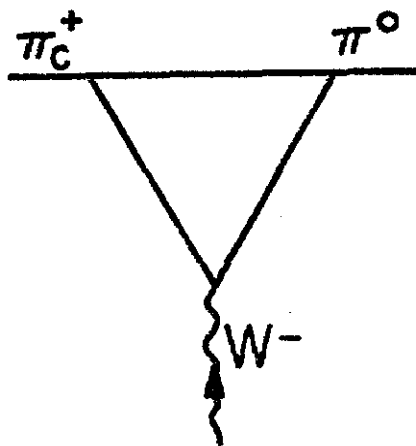
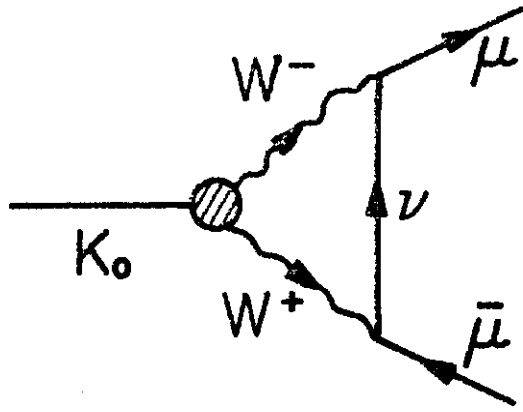
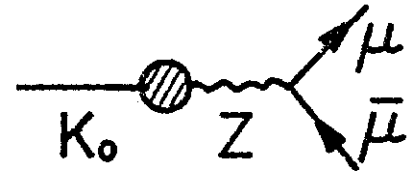


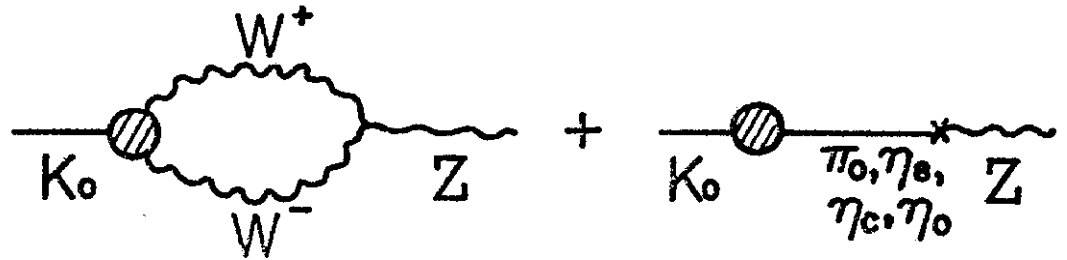
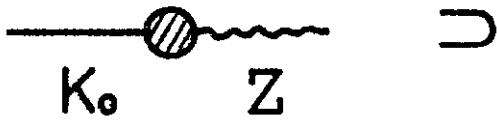
FIG. 2



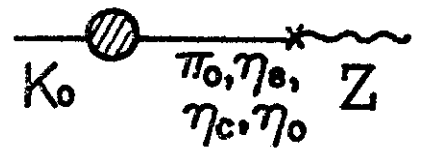
(a)



(b)



(c)



(d)

FIG. 3

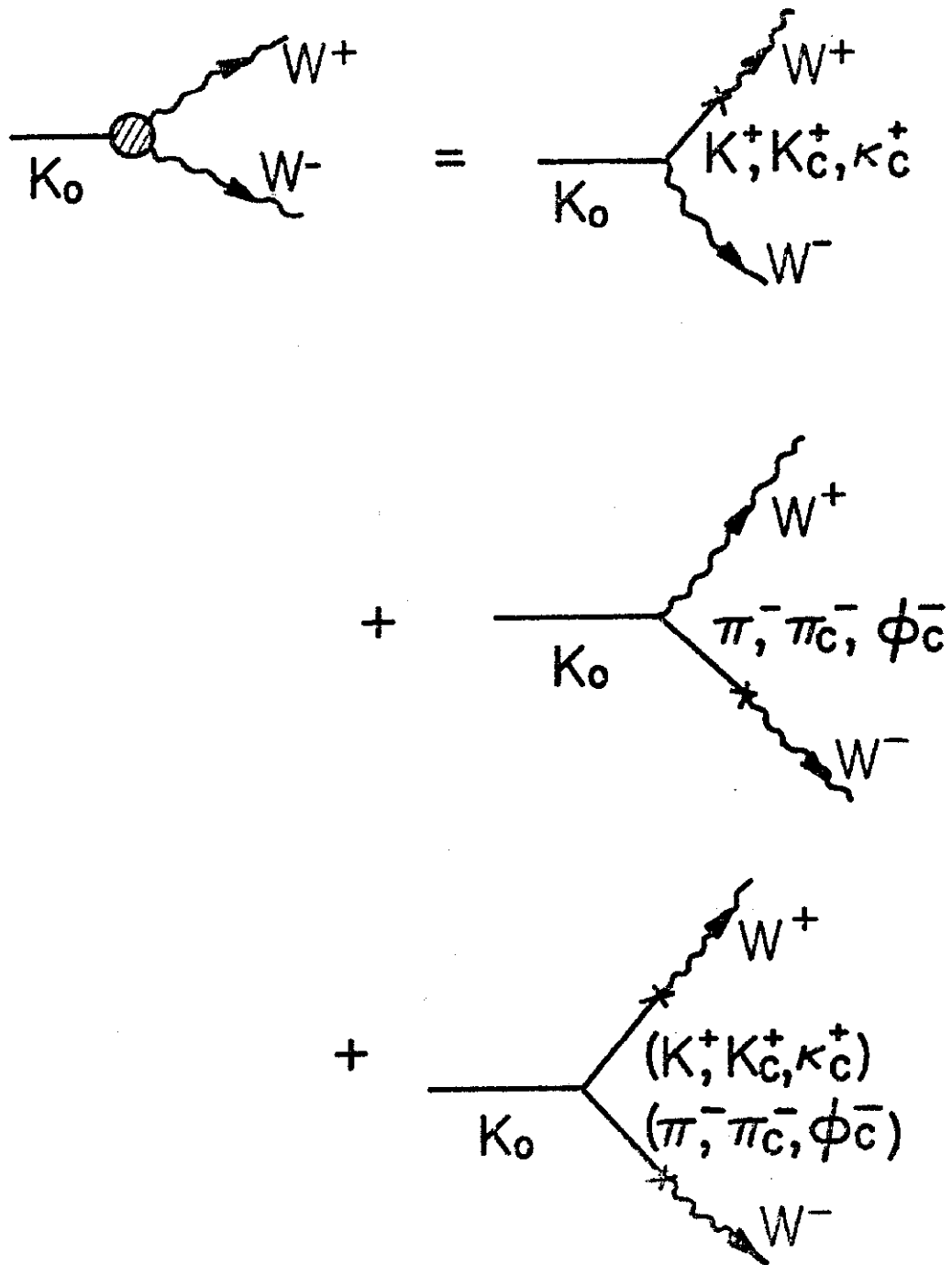


FIG.4

$$\begin{aligned}
 & K_0 \text{---} \textcircled{\text{---}} \text{---} \pi_0 = \\
 & \begin{array}{c}
 \text{---} K_0 \text{---} \text{---} \pi_0 \text{---} \\
 \text{---} \text{---} W^\pm \text{---} \\
 \text{---} \text{---} \\
 \text{---} K_0 \text{---} \pi_0 \text{---} \\
 + \\
 \text{---} K_0 \text{---} \pi_0 \text{---} \\
 \text{---} W^+ \text{---} \\
 \text{---} \text{---} \\
 \text{---} K_0 \text{---} \pi_0 \text{---} \\
 + \\
 \text{---} K_0 \text{---} \pi_0 \text{---} \\
 \text{---} W^\pm \text{---} \\
 \text{---} K_0 \text{---} \\
 \text{---} K_0 \text{---} \pi_0 \text{---} \\
 + \\
 \text{---} K_0 \text{---} \pi_0 \text{---} \\
 \text{---} W^+ \text{---} \\
 \text{---} \text{---} \\
 \text{---} K_0 \text{---} \pi_0 \text{---}
 \end{array}
 \end{aligned}$$

where,

$$\begin{array}{c}
 \text{---} K_0 \text{---} \\
 \text{---} W^\pm \text{---} \\
 \text{---} K_0 \text{---}
 \end{array}
 =
 \begin{array}{c}
 \text{---} K_0 \text{---} \\
 \text{---} W^\pm \text{---} \\
 \text{---} K_0 \text{---}
 \end{array}
 +
 \begin{array}{c}
 \text{---} K_0 \text{---} \\
 \text{---} W^\pm \text{---} \\
 \text{---} K_0 \text{---}
 \end{array}$$

FIG. 5

$$\begin{array}{c} \longrightarrow \\ K_0 \end{array} \begin{array}{c} \text{[hatched box]} \\ \longrightarrow \\ \chi \end{array} = \begin{array}{c} \longrightarrow \\ K_0 \end{array} \begin{array}{c} \text{[hatched circle]} \\ \longrightarrow \\ \chi \end{array} + \begin{array}{c} \longrightarrow \\ K_0 \end{array} \begin{array}{c} \text{[hatched circle]} \\ \longrightarrow \\ \chi \end{array} \begin{array}{c} \pi_0, \eta_0 \\ \eta_c, \eta_c \end{array}$$

$$\begin{array}{c} \longrightarrow \\ K_0 \end{array} \begin{array}{c} \text{[hatched circle]} \\ \longrightarrow \\ \chi \end{array} \begin{array}{c} (IPI) \end{array} = \begin{array}{c} \longrightarrow \\ K_0 \end{array} \begin{array}{c} K^+, K_c^+, \pi_c^-, (\kappa_c^+, \phi_c^-, \kappa^+) \\ \text{[triangle with } W^{\mp} \text{ and } s^{\pm} \text{]} \\ \longrightarrow \\ \chi \end{array}$$

(a)

$$\Sigma \equiv \begin{array}{c} \longrightarrow \\ K_0 \end{array} \begin{array}{c} \text{[hatched circle]} \\ \longrightarrow \\ \chi \end{array} = \begin{array}{c} \text{[wavy line } W \text{]} \\ K^+, \kappa^+ \\ \longrightarrow \\ K^0 \pi^-, \phi^-, \pi_c^-, \phi_c^- \end{array}$$

(b)

$$+ \begin{array}{c} \text{[triangle with } s^+ \text{]} \\ (\kappa_c^+, \kappa_c^+) \downarrow (\pi_c^+, \phi_c^+) \\ \longrightarrow \\ K_0 (\phi_c^-, \pi_c^-) \end{array} + \begin{array}{c} \text{[triangle with } s^- \text{]} \\ (\phi_c^-, \pi_c^-) \downarrow (\kappa_c^-, \kappa_c^-) \\ \longrightarrow \\ K_0 (\kappa_c^+, \kappa_c^+) \end{array}$$

(c)

(d)

$$+ \begin{array}{c} \text{[triangle with } s^+ \text{]} \\ (\kappa_c^+, \kappa_c^+) \downarrow (\phi_c^+, \pi_c^+) \\ \longrightarrow \\ K_0 \end{array}$$

(e)

$$\begin{array}{c} \text{[triangle with } s^+ \text{]} \\ (\kappa_c^+, \kappa_c^+) \downarrow (\phi_c^+, \pi_c^+) \\ \longrightarrow \\ K_0 \end{array}$$

(e)

FIG. 6



FIG. 7

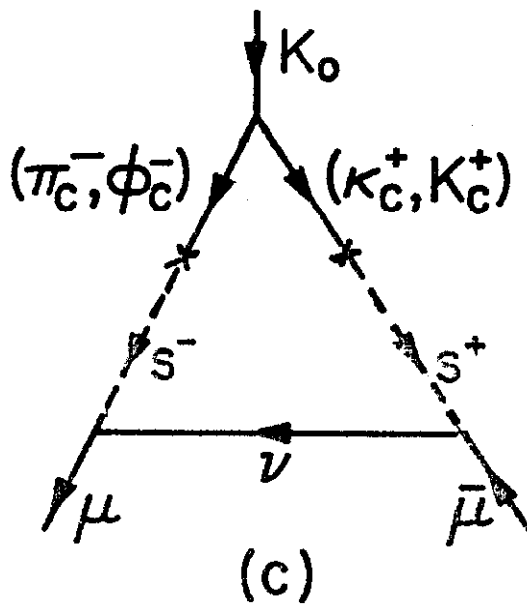
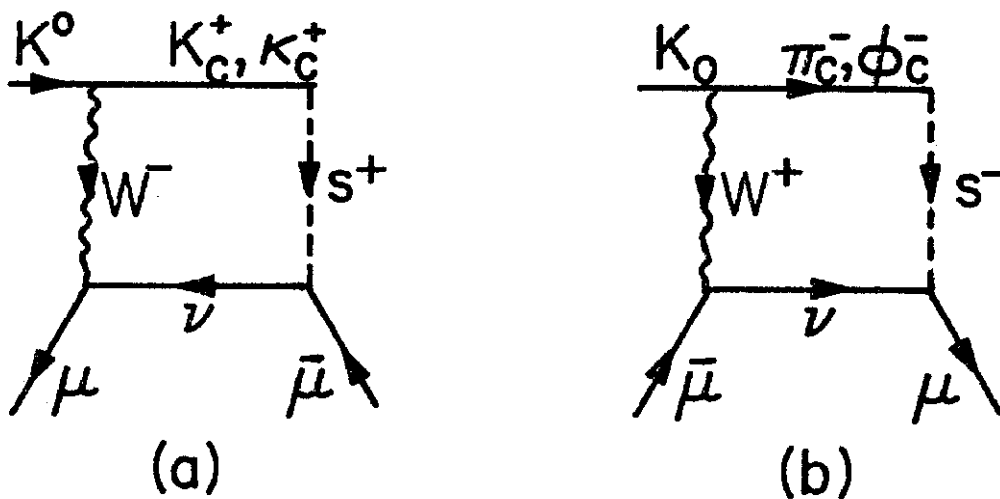


FIG. 8

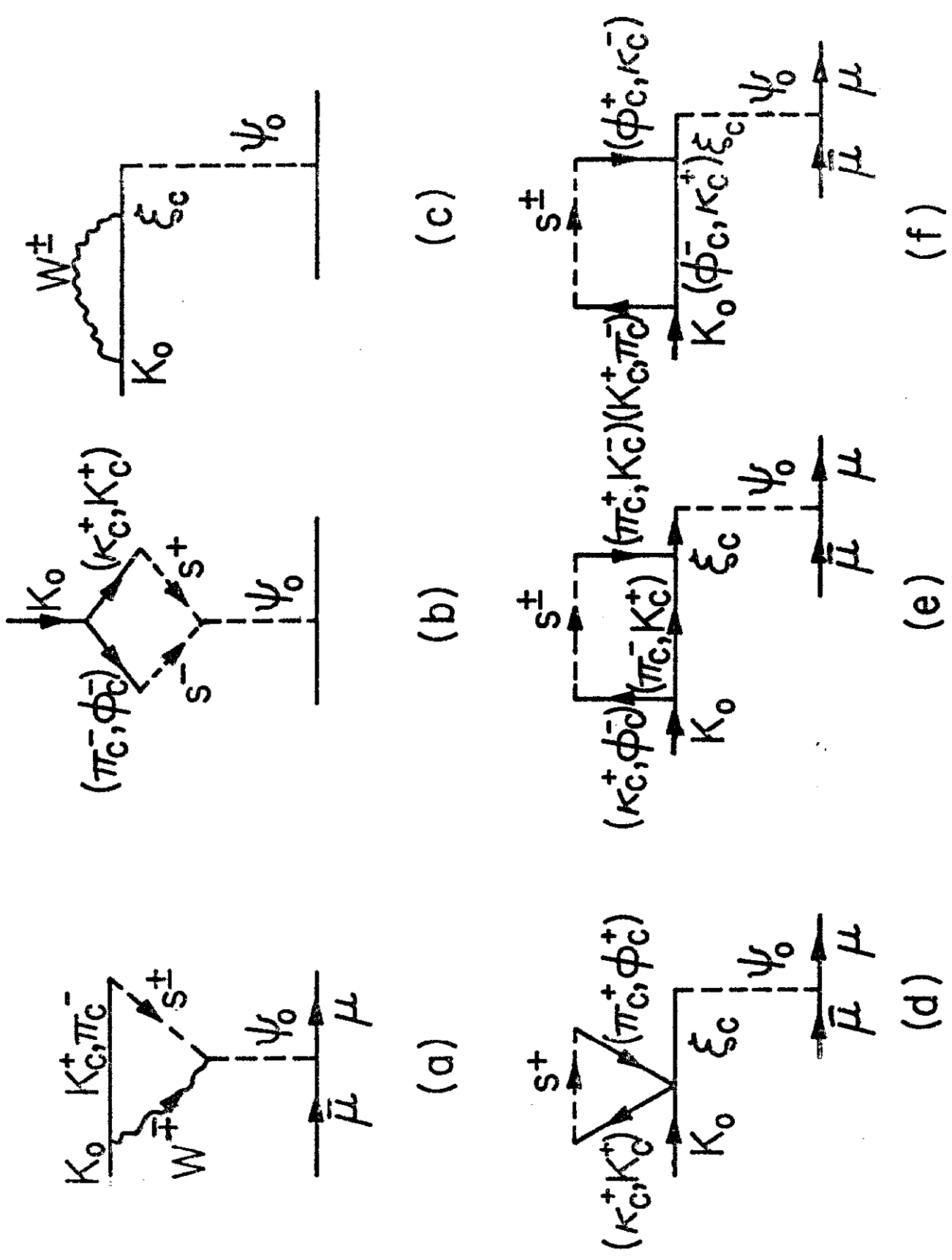


FIG. 9

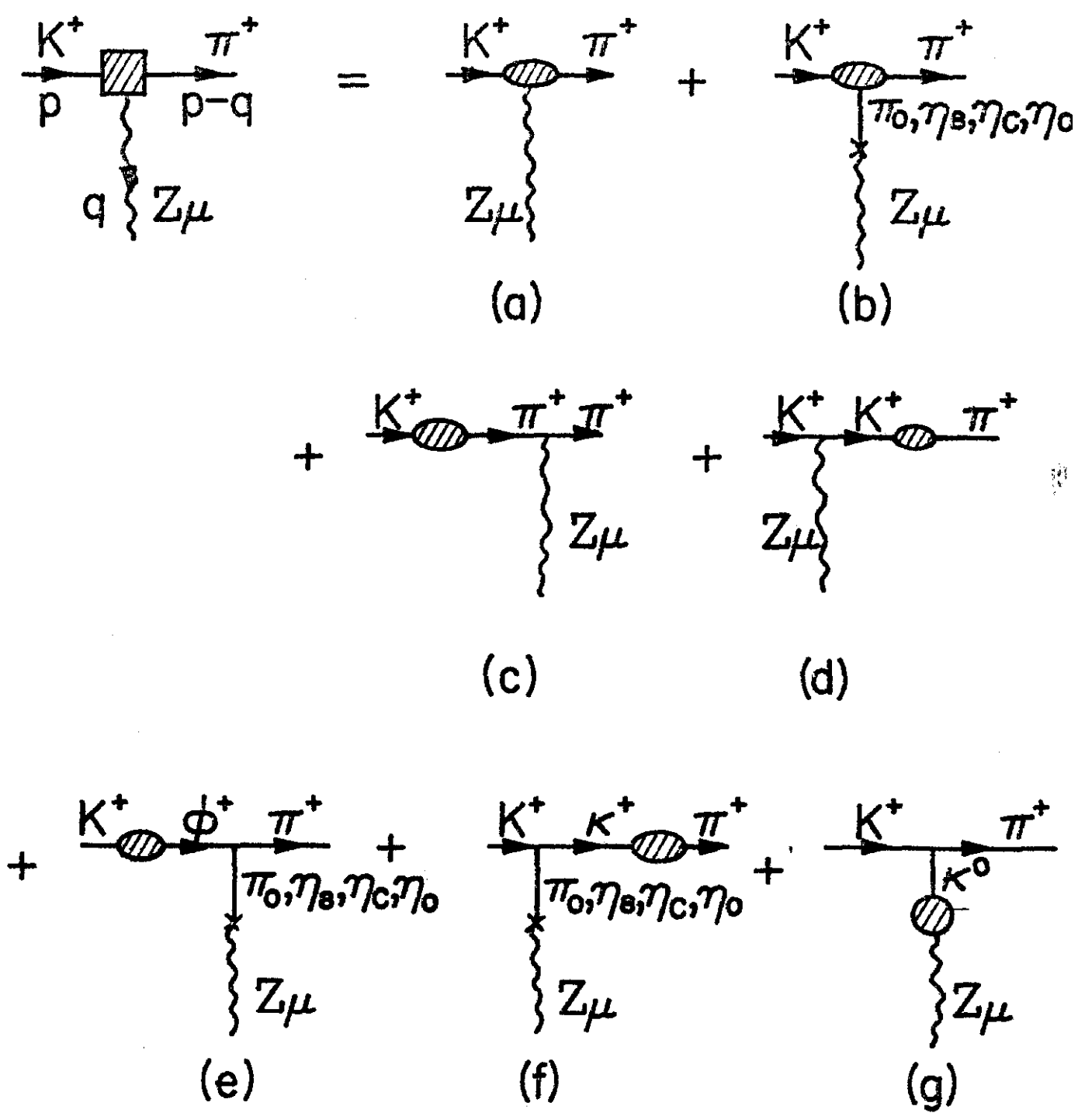
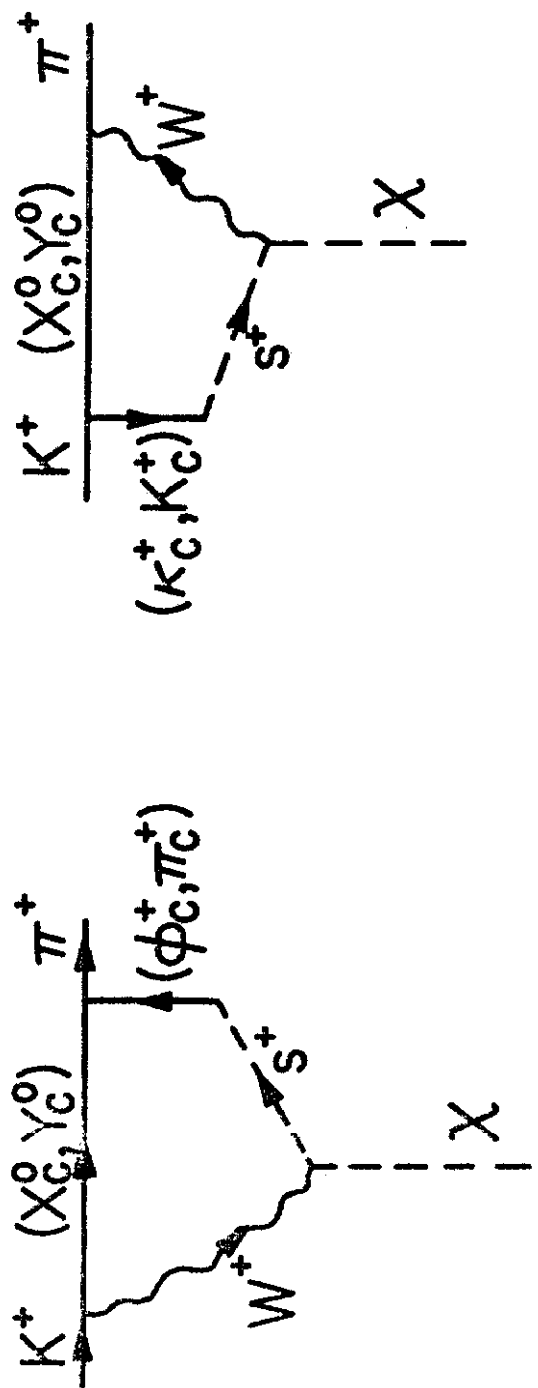


FIG. 10



(a)

(b)

FIG. 12

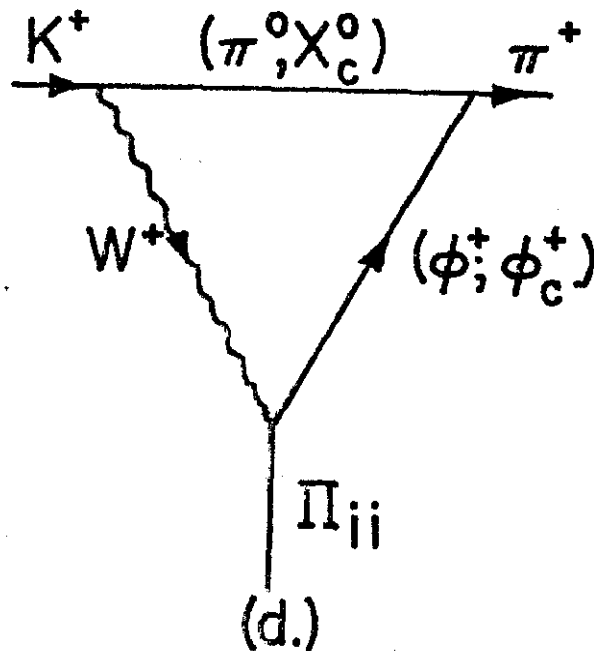
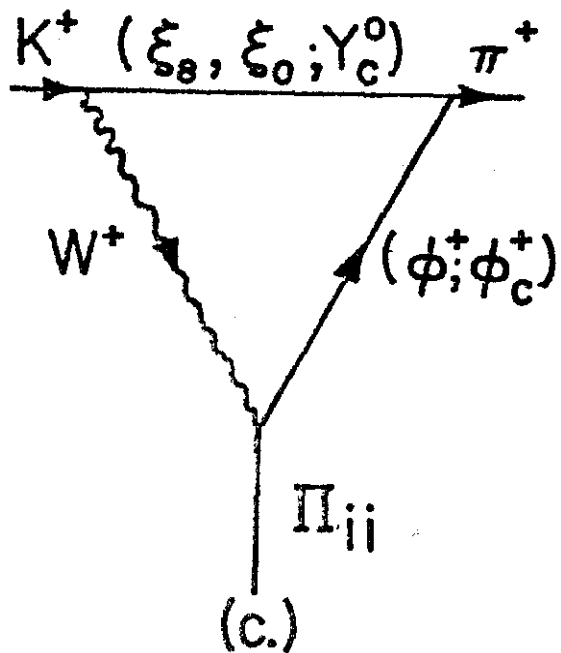
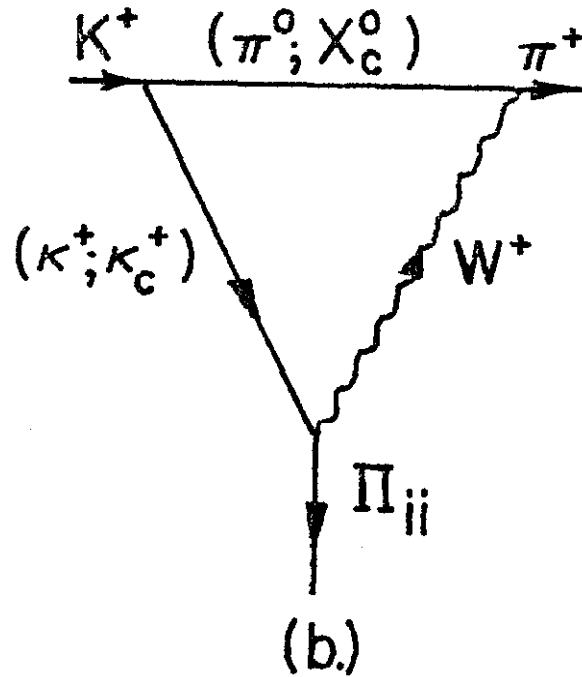
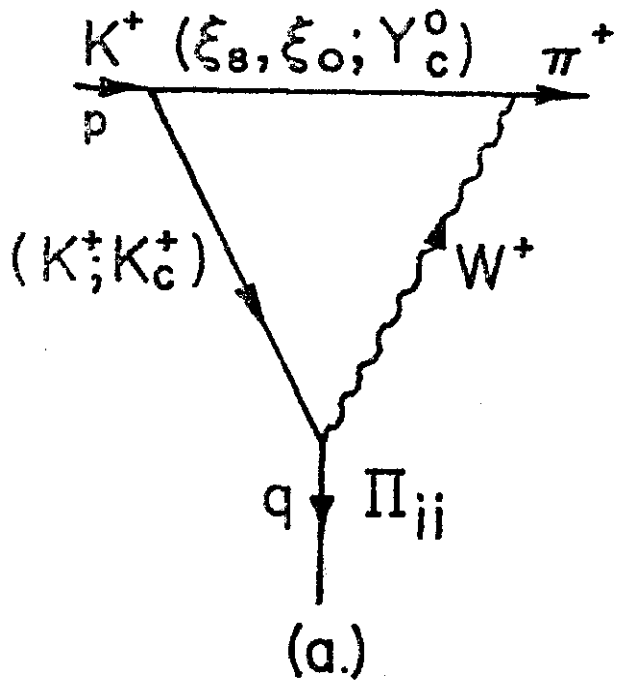


FIG. 13
continued on next page

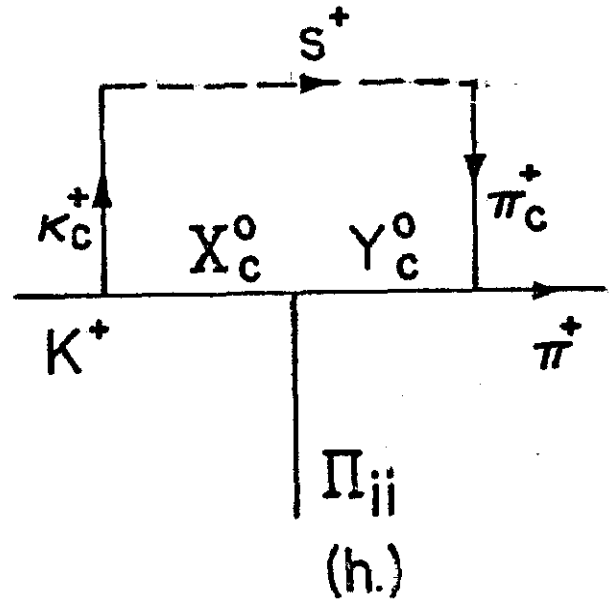
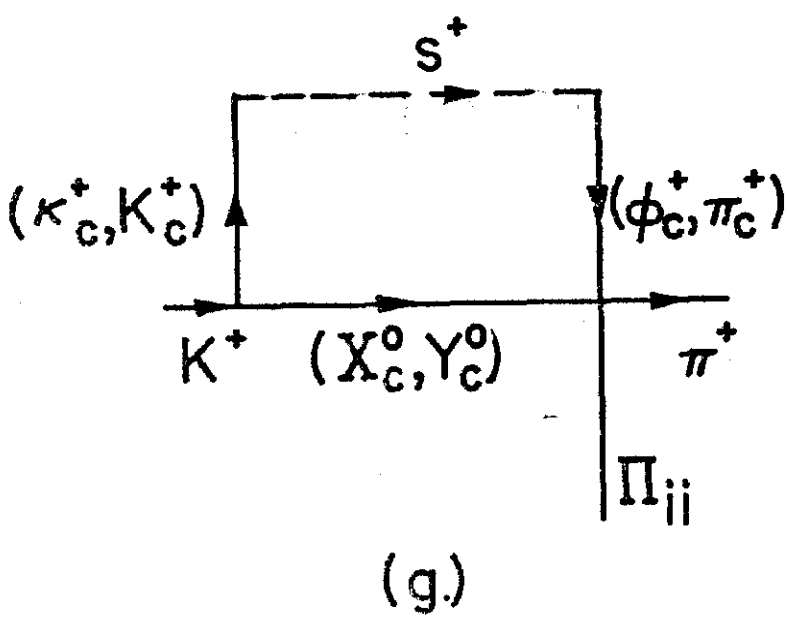
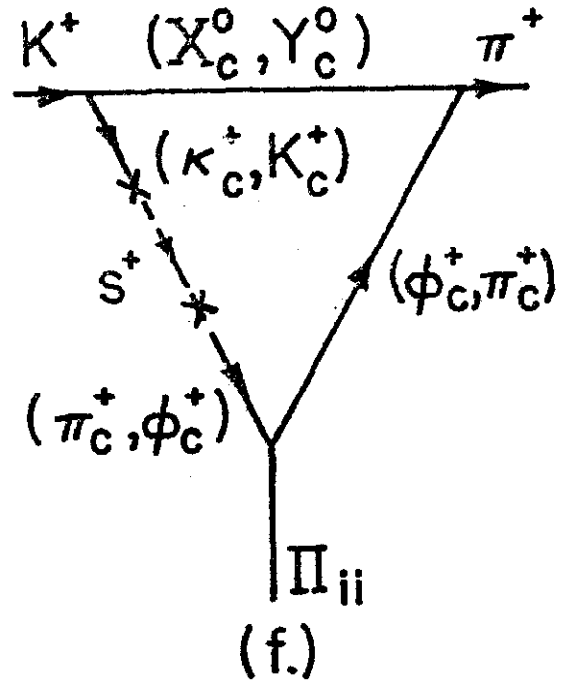
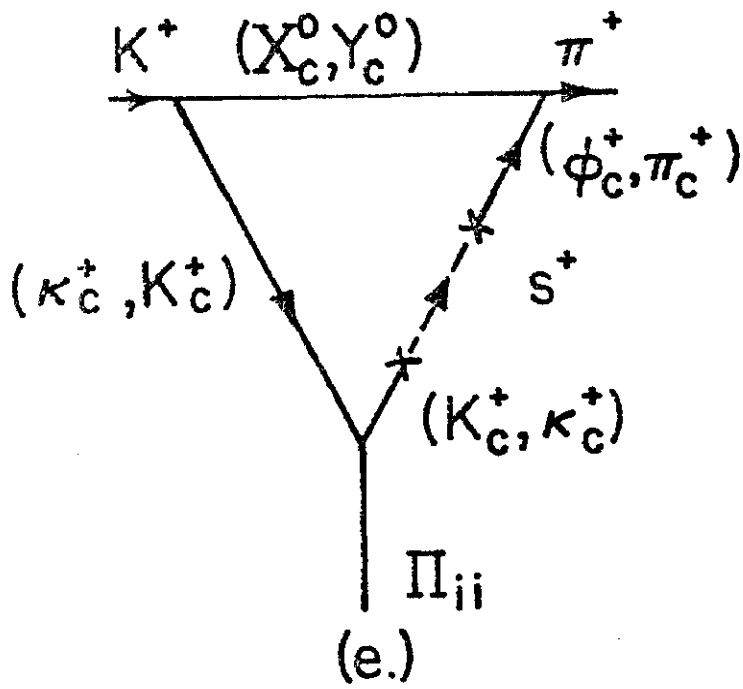


FIG. 13
continued

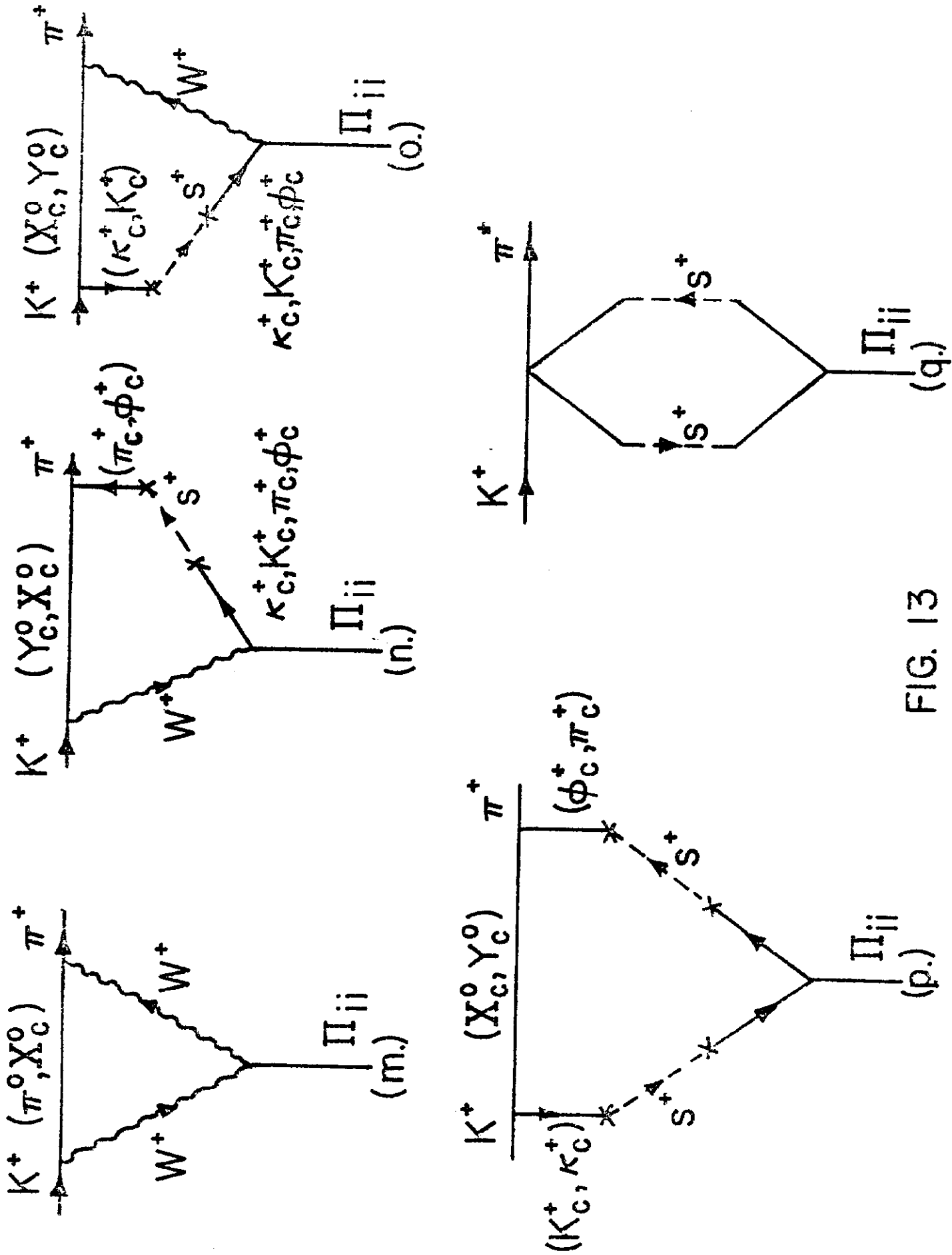


FIG. 13

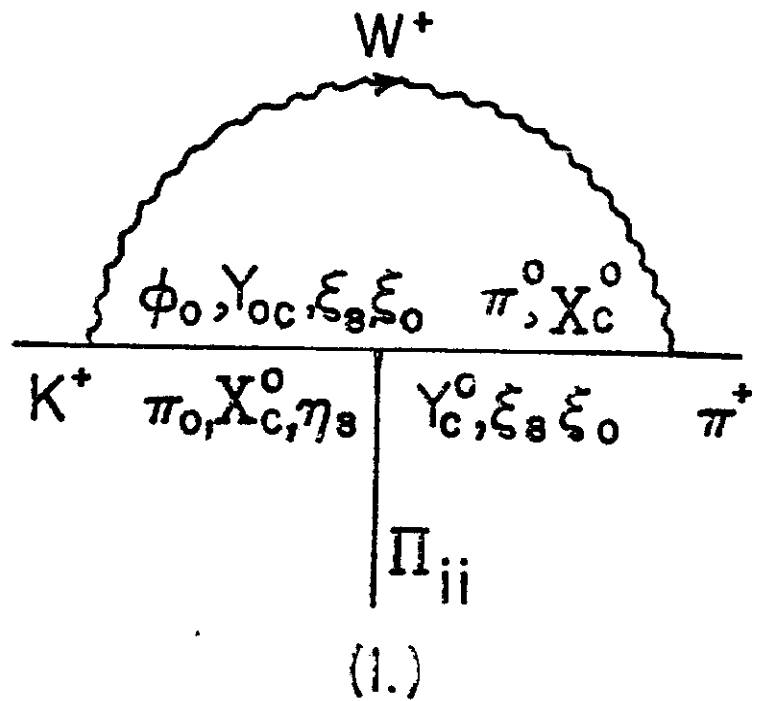
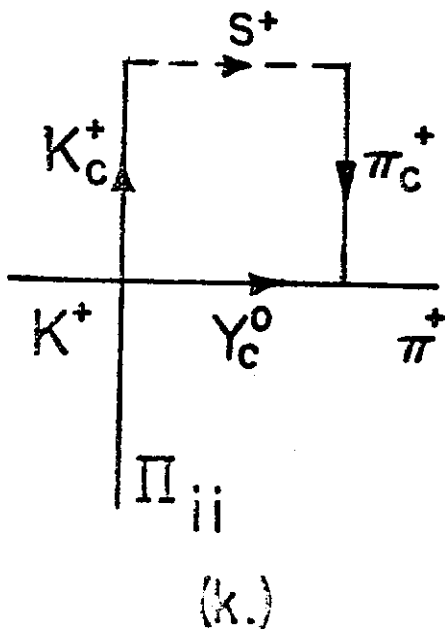
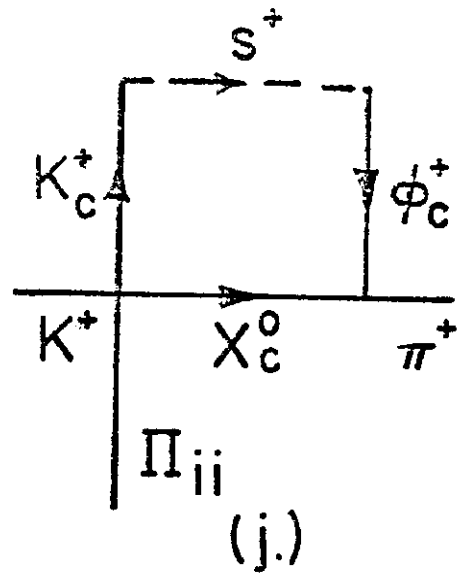
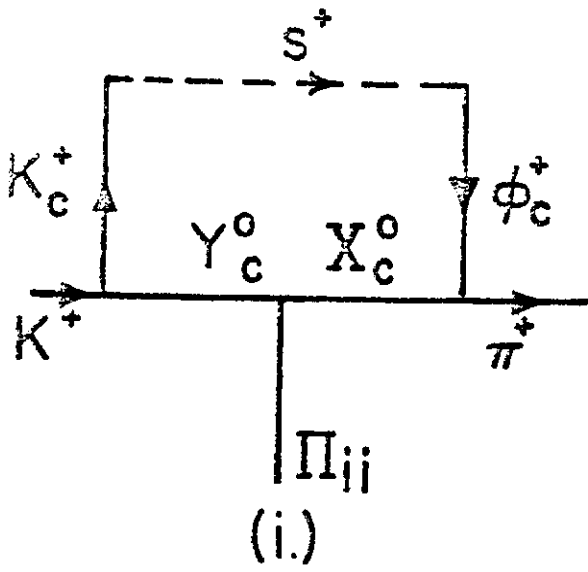


FIG. 13
continued

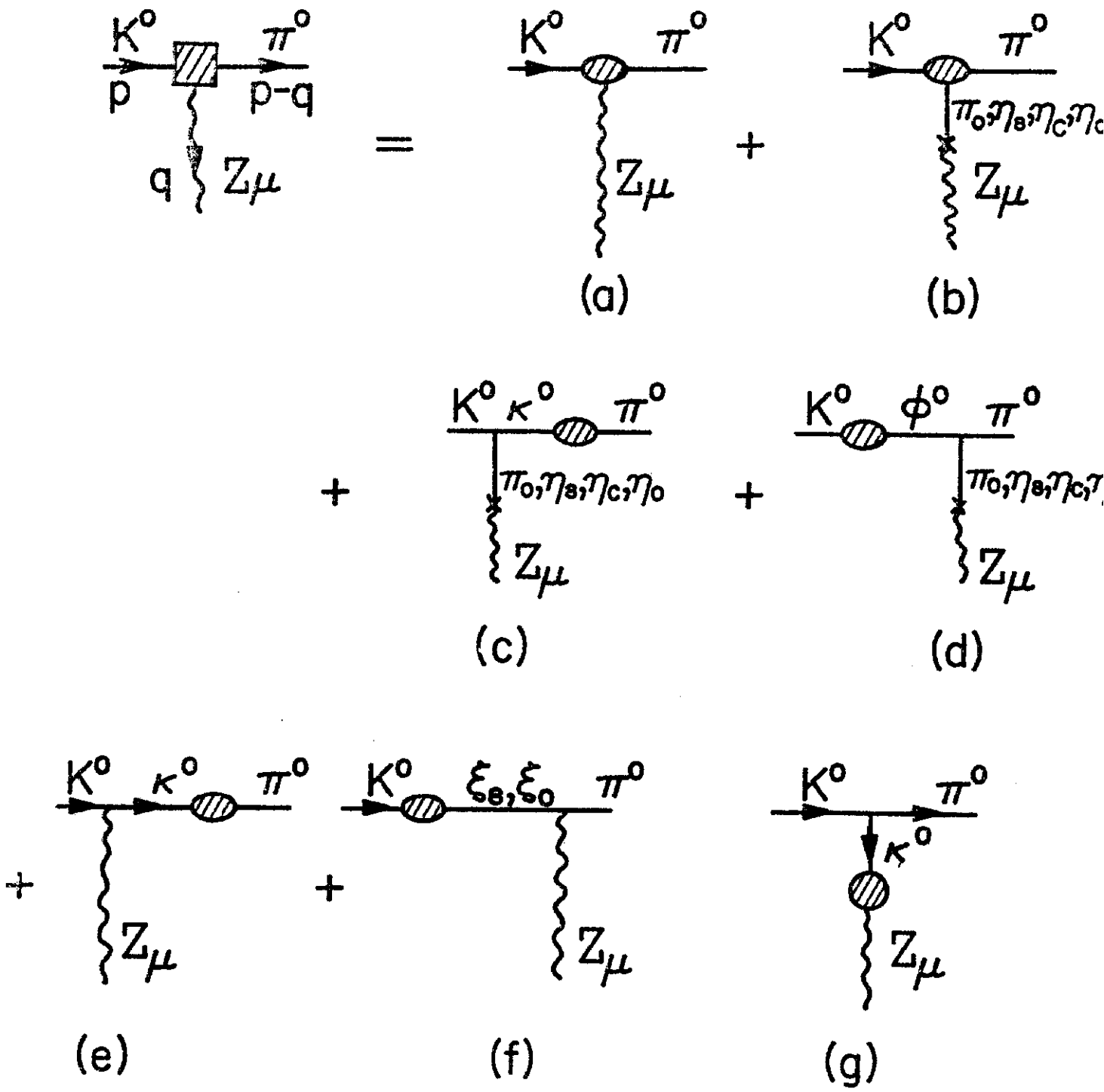
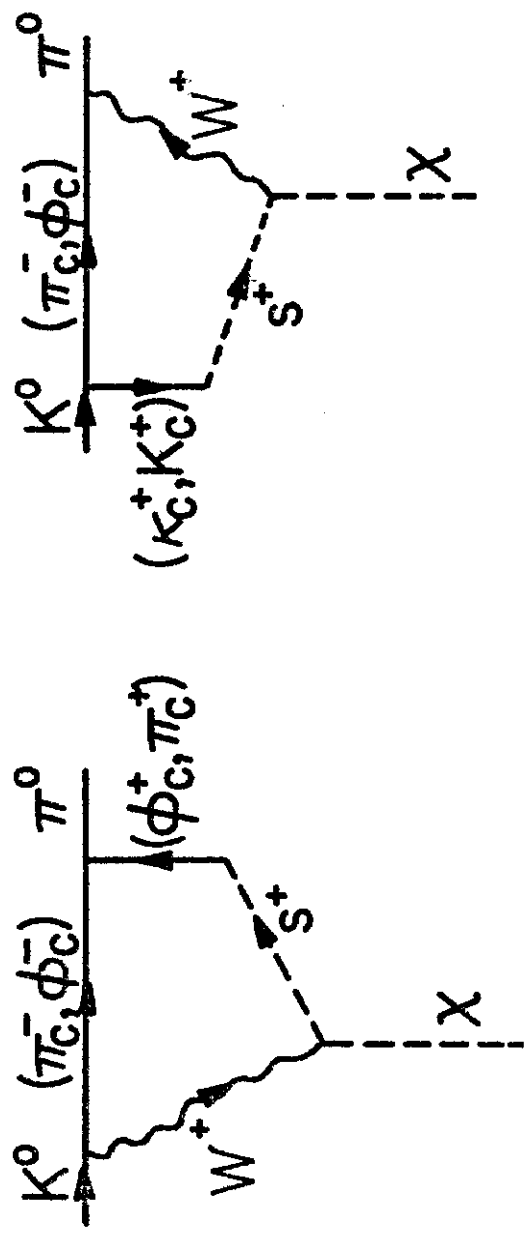


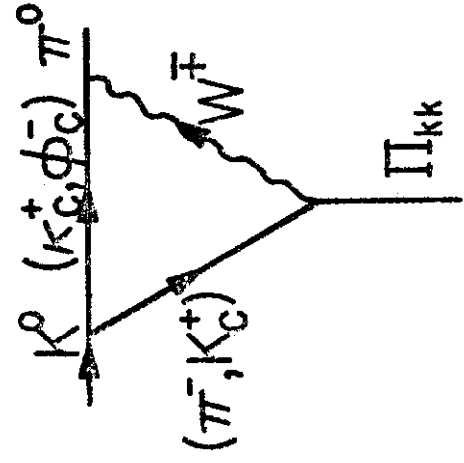
FIG. 14



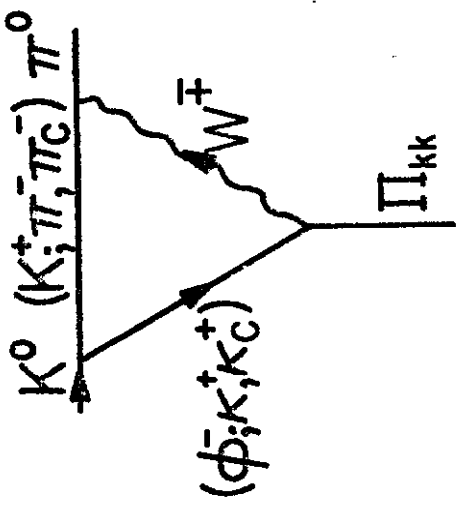
(b)

(a)

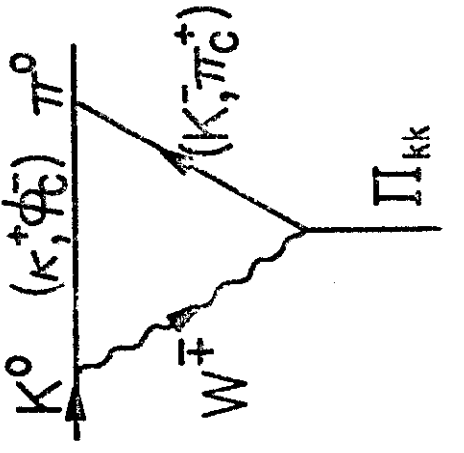
FIG. 16



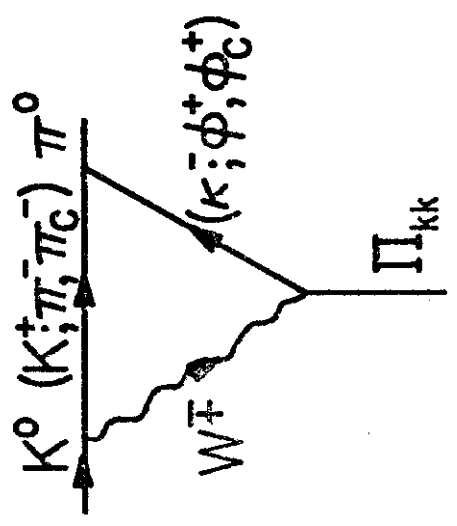
(a)



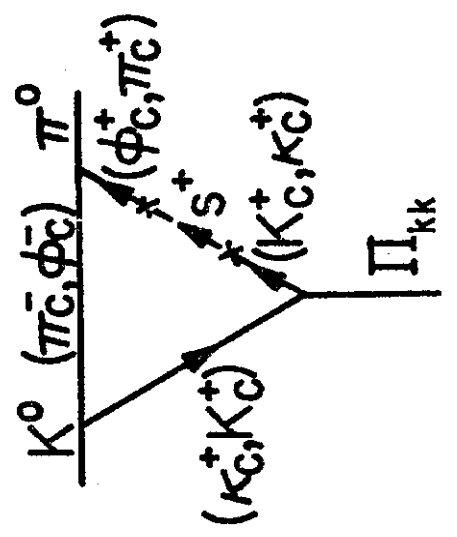
(b)



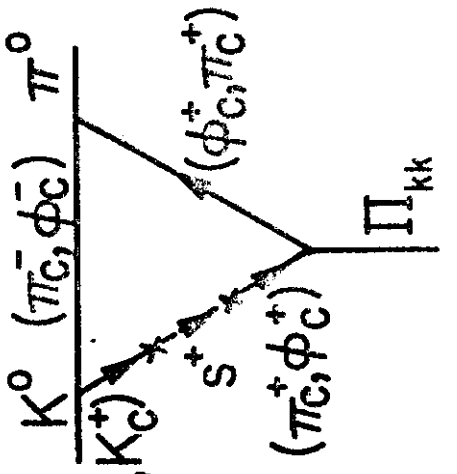
(c)



(d)

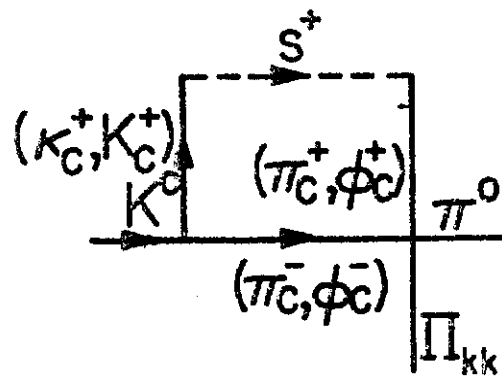


(e)

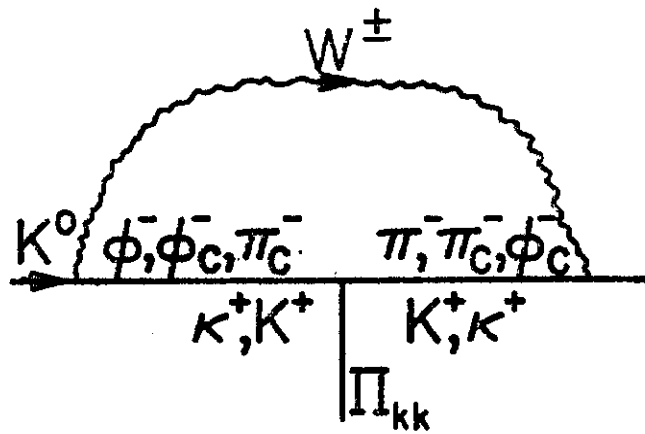


(f)

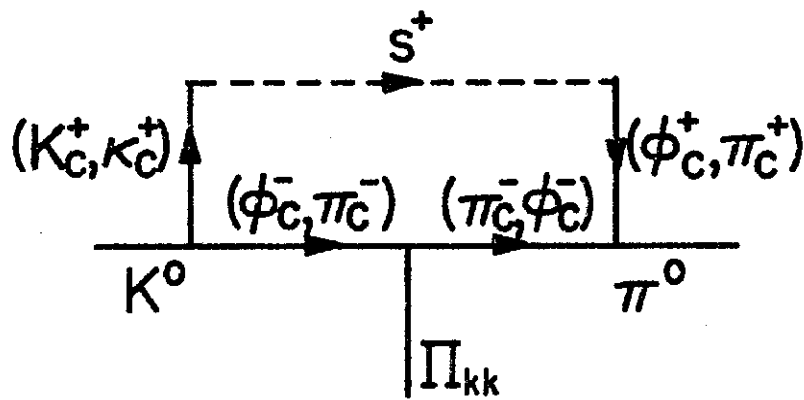
FIG. 17



(g)



(h)



(i)

FIG. 17
(continued)

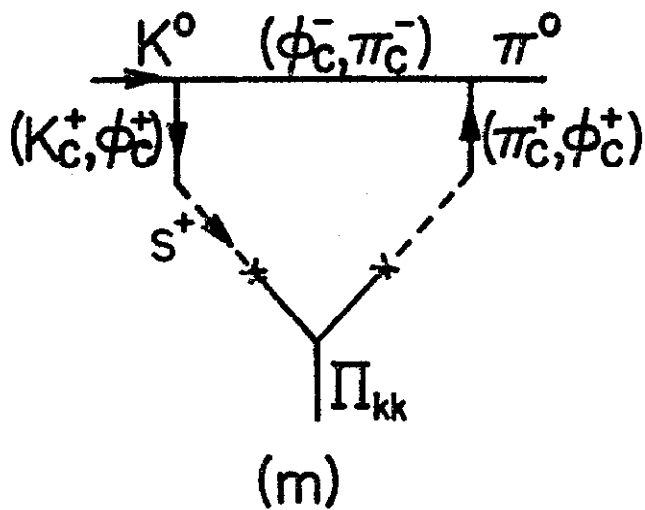
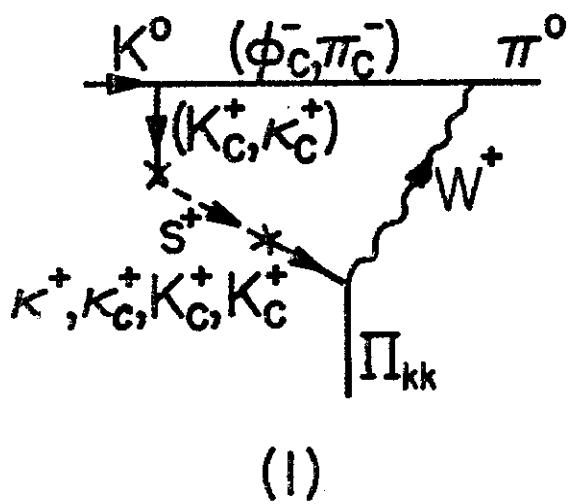
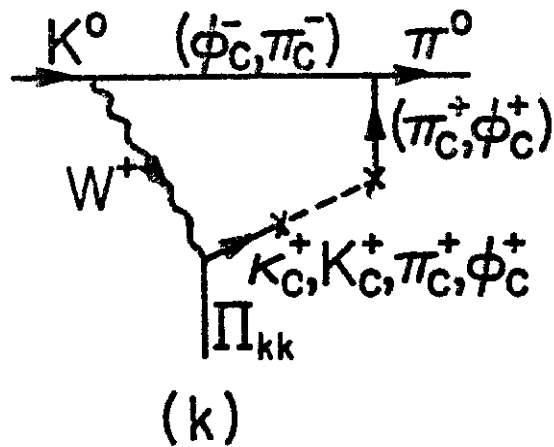
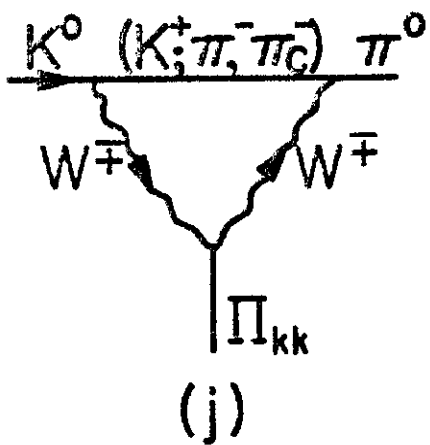
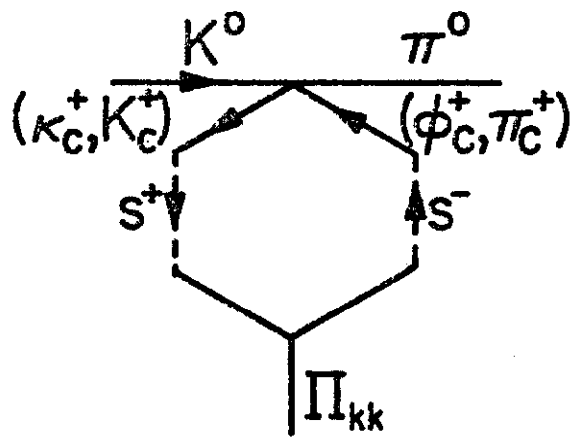
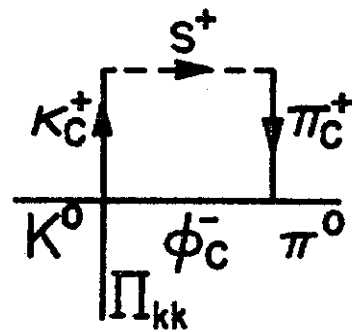


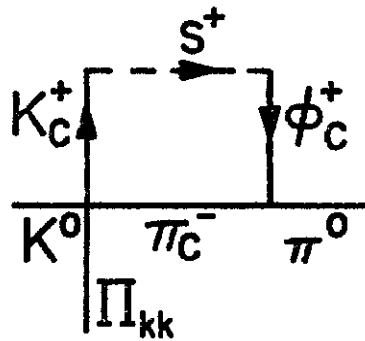
FIG. 17
(continued)



(n)



(p)



(q)

FIG. 17
(continued)

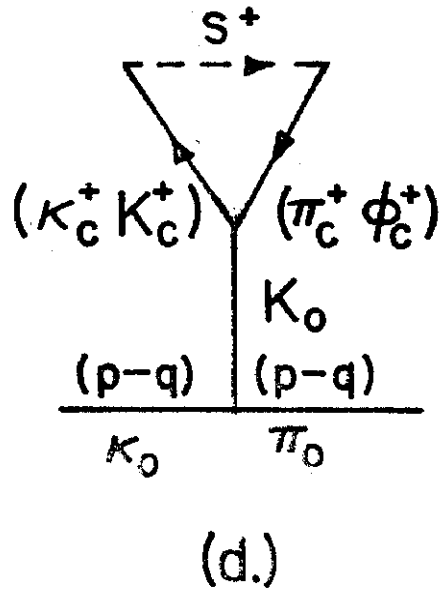
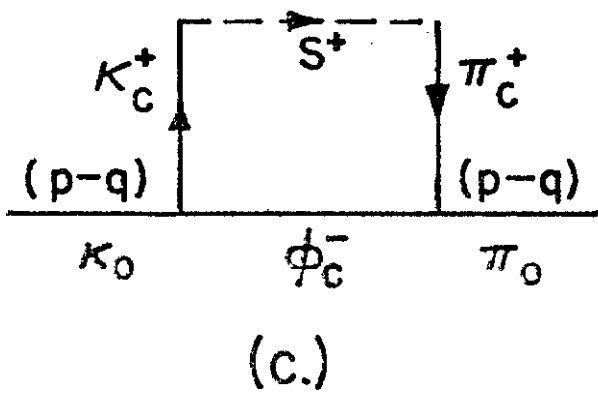
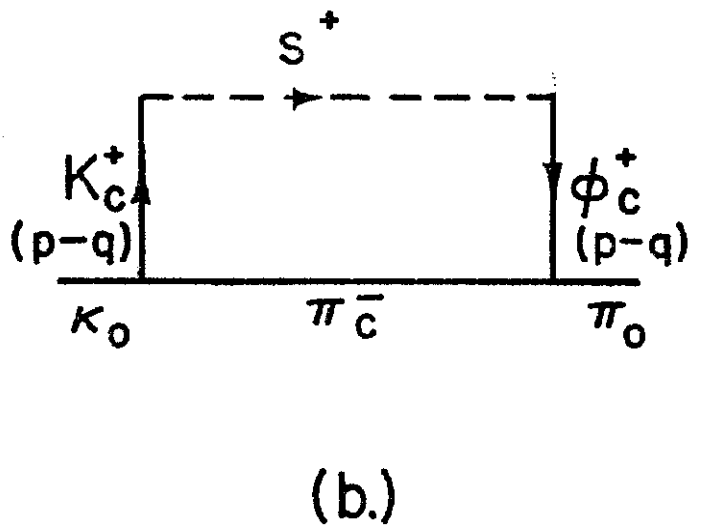
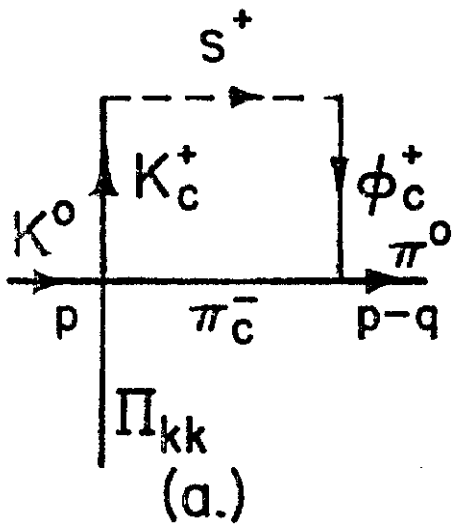
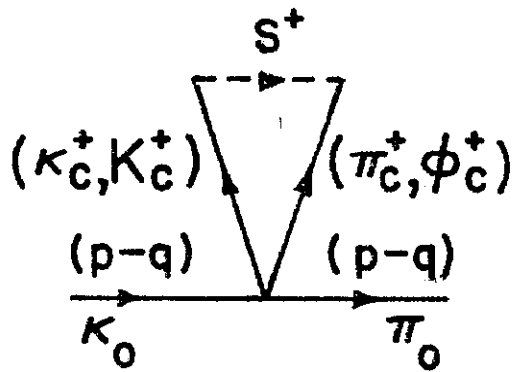
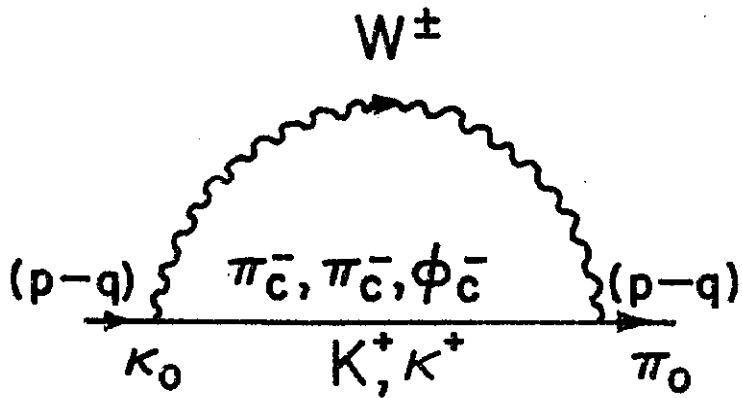


FIG. 18



(e.)



(f.)

FIG. 18
(continued)

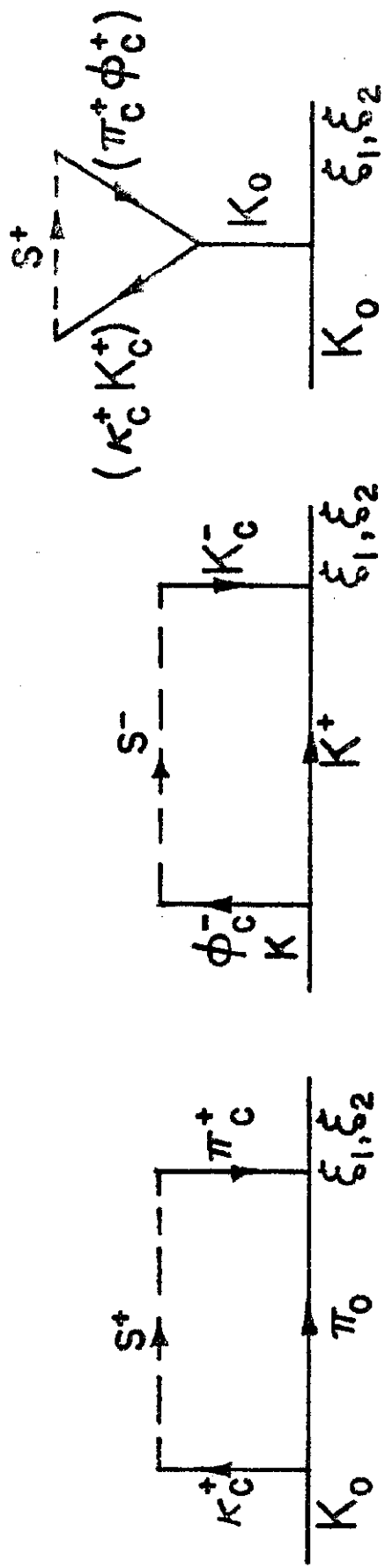


FIG. 19

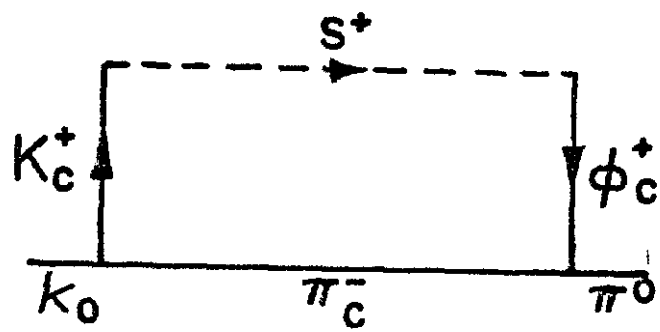


FIG. 20

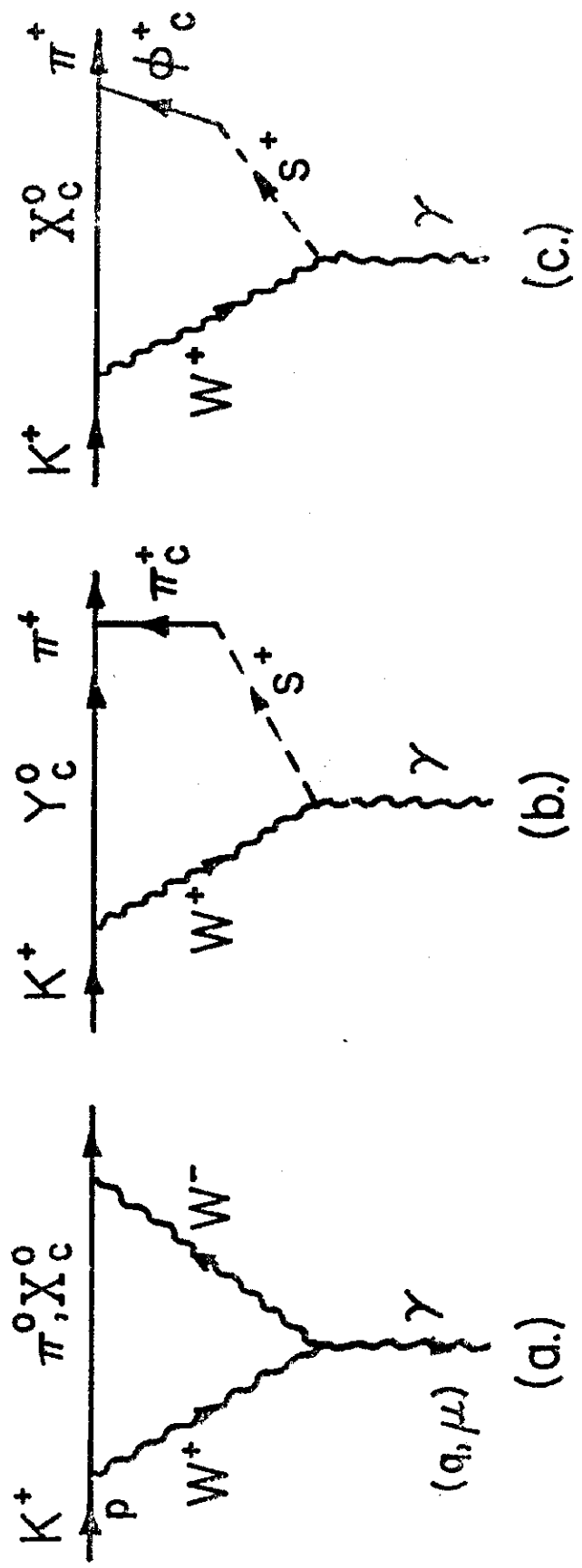


FIG. 21

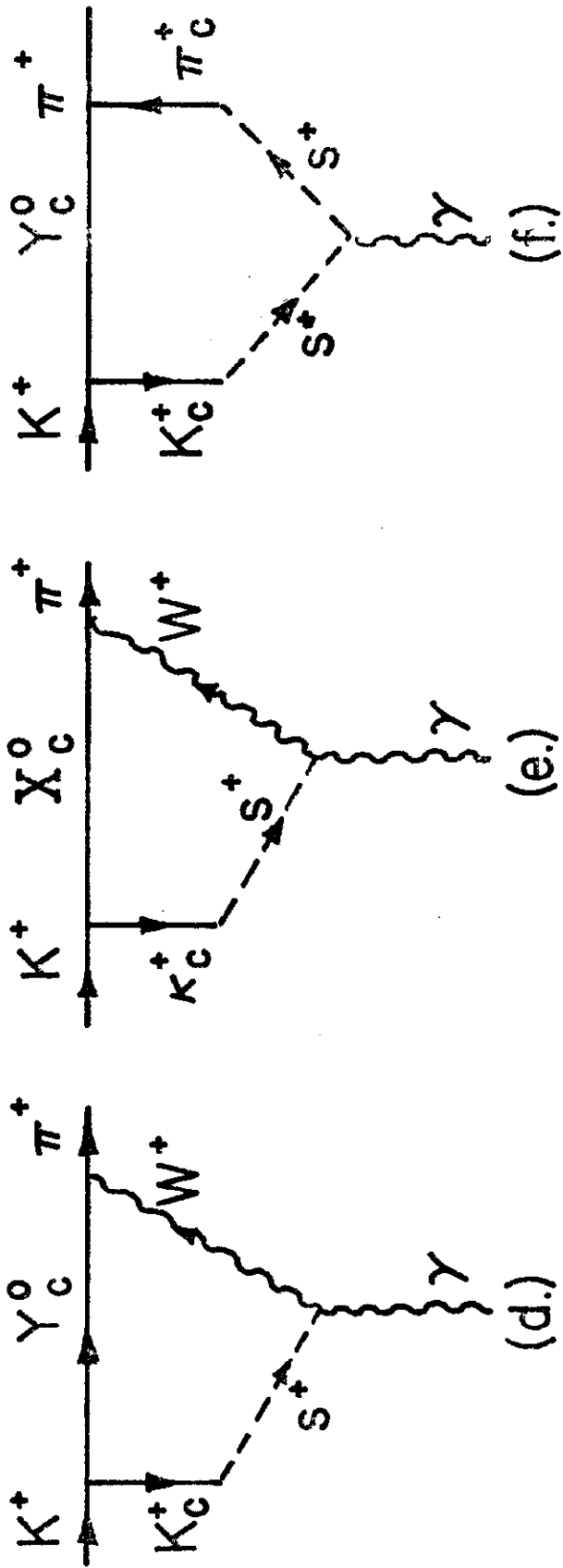


FIG. 21
(continued)

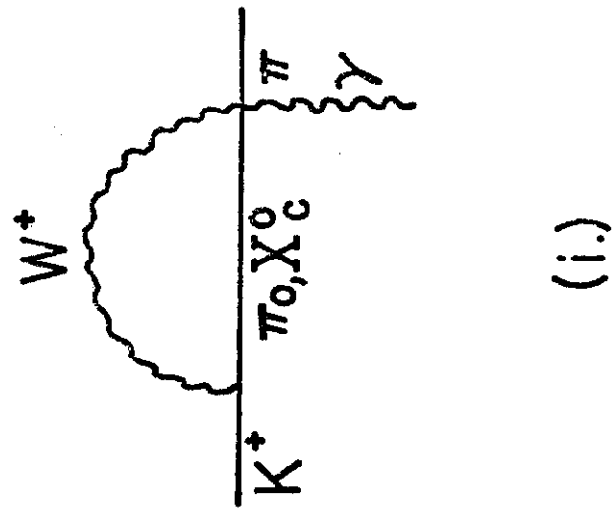
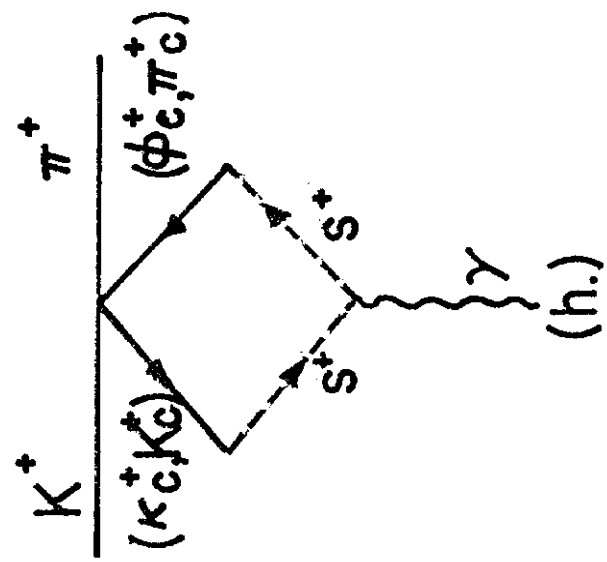
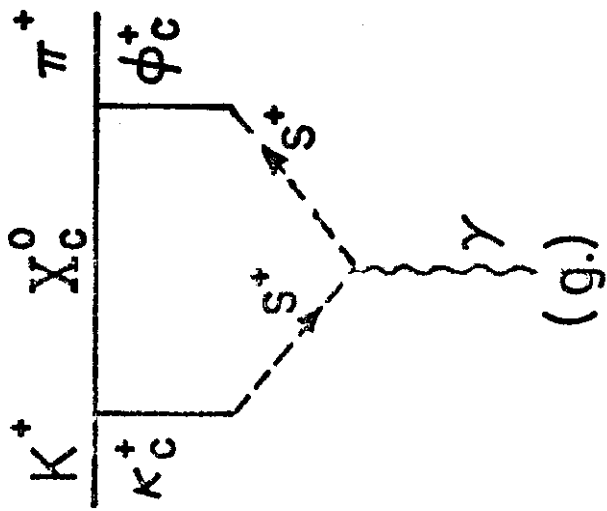


FIG. 21
(continued)

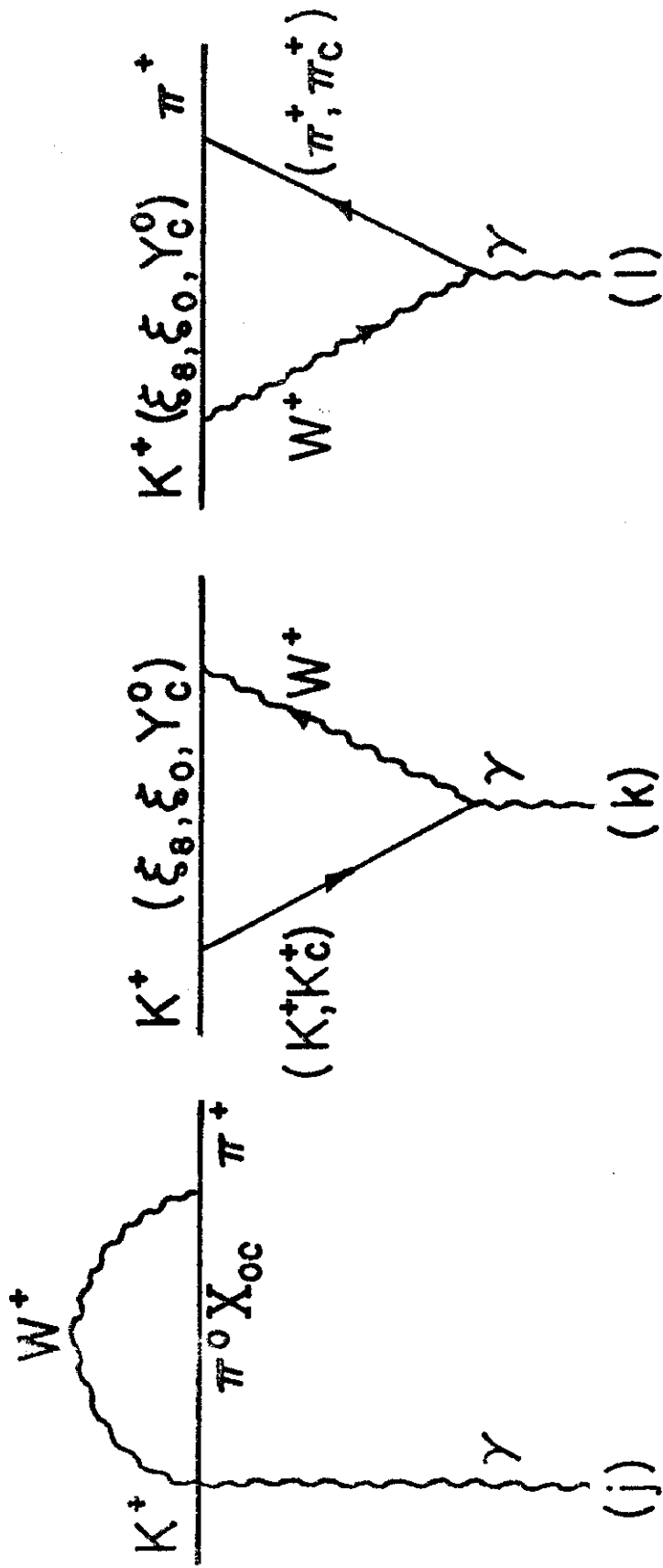


FIG. 21
(continued)

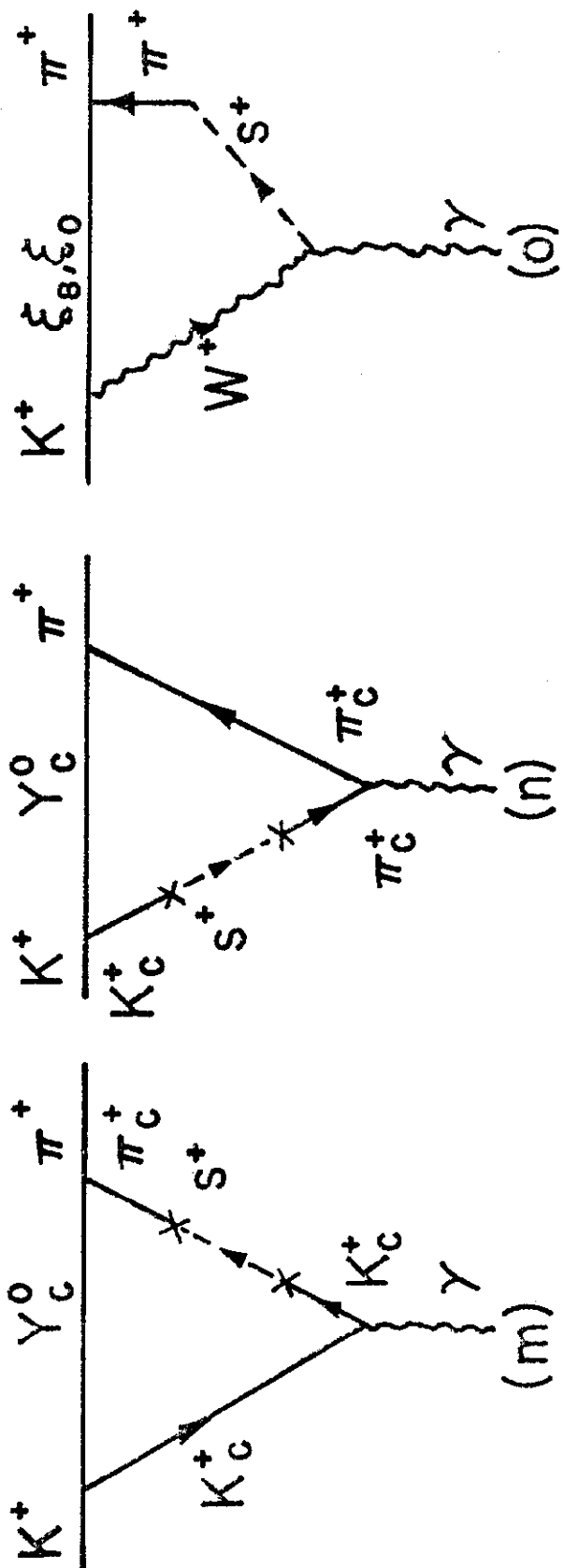


FIG.21
(continued)

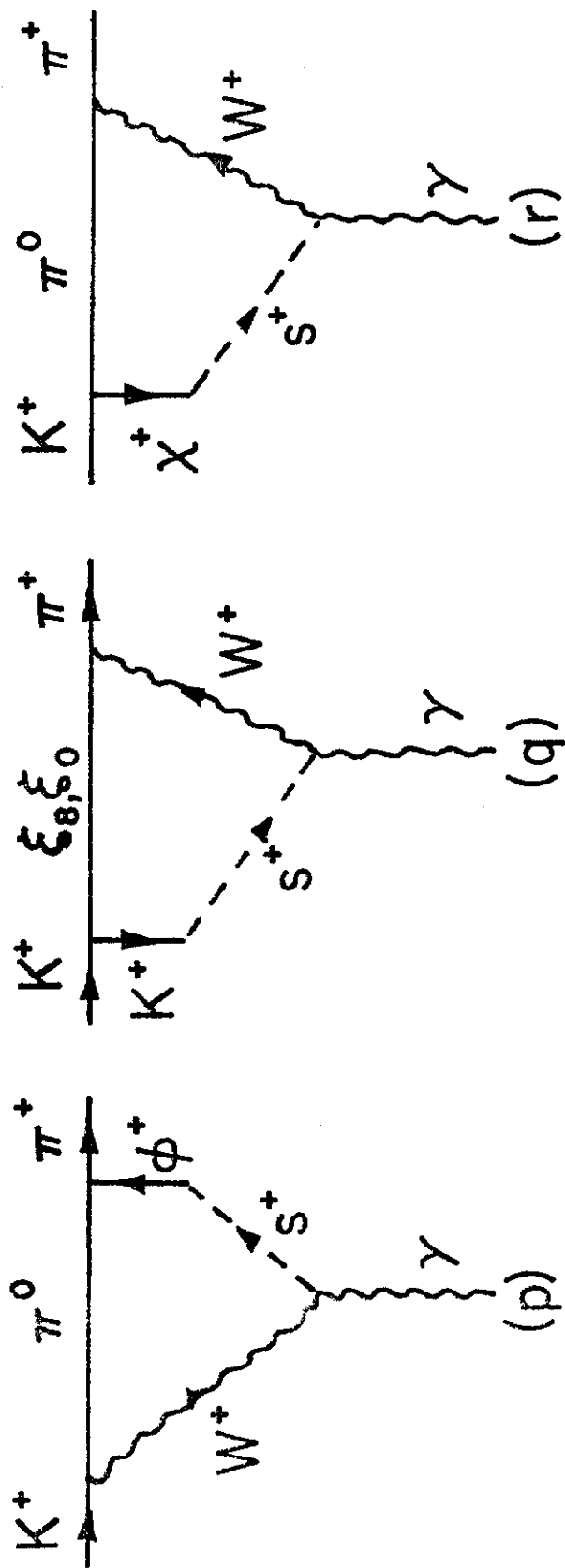


FIG. 21
(continued)

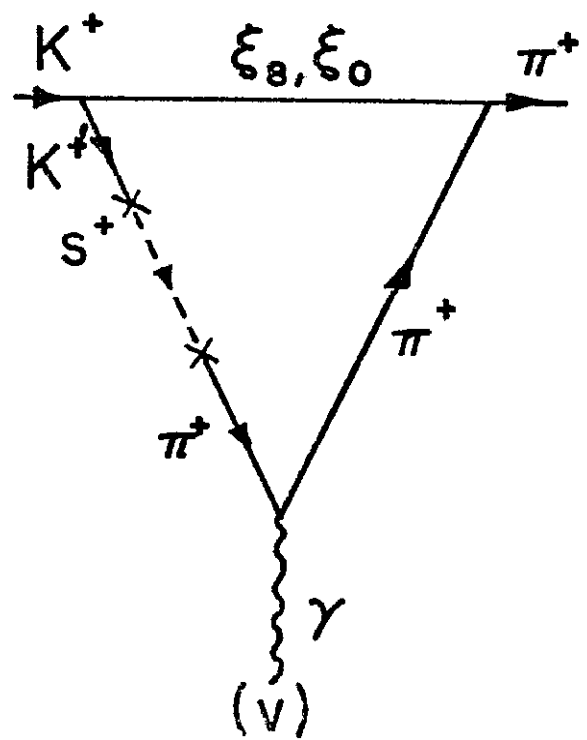
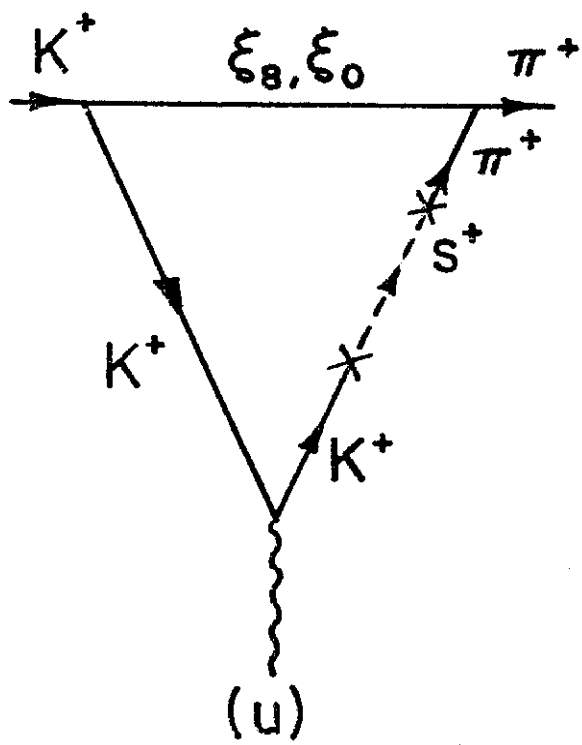
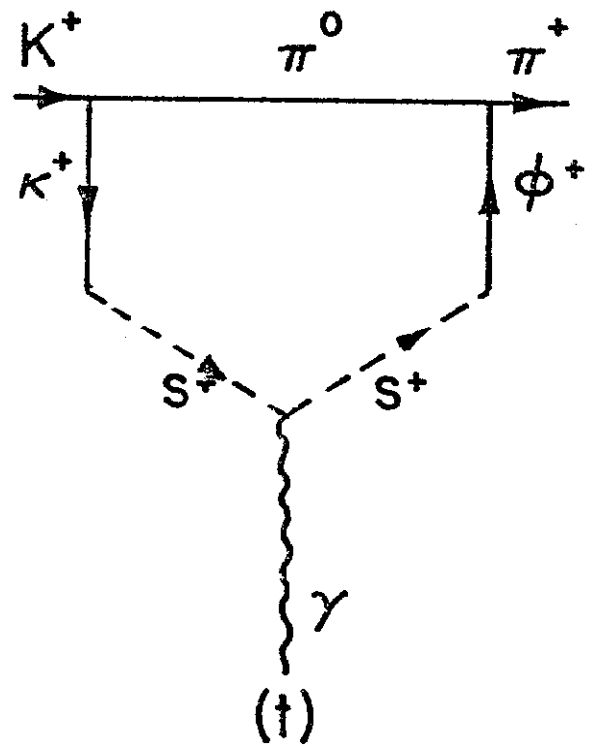
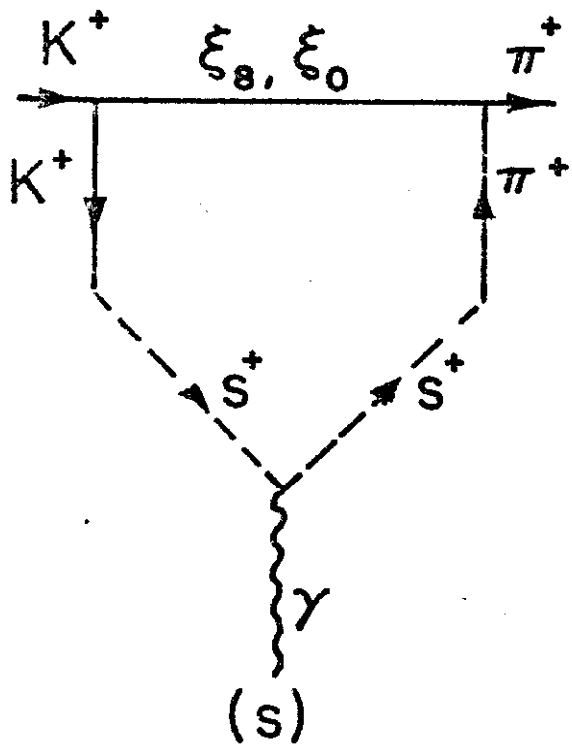
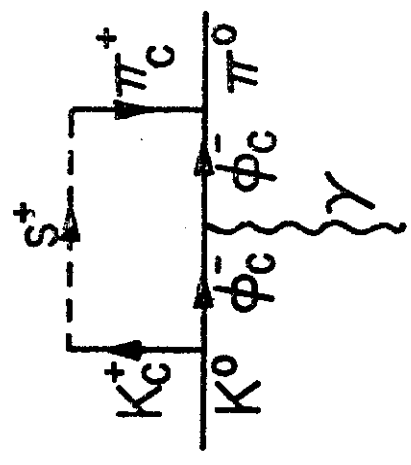
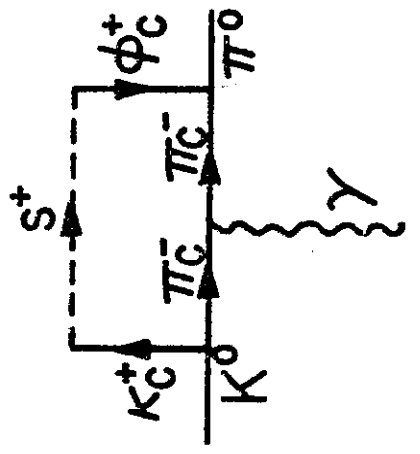
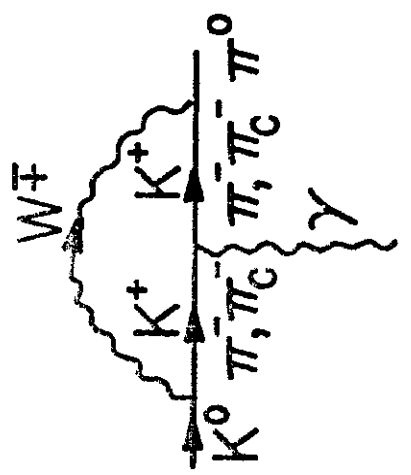


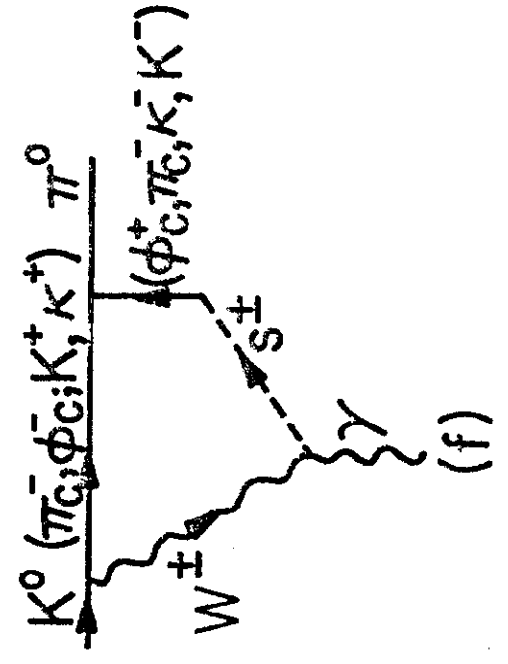
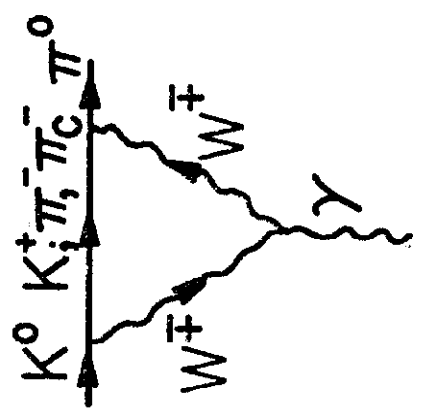
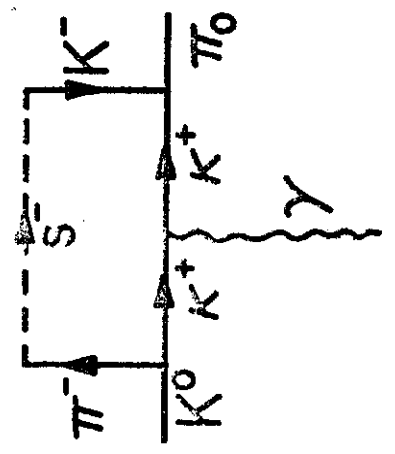
FIG. 21



(a)

(b)

(c)



(d)

(e)

(f)

FIG. 22

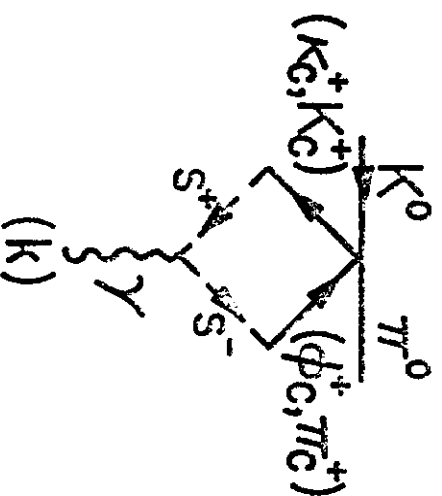
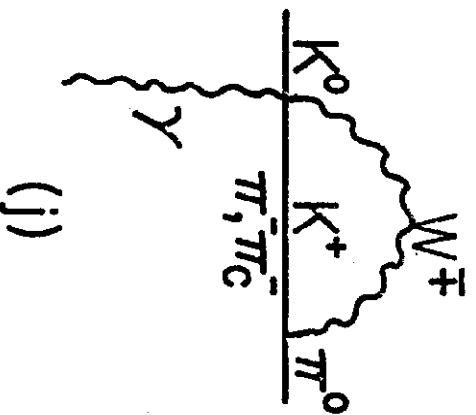
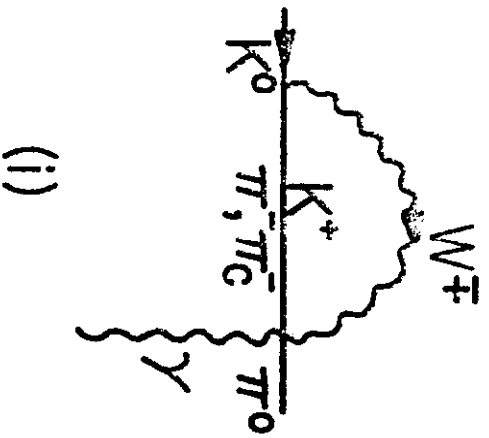
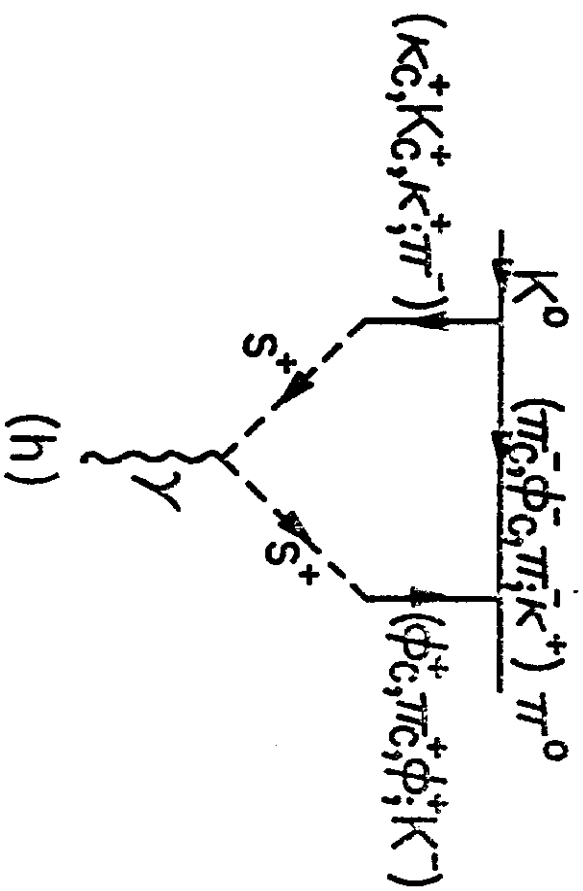
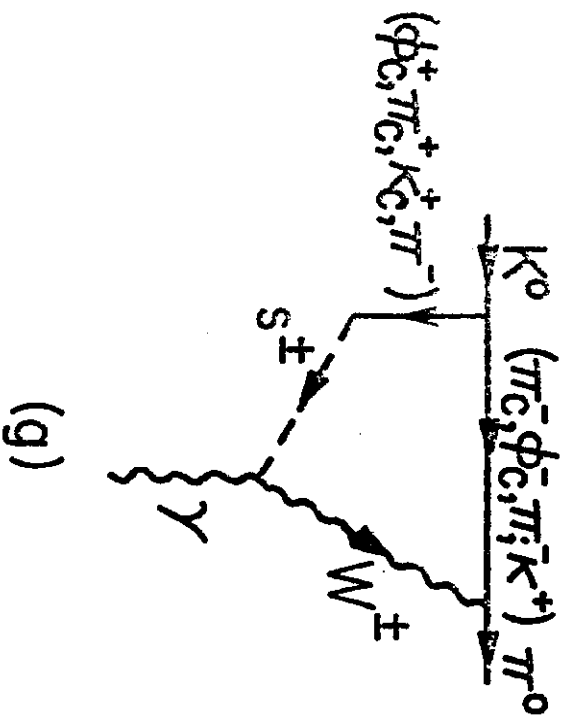
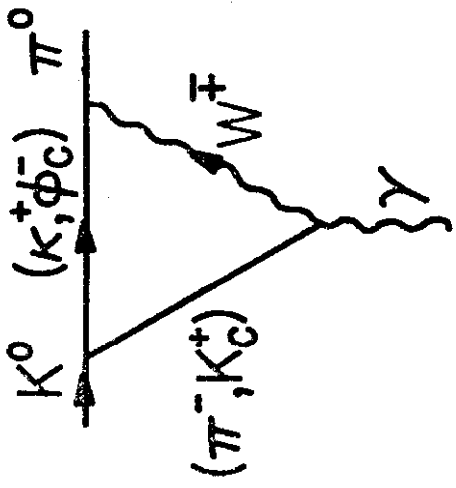
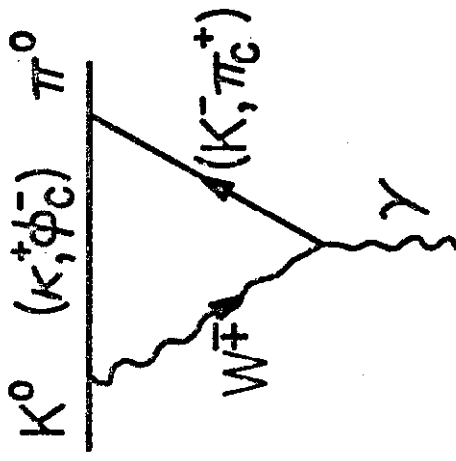


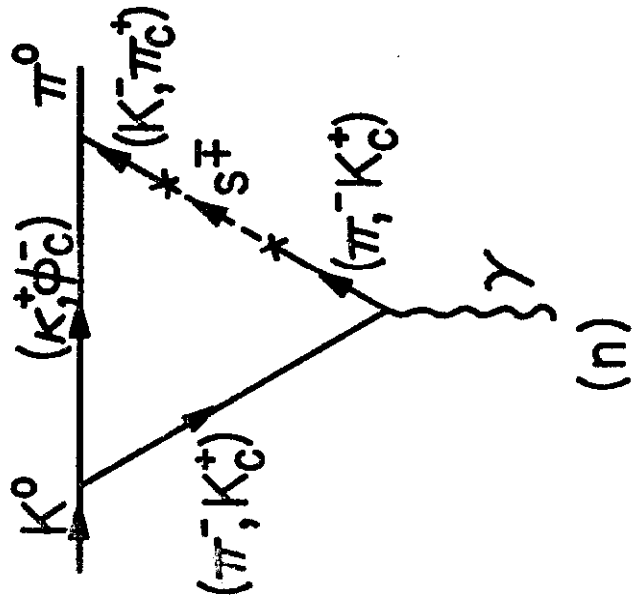
FIG. 22
 (continued)



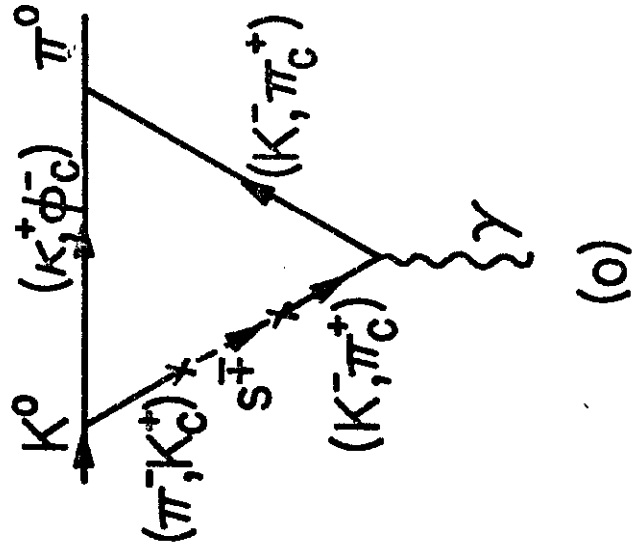
(l)



(m)

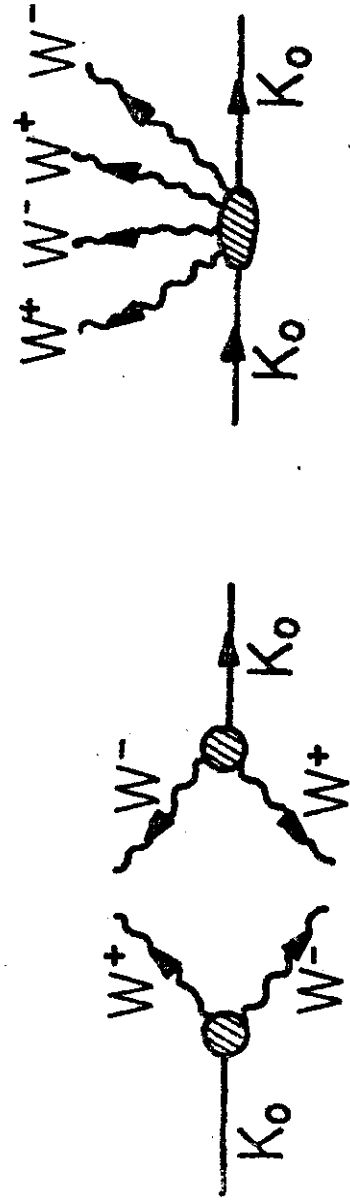


(n)



(o)

FIG. 22
(continued)

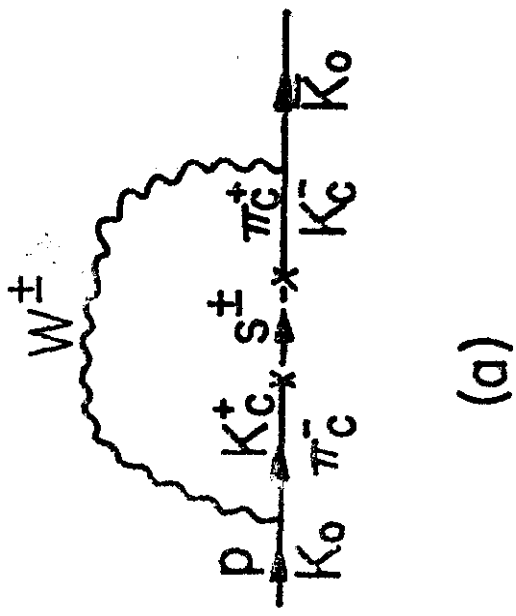


(a)

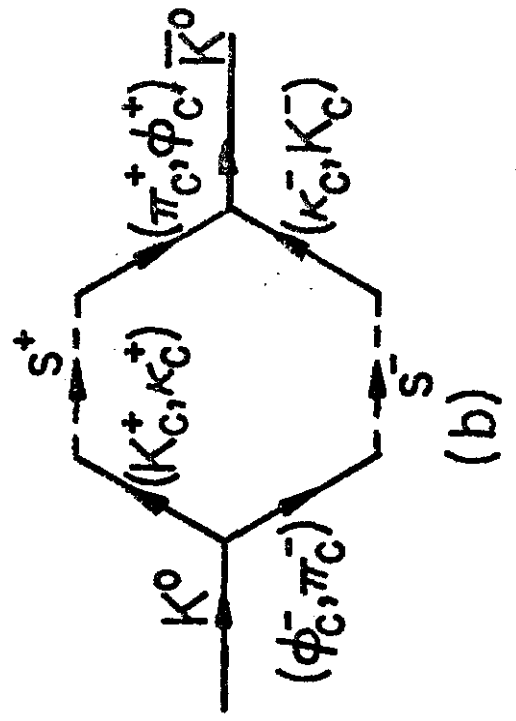
(b)

closing the w lines in (a) generates the one loop diagrams
 " " " " (b) " " two loop diagrams

FIG. 23



(a)

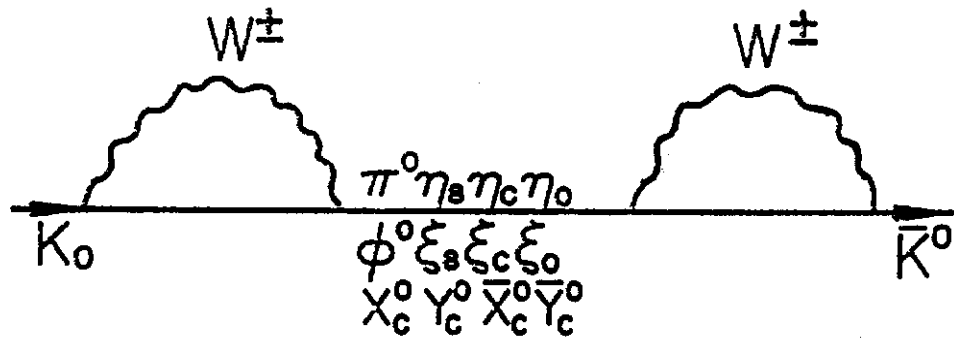


(b)

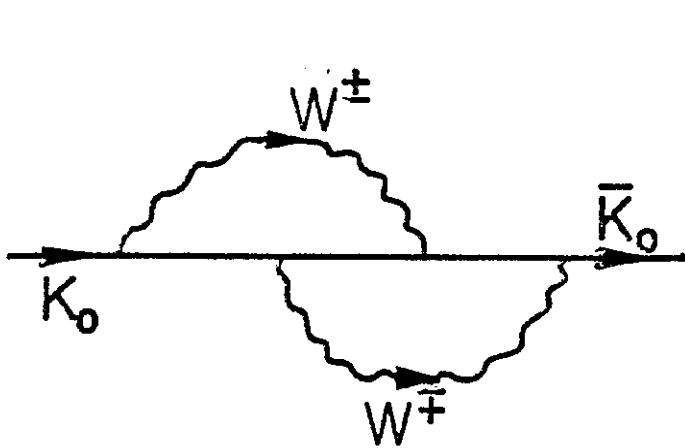
FIG. 24

Note: Henceforth, whenever an intermediate or a final state is unlabeled or incompletely labeled, the diagram stands for sum over all possibilities.

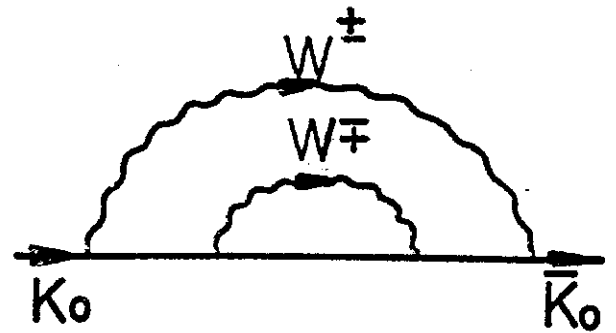
Class I



(a)



(b)



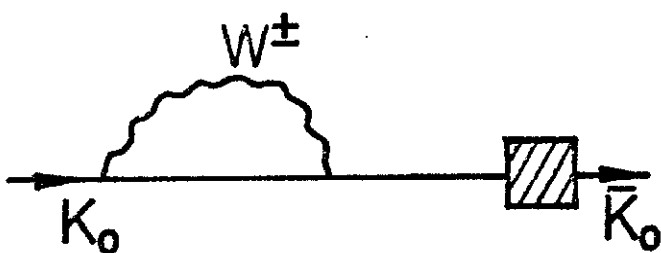
(c)

FIG. 25

Class 2

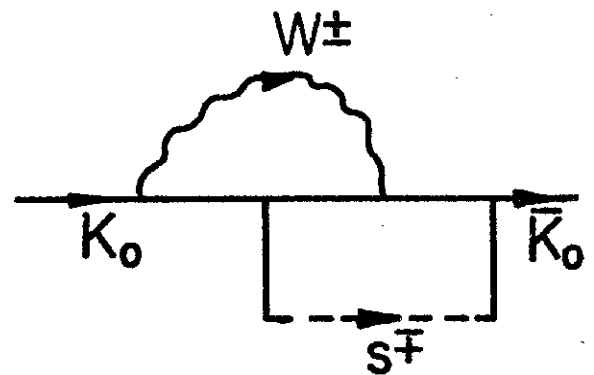
Note: M.R. means mirror reflection in a vertical line
(except for the labels K_0, \bar{K}_0)

 = sum of all one loop, self energy diagrams
not involving a W propagator.



+ M.R.

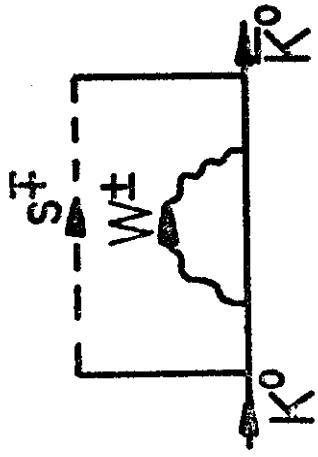
(d)



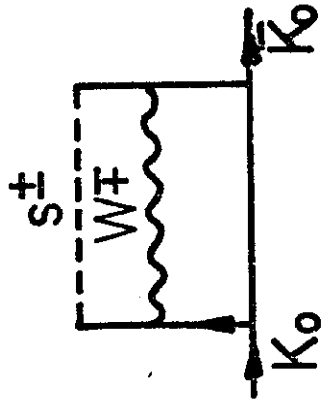
M.R.

(e)

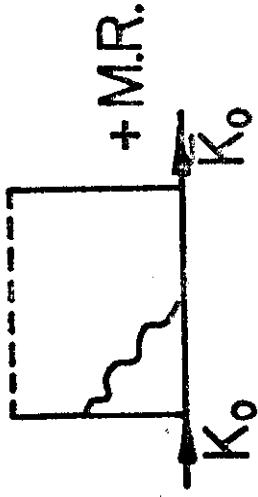
FIG. 25
(continued)



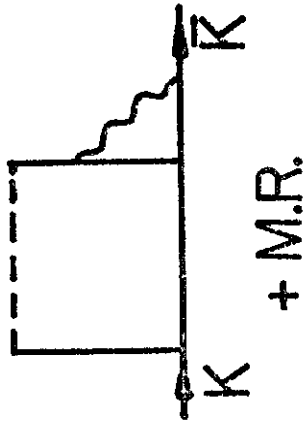
(f)



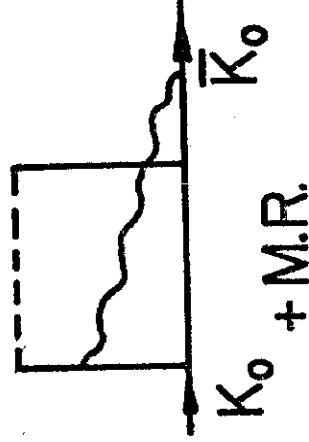
(g)



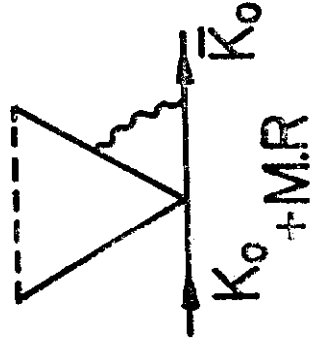
(h)



(i)

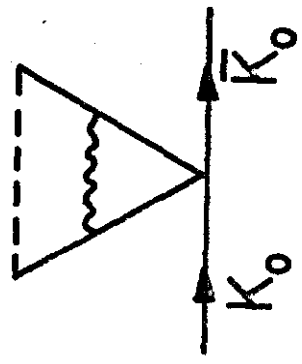


(j)

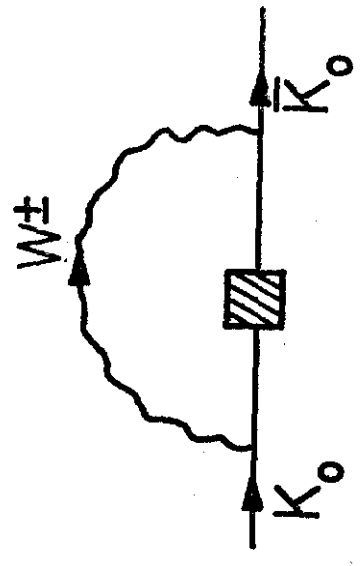


(k)

FIG. 25
(continued)



(l)



(m)

FIG. 25
(continued)

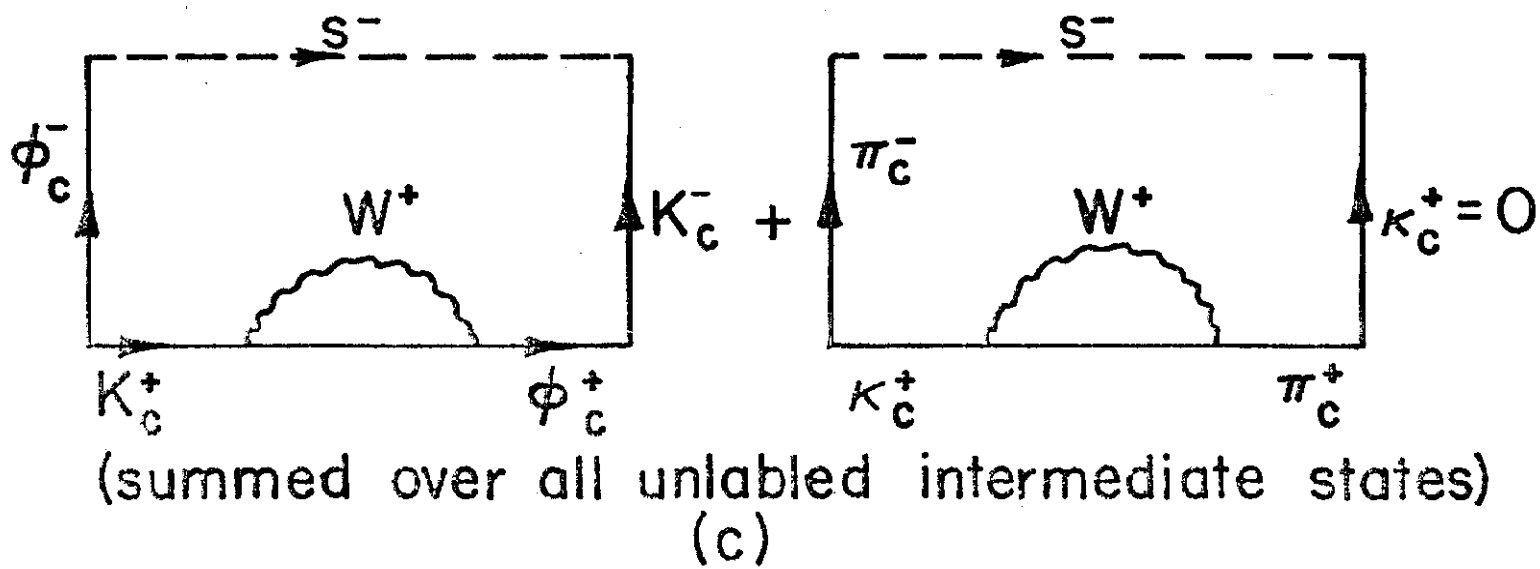
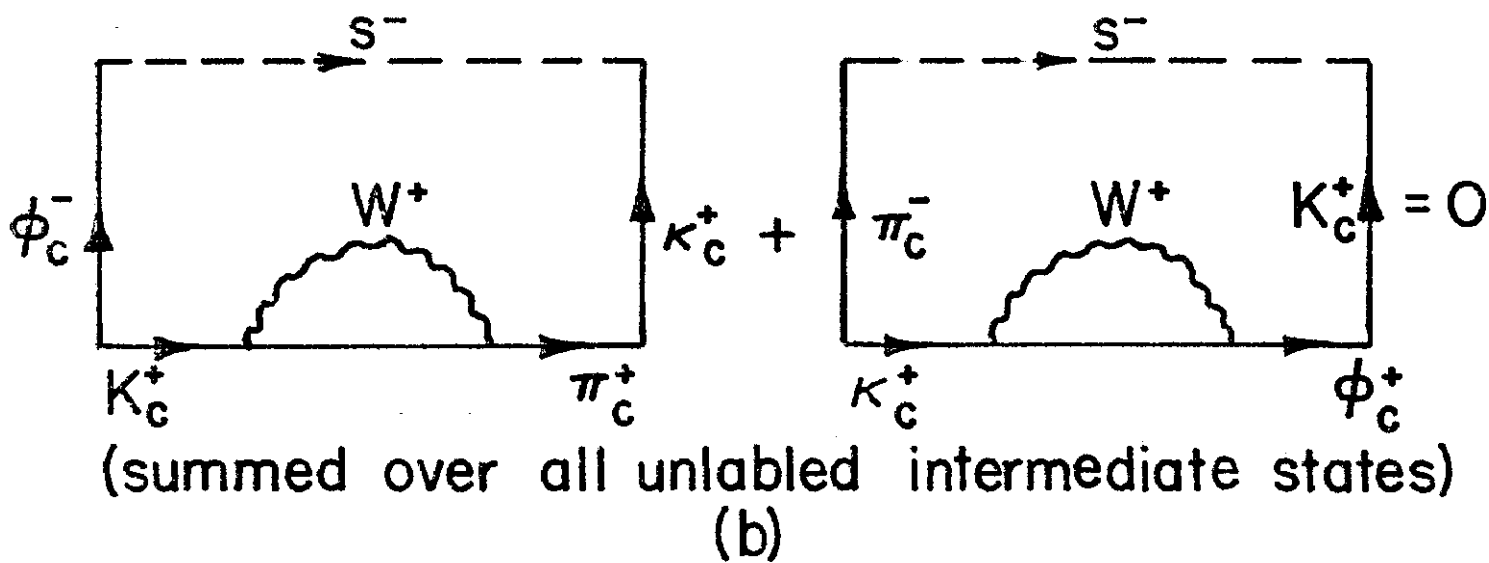
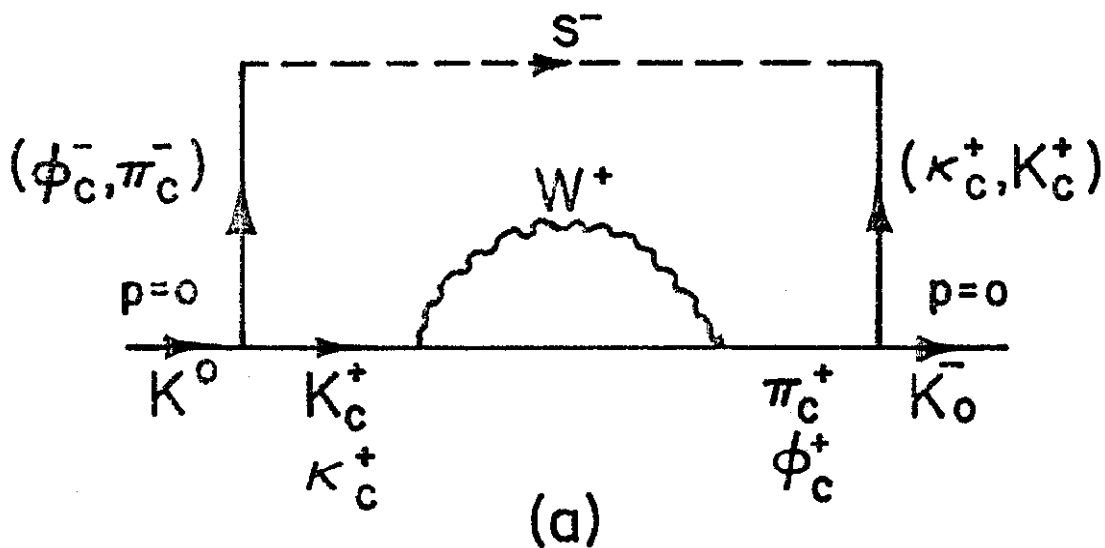
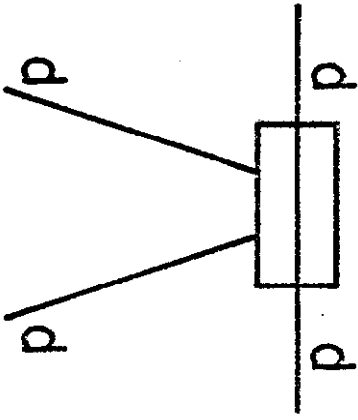


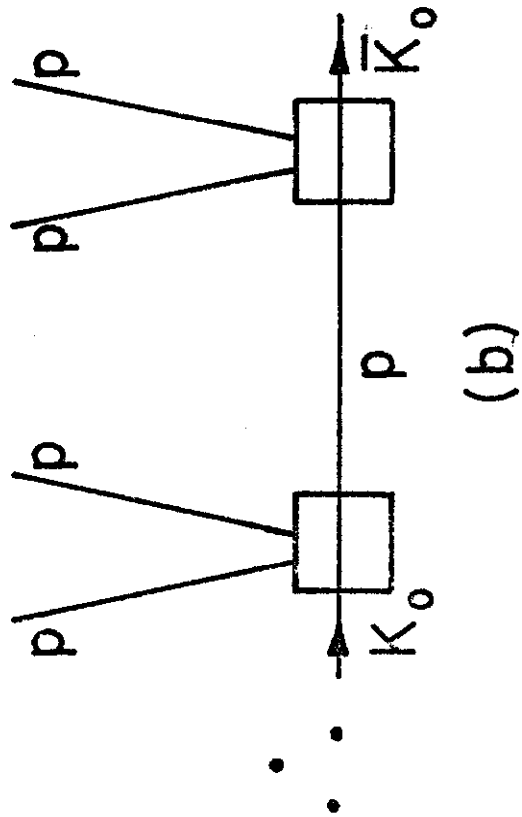
FIG. 26



(a)

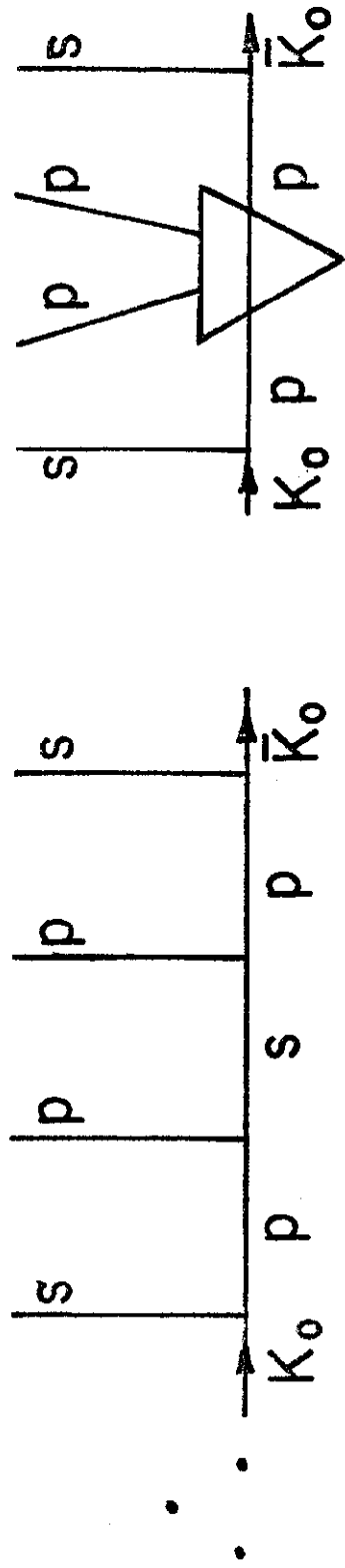
does not have terms proportional
to μ^2 for any given external
4 p. s. mesons.

FIG. 27



does not have terms
proportional to μ^4, μ^2 .

FIG. 27
(continued)



does not have terms proportional to μ^2 .

(c)

FIG. 27
(continued)

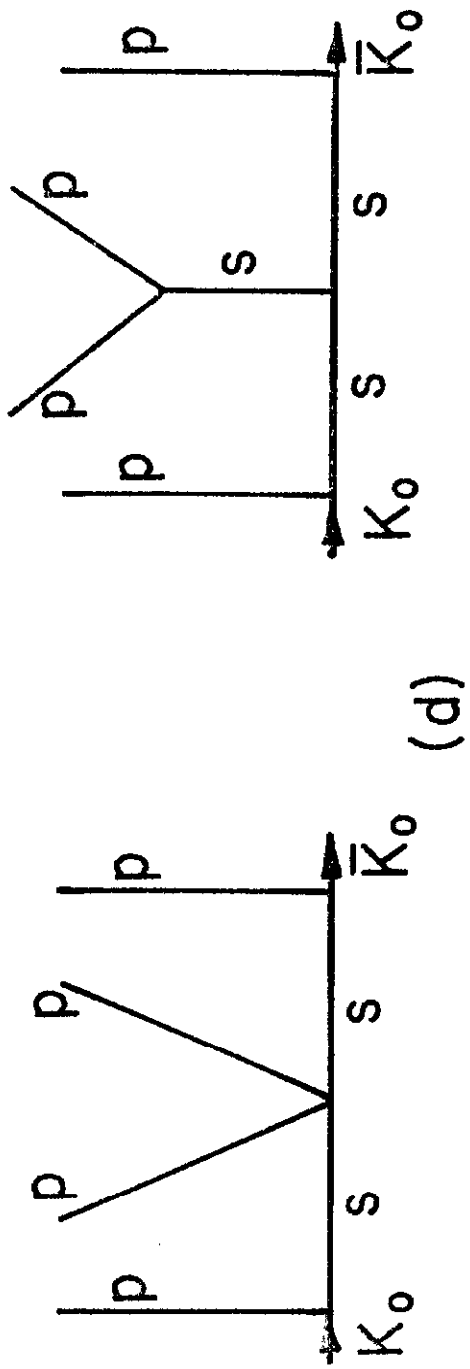


FIG. 27
(continued)

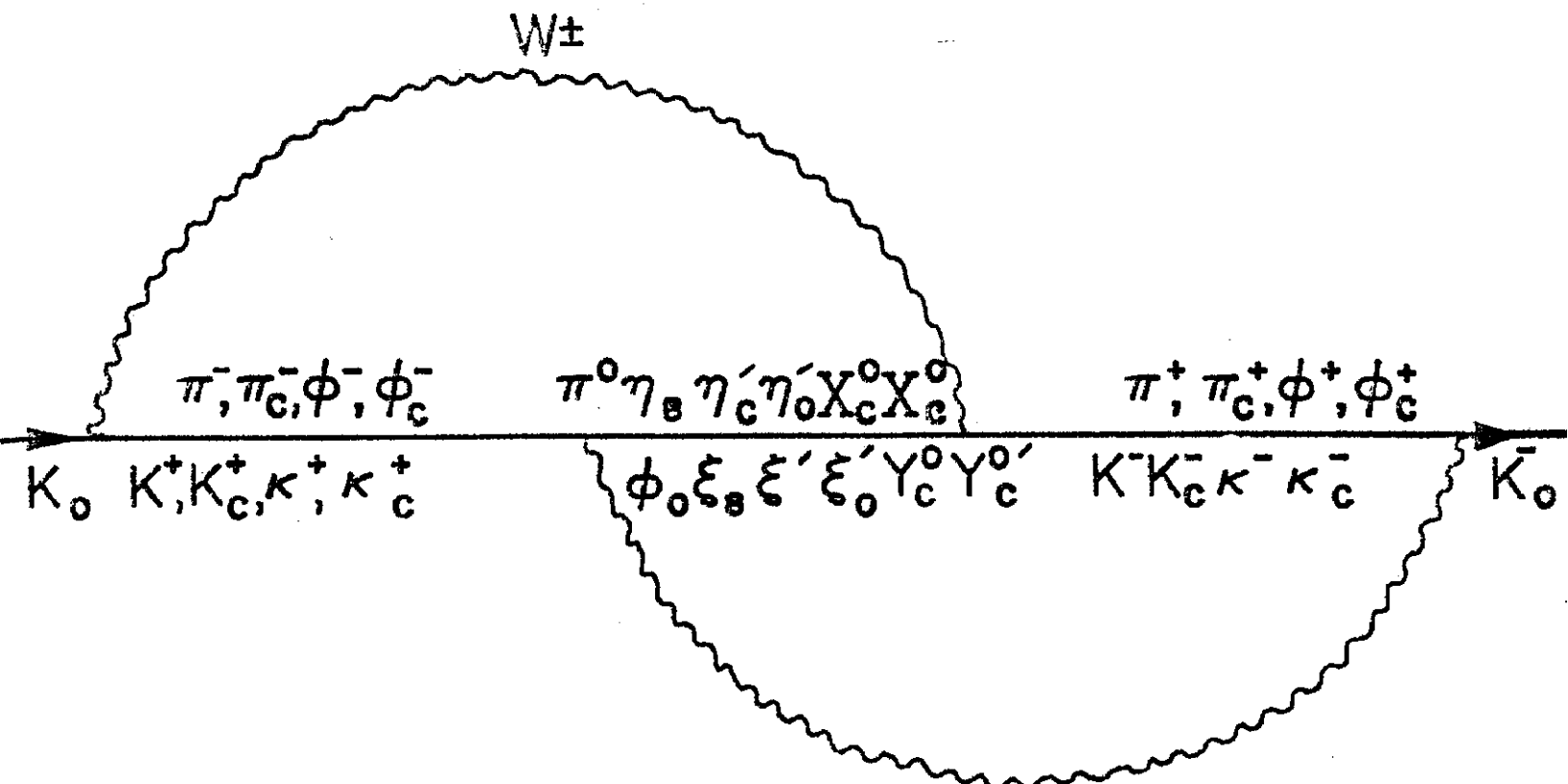


FIG. 28

W^\mp

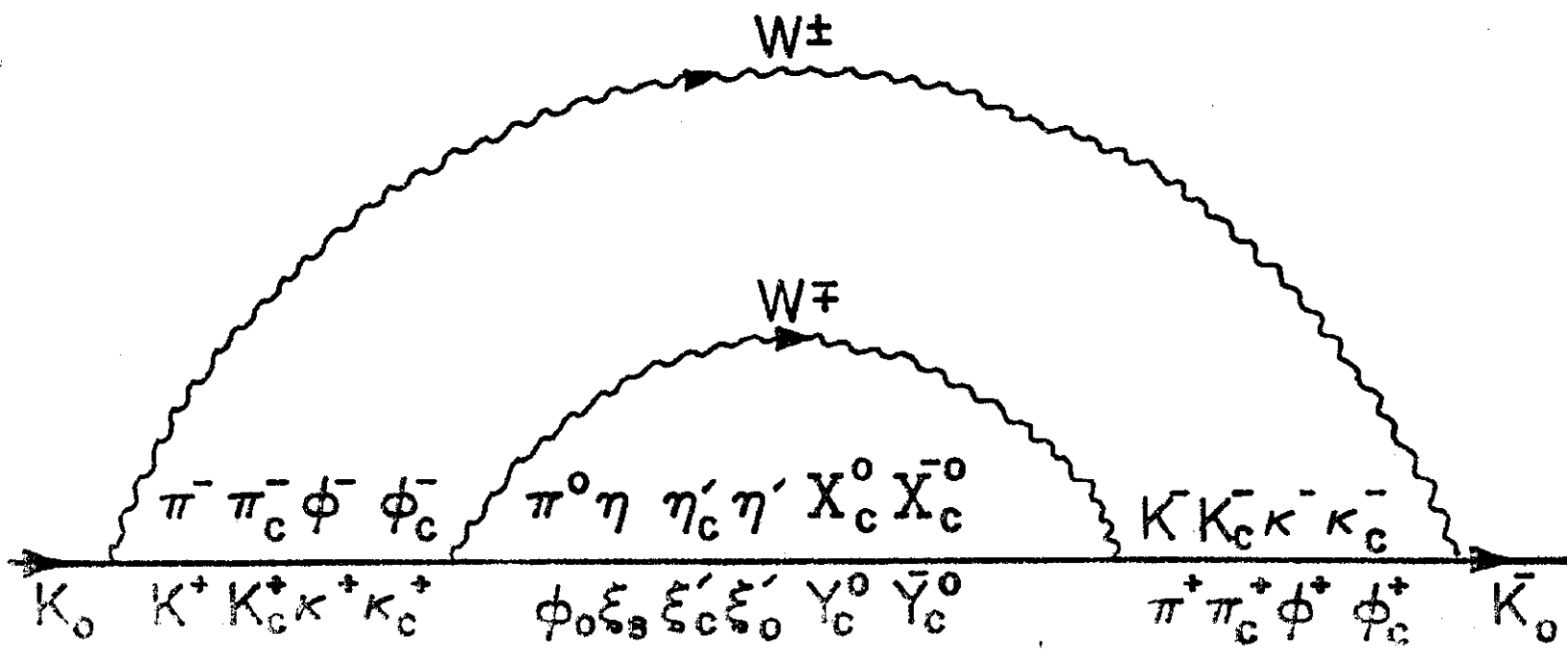


FIG. 29

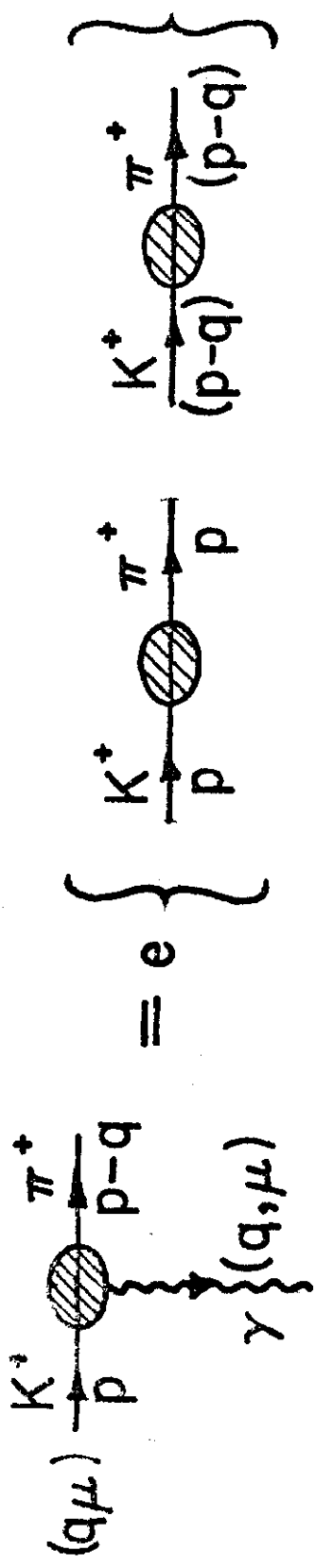


FIG. 30

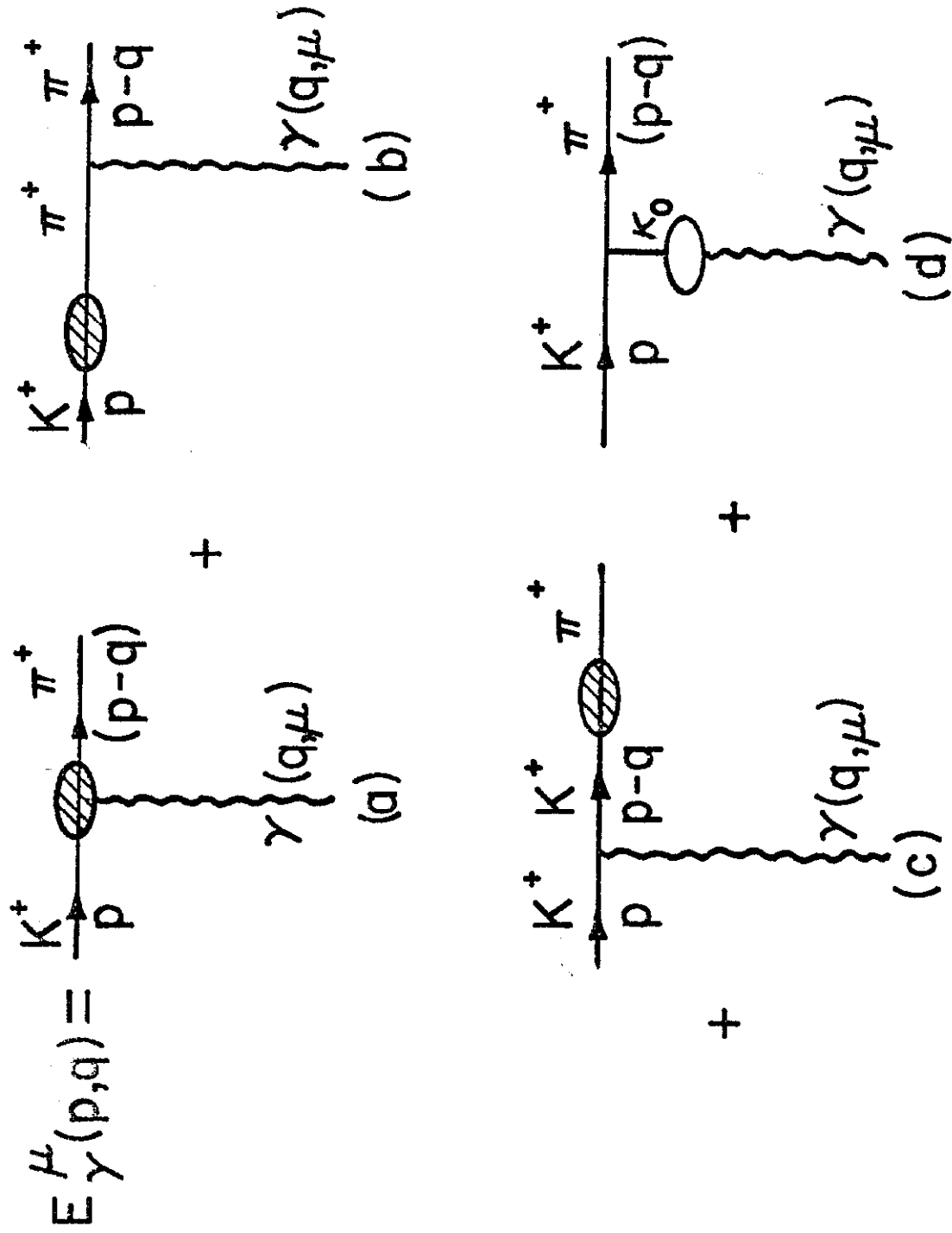


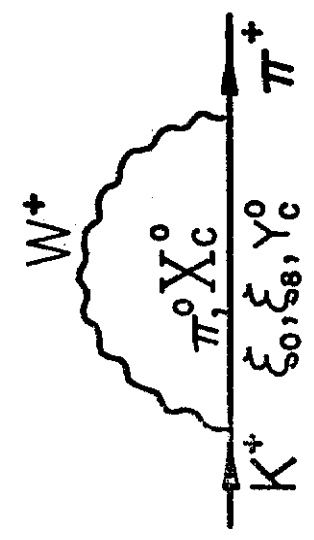
FIG. 31

$$E_{0\gamma}^{\mu}(p,q) = \text{Diagram 1} + \text{Diagram 2}$$

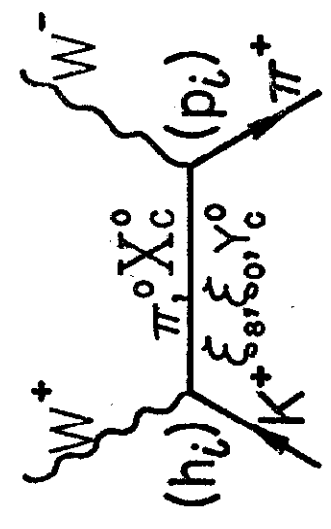
Diagram 1: A horizontal line labeled K^0 has a shaded circle on it. A wavy line labeled $\gamma(q,\mu)$ originates from the shaded circle. A vertical line labeled K^0 extends upwards from the shaded circle to a horizontal line labeled π^0 .

Diagram 2: A horizontal line labeled K^0 has a shaded circle on it. A wavy line labeled $\gamma(q,\mu)$ originates from the shaded circle. A vertical line labeled K^0 extends upwards from the shaded circle to a horizontal line labeled π^0 .

FIG. 32

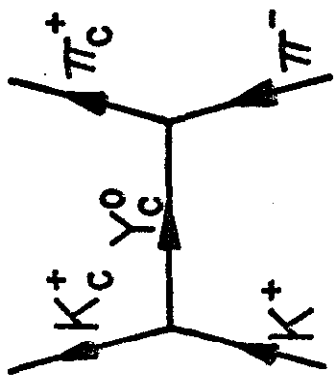


(a)

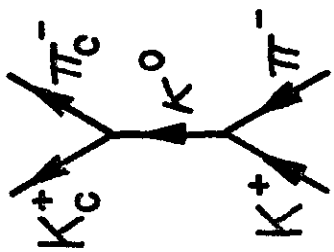


(b)

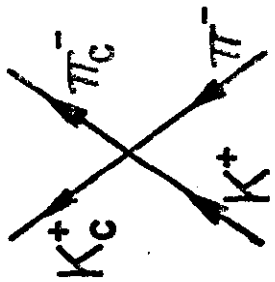
FIG. 33



(a)

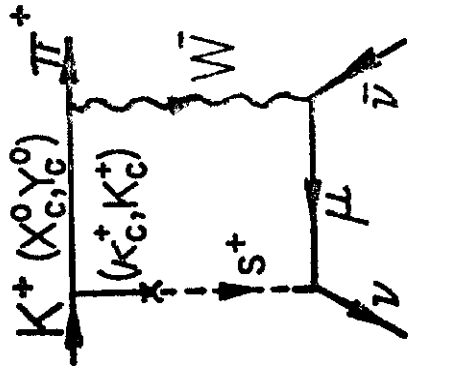


(b)

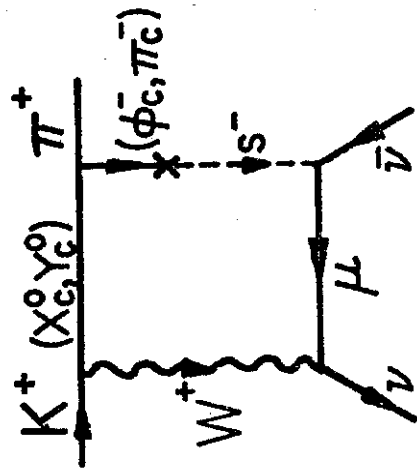


(c)

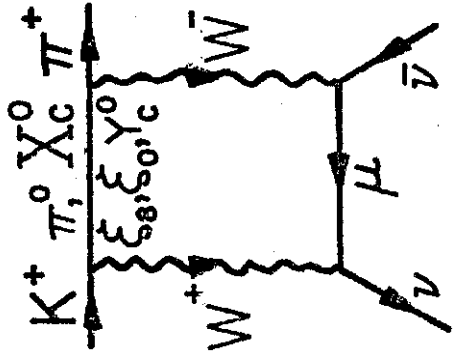
FIG. 34



(a)

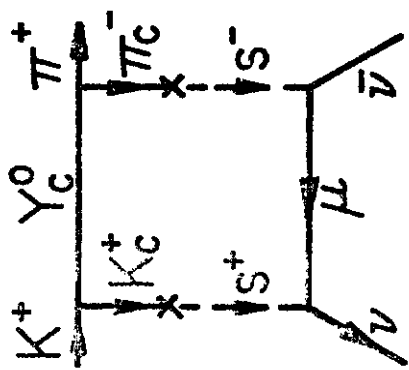


(b)

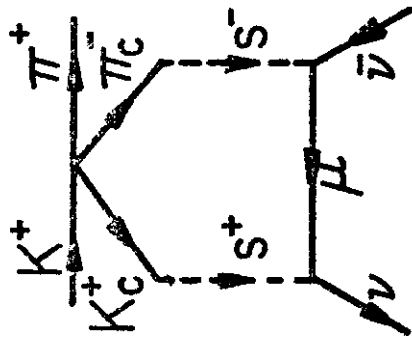


(c)

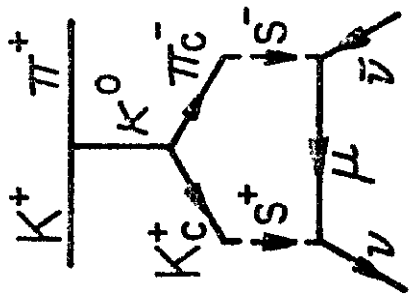
FIG. 35



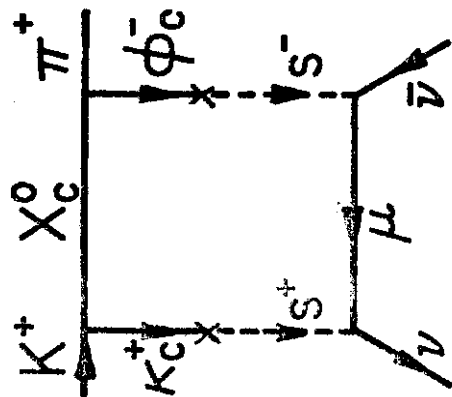
(d)



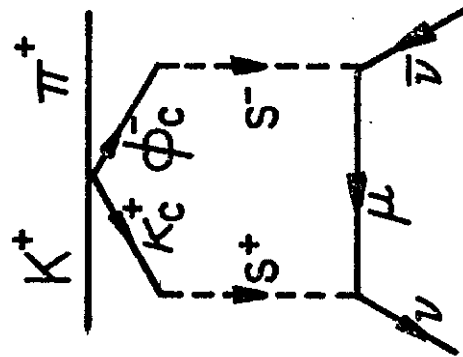
(e)



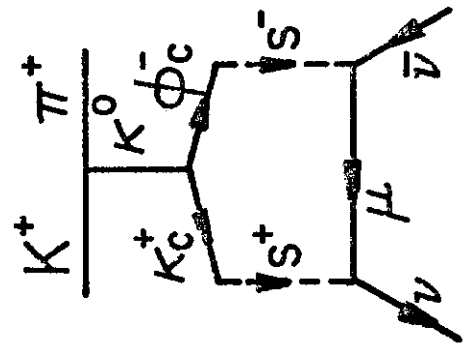
(f)



(g)

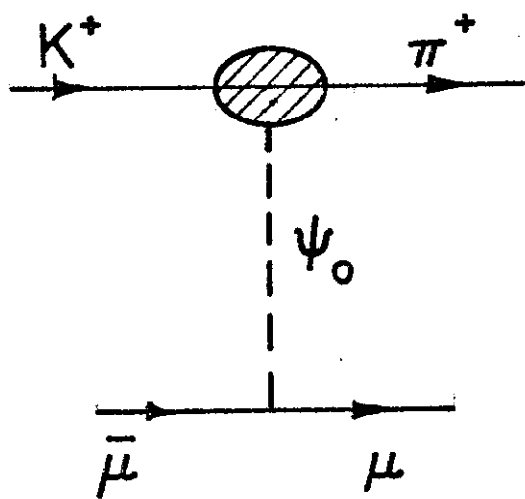


(h)

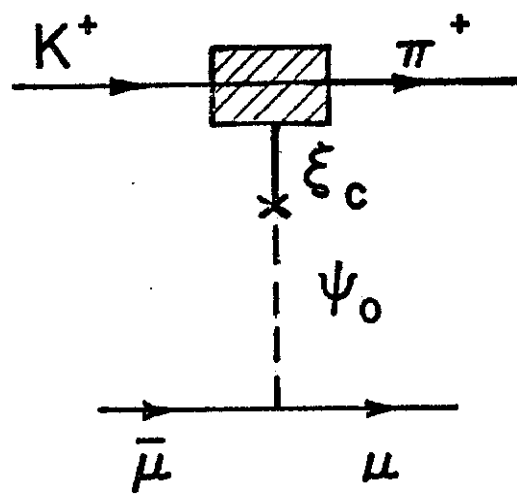


(i)

FIG. 35
continued



(a)



(b)

FIG. 36

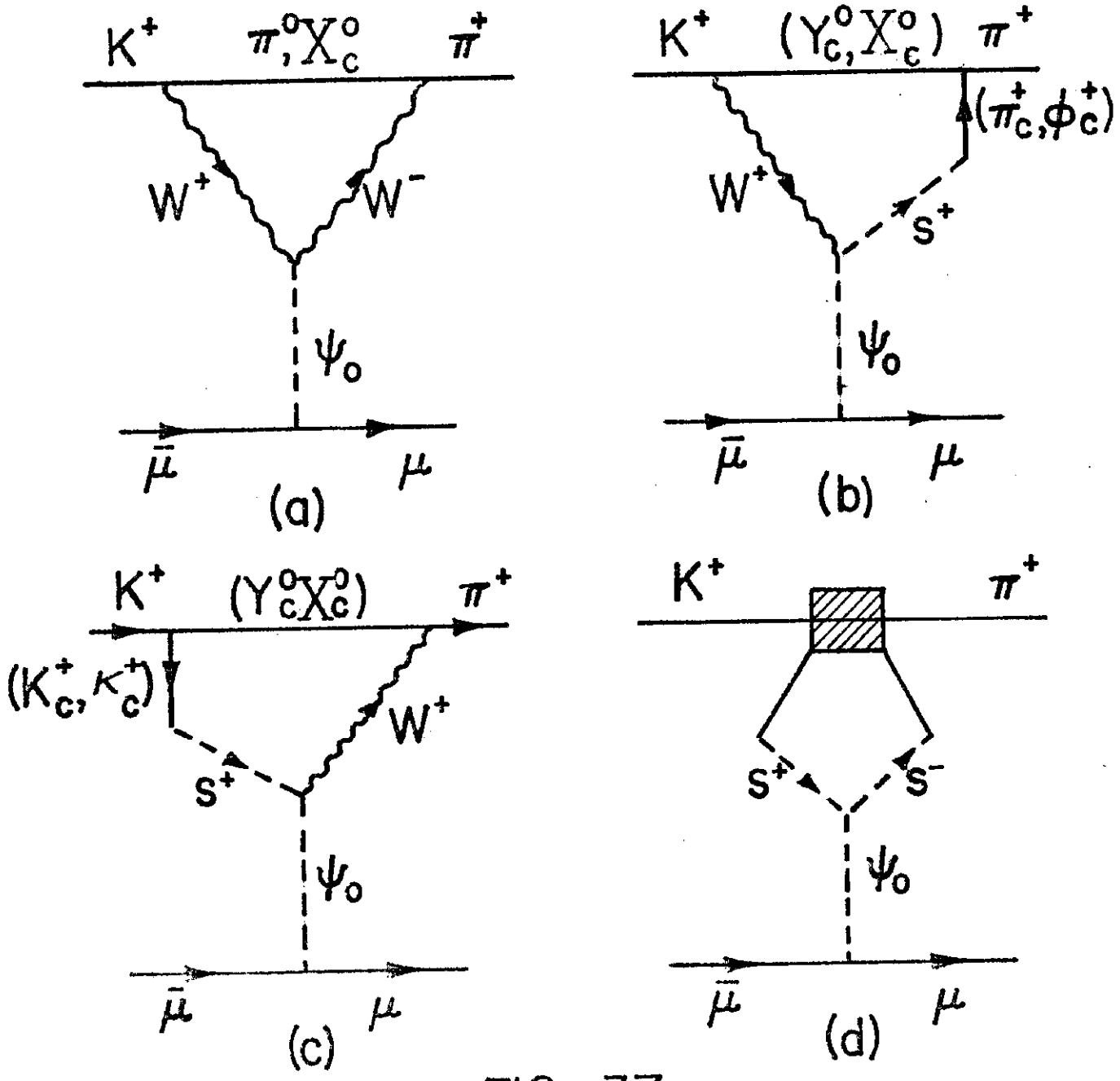


FIG. 37

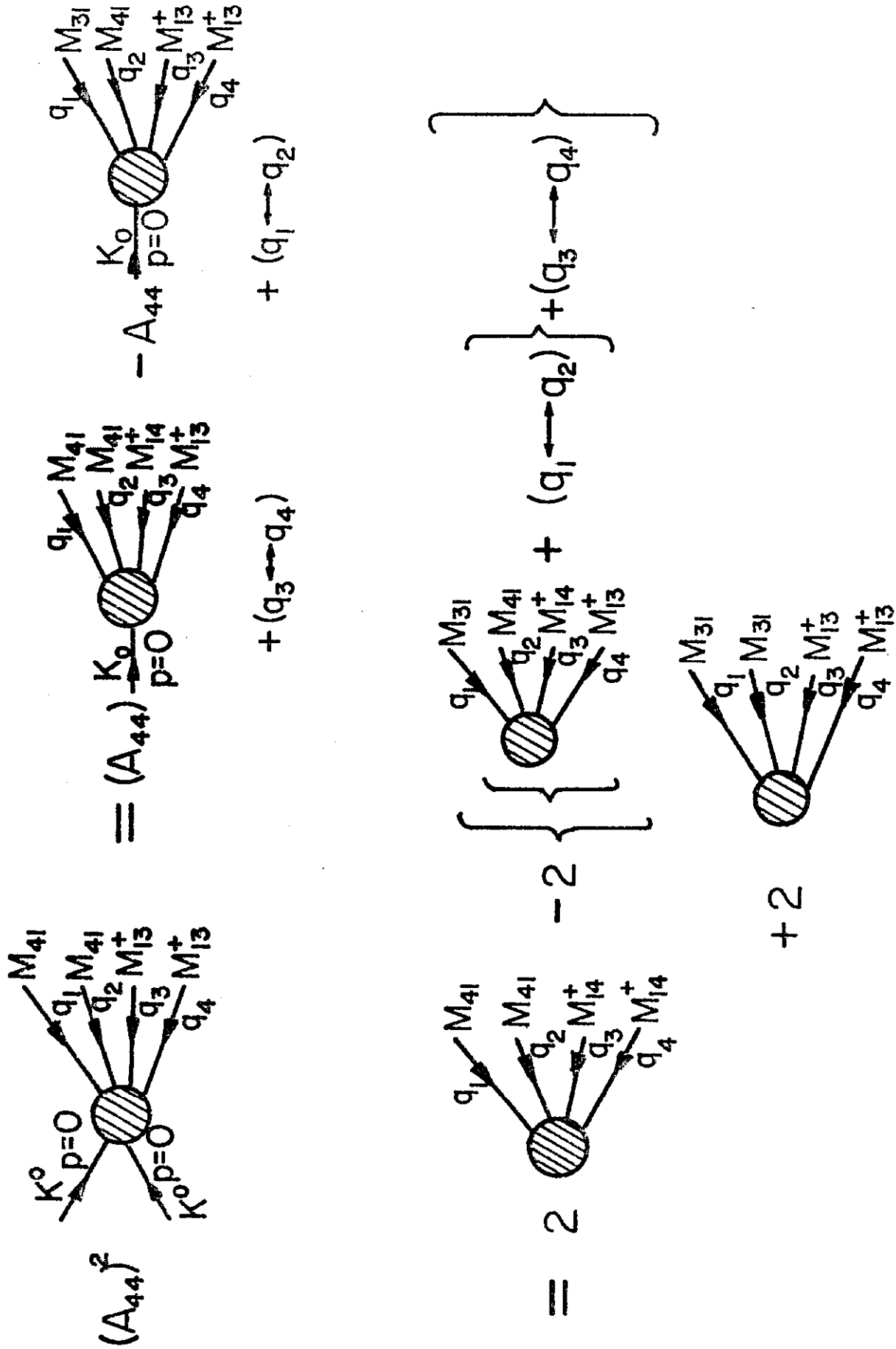


FIG. 38

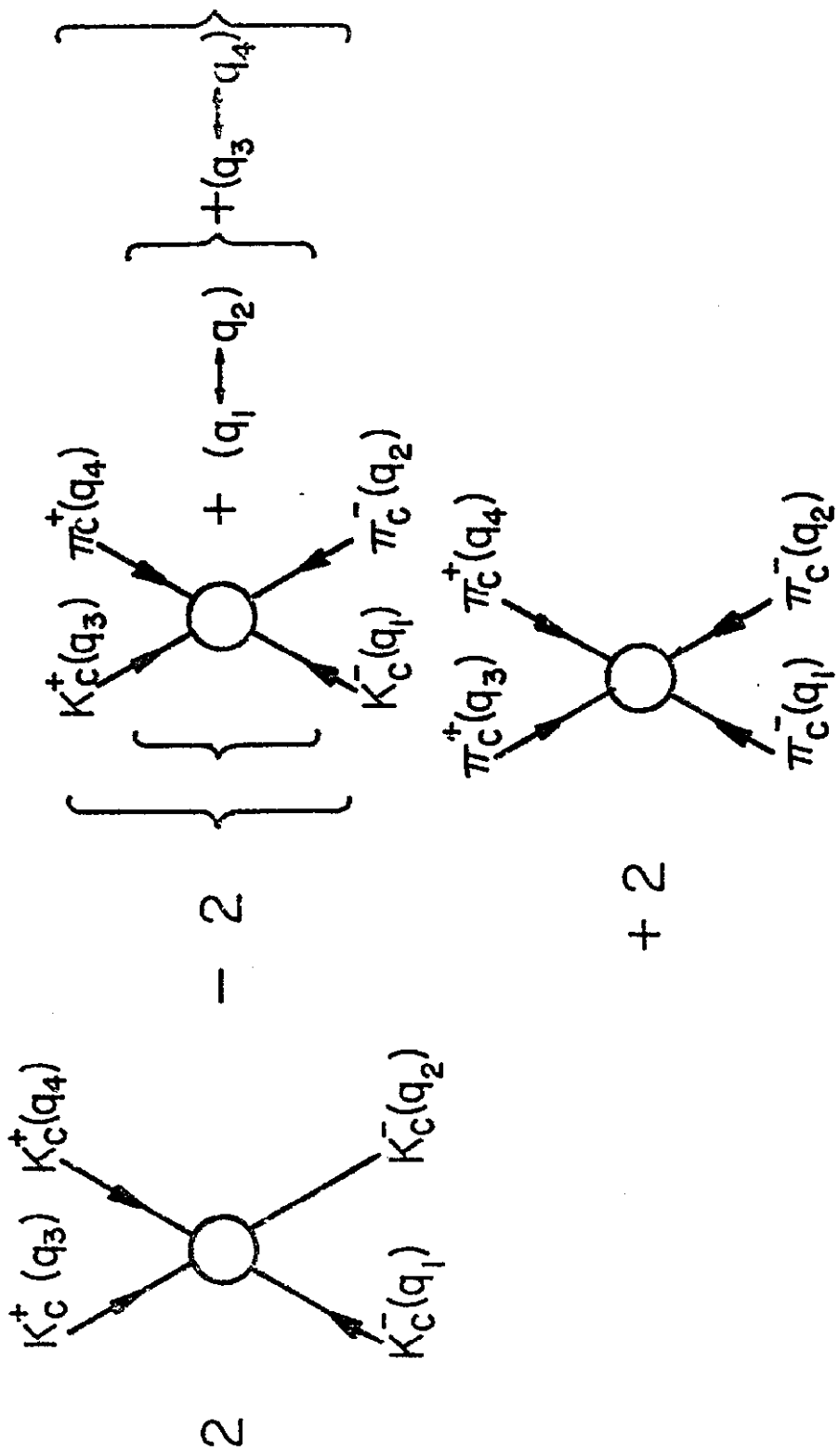


FIG. 39